Rockefeller University
Digital Commons @ RU

Student Theses and Dissertations

2016

Aversive Olfactory Imprinting in Caenorhabditis Elegans

Xin Jin

Follow this and additional works at: http://digitalcommons.rockefeller.edu/student_theses_and_dissertations

 Part of the Life Sciences Commons

Recommended Citation
Jin, Xin, "Aversive Olfactory Imprinting in Caenorhabditis Elegans" (2016). *Student Theses and Dissertations.* Paper 310.

This Thesis is brought to you for free and open access by Digital Commons @ RU. It has been accepted for inclusion in Student Theses and Dissertations by an authorized administrator of Digital Commons @ RU. For more information, please contact mcsweej@mail.rockefeller.edu.

AVERSIVE OLFACTORY IMPRINTING IN *CAENORHABDITIS ELEGANS*

A Thesis Presented to the Faculty of

The Rockefeller University

in Partial Fulfillment of the Requirements for

the degree of Doctor of Philosophy

by

Xin Jin

June 2016

© Copyright by Xin Jin 2016

AVERSIVE OLFACTORY IMPRINTING IN *CAENORHABDITIS ELEGANS*

Xin Jin, Ph.D.

The Rockefeller University 2016

Early memories are especially robust and enduring, among which the most evocative example is imprinting. Imprinting was first described in newly hatched geese that form a lasting attachment to the first moving object they see. As observed in many animal species, imprinting is a process in which a sensory cue presented early in animal's life – a critical period – subsequently gains unique access to ecologically relevant behaviors. Little is known about the molecular and neural underpinnings of imprinting. I have used *C. elegans* as a model organism to study imprinting because of its compact and well-characterized nervous system, an armory of available genetic tools, and a versatile behavioral repertoire. Using a ethologically relevant training regime, I found that exposing newly hatched larvae *C. elegans* to pathogenic bacteria can generate an aversive memory of bacterial odors that is sustained into adulthood (4 days), in contrast to training of adults that results in a medium-term memory that lasts for less than a day. This long-lasting aversive memory is specific to the experienced pathogen and has a critical period in the first larval stage (L1), and is defined as a form of aversive imprinting. Through chemical-genetic silencing of candidate neurons, I identified neurons essential for memory formation but not for memory retrieval (interneurons AIB and RIM), and complementary neurons essential for memory retrieval but not for memory formation (interneurons AIY and RIA) (Chapter 2). The RIM memory formation neurons synthesize

the neuromodulator tyramine, which is required in the L1 stage for learning. This learning signal is transmitted to the AIY memory retrieval neurons by the tyramine receptor SER-2, which is required for imprinted aversion but not for adult learned aversion (Chapter 3). Tyramine modulation bridges the two subcircuits by linking tyramine production during learning with memory retrieval days later. Functional calcium imaging indicates that early imprinting experience modifies neuronal activity and output of the memory circuit. Among several neurons examined, changes in RIA best express the context and specificity of the imprinted memory (Chapter 4). Combining classical neuroethology, molecular genetics, and functional imaging, I have mapped distinct groups of neurons required for the formation and retrieval of an imprinted memory, defined neuromodulation that enables this critical period learning (tyramine and SER-2), and identified neuronal activity changes associated with memory. These findings provide insight into neuronal substrates of different forms of learning and memory, and lay a foundation for further understanding of early plasticity.

ACKNOWLEDGEMENTS

Graduate school and my mid 20s were a time with rapid scientific and personal growth. I am grateful to have spent this time at Rockefeller with this lovely crowd. First of all, I want to thank my advisor Cori for her encyclopedic knowledge, scientific creativity, and her great leadership. Coming to Rockefeller with organic chemistry training, I have learned every bit of neuroscience that I know from Cori and the team she led. I am forever indebted to her for all the scientific guidance, career advice, and emotional support.

I want to thank my dissertation committee members, Marc Tessier-Lavigne, Shai Shaham and Vanessa Ruta, for helpful advice and encouragement along five years; my external examiner Bence Ölveczky for traveling here from Boston to share with us his insights. Yun Zhang pioneered the study of the adult associative learning, which is the basis of my entire thesis; she also has been an important mentor to me.

Navin Pokala is the Daedalus in the lab – he developed various genetic tools to monitor and manipulate neuronal activities, which made many of my experiments possible. I miss his scientific generosity and collaborative energy. Sara Abrahamsson designed the multi-focal microscope that allows my dream experiment of recording many neurons simultaneously; her charming personality makes working in a cold dark room actually fun. Anthony Santella and Zhirong Bao have helped us analyze the early multi-neuron imaging results; Phil Kidd, a brilliant physicist recently joined the lab, has been actively collaborating with us on the imaging analysis. Elias Scheer worked with me during his rotation and I love his creativity and energy.

In the past five years, I am indebt to my baymates Steve Flavell and Margaret Ebert for scientific advice and discussions almost on a daily basis. Andrew Gordus and Sagi Levy are savvy quantitatively and have taught me lots of math and statistics. Dirk Albrecht, who kindly mentored me during rotation and introduced me to the world of *C. elegans*. Christine Cho, working on another associative learning behavior in the lab, has been generously sharing reagents and ideas. Josh Greene, an incredible biologist and a dear friend, joined the lab together with me and have been supportive scientifically and personally along the way. May Dobosiewicz, Donovan Ventimiglia, Alejandro Lopez, Meghan Lockard, Johannes Larsch, and Tapan Maniar: it is my pleasure to work with such a bright, kind, and fun group. I also want to thank the staff team for taking good care of us: Holly Hunnicutt, Priscilla Kong, Hernan Jaramillo, Manoush Ardzivian. Our lab pet, the bearded dragon Puff, has been a shiny example of how to live in my stressful times.

Outside of the Bargmann lab, I have received lots of help from Michael Hendricks on the RIA neuronal imaging experiments; Marc Tessier-Lavigne, Cynthia Duggan, Elaine Fuchs and Ya-Chieh Hsu for mentoring me in first-year rotations; Matt Meselson for giving me the privilege to be his teaching assistant during his time at Rockefeller and showing me the coexistence of scientific rigor and elegance of humanity.

Many thanks go to the Dean's office for all the support, as well as the HHMI international predoctoral fellowship for the funding and meeting opportunities.

My very good friends and classmates, Sasa Jereb, Emily Dennis, Yi-Hsueh Lu, Tamara Ouspenskaia, Wen Jiang, Michelle Siao, and Steven Serene for help with my thesis project and fellowship interviews. My friends outside of Rockefeller, Connie Kang,

Kim Dietz, Helen Hou, Xiaolei Gu, Uri Bram, and Herbert Wu for all the fun time and fashion advice. My talented friend and illustrator Janny Ji for making the artwork.

Most importantly, I want to thank my family for their unconditional love and support. 我衷心感谢我的父亲母亲多年来始终鼓励我追求自己想要的东西，成为我想要成为的人。他们的善良，趣味和坚韧永远是我学习的榜样。

In my late teen, I read a short story titled *Aleph* by Jorge Borges – *Aleph* is a point in space that contains all the points, a concentrated universe, and a miniature of the complex world without distortions. I was then in China, reading the Chinese translation, and probably too young to read Borges. Little did I know that ten years later, I would be living in New York City, speaking English mostly everyday, and still too young to understand Borges to the extent that I would like to (only the last part remains the same). And I have the luck to behold the *Aleph* of neuroscience.

TABLE OF CONTENTS

LIST OF FIGURES

LIST OF TABLES

CHAPTER 1:

Introduction

Learning, a general feature of the nervous system, allows animals to incorporate environmental information into behavioral strategies for optimal fitness. Although learning can occur at any stage of life, early memories are often the most influential and long lasting. One of the most evocative examples of early learning is imprinting, which causes a profound if not permanent modification of animal behavior resulting from a brief sensory experience at a specific time (Scott, 1962). Imprinting was first described in newly hatched birds such as chicks or geese, which form a life-long attachment to the first moving object they see (Lorenz, 1935). Following these classical neuroethological studies, imprinting has been reported in a variety of animals, and particularly in olfactory and gustatory behaviors (Hudson, 1993).

In the early stages of life, the nervous system goes through tremendous expansion and cellular growth, as well as cell death and axonal pruning (Lichtman and Balice-Gordon, 1990; Lichtman and Colman, 2000; Sanes and Lichtman, 1999). One hypothesis is that, imprinting in the critical period might modulate neural wiring or synaptic strength using these developmental processes (Hensch, 2005). However, little is known about the neural basis of imprinting, and the following questions still remain: what are the sites of formation and retrieval of an imprinted memory? What are the similarities and differences between imprinted memory and memories that are formed later in life? What is changed in neural circuits in early learning? How similar is such learning in different species?

In this chapter, I will discuss classical neuroethological studies showing how early experience has a long-term impact on animal behaviors; and describe examples of

associative learning behavior in animals, with a particular focus on the nematode *C. elegans*.

Konrad Lorenz: father of ethology and "mother of foster birds"

Imprinting was first described by the Austrian biologist Konrad Lorenz in the 1960s. By studying the instinctive behaviors of greylag geese, Lorenz made the insight that geese form strong bonds with the first moving object they see after hatching, without any reward or punishment association (Lorenz, 1979). This object is usually the mother goose, but she could be replaced by a toy, another animal, or Lorenz himself. Strikingly, geese that imprinted on Lorenz not only followed him everywhere, but also formed a long-term emotional attachment to him or other humans, and had no interest in socializing or copulating with other geese (Lorenz, 1935).

What is the neural substrate allowing such a strong memory? Visual imprinting of chicks has been studied in the laboratory using functional neuronal imaging. Presenting an image of a blue dot to a newly hatched chick is sufficient to drive approach behavior to this trained image, the memory of which lasts until adulthood (Nakamori et al., 2013). fMRI recordings show that activity in several parts of the chicks' brain associated with the establishment of this image imprinting, including the visual wulst (analogous to the visual cortex in mammals) and intermediate medial mesopallium (analogous to mammalian association cortex). After the attachment is formed, the imprinted object can elicit strong responses in brain areas including the hypopallium densocellulare and

intermediate medial mesopallium, a process dependent on the neurotransmitter glutamate (Nakamori et al., 2013). The detailed mechanisms of this phenomenon remain unknown.

Imprinting behaviors in other animals

Emotional bonding of geese is not the only example of imprinting. Attachment learning is present in many species, from rodents to non-human primates. In rats, infant attachment is mainly achieved through recognition of maternal odors (Leon, 1992). This early odor imprinting is enabled by the release of the neurotransmitter norepinephrine from a brain region called the locus coeruleus (LC), which modulates neural activity in the olfactory bulb and piriform cortex (Landers and Sullivan, 2012).

Similarly, in juvenile zebrafish, olfactory imprinting occurring during a 24-hour time window on post-fertilization day 6 profoundly affects kinship recognition. Larvae that were exposed to odors of their kin either before or after this critical time window fail to recognize the kin (Gerlach et al., 2008). However, exposure to non-kin odors during the critical period is not sufficient to produce kin-like recognition behavior; this represents a limitation of learning flexibility, suggesting that imprinted kin recognition may require extra matchings. One possible reason for such a limitation is that imprinting could require a hardwired ligand-receptor matching that is only present in kins, such that exposure to non-kin odor ligands would not match the receptor, hence the failure to induce imprinting.

Early experiences of smell or taste can lead to long-term and sometimes irreversible changes in animals' behavioral preferences. Young Pacific salmon are known

for their seasonal homing to natal stream for reproduction, a process that relies primarily on olfactory memories (Nevitt et al., 1994; Semke et al., 1995). Juvenile coho salmon that were exposed to the chemical morpholine, and then released into Lake Michigan, migrate to a stream supplemented with morpholine, but not to streams with other chemicals, suggesting homing to olfactory cues (Hasler and Cooper, 1976; Scholz et al., 1976). Electrophysiological studies show that the formation of imprinted memory in salmon correlates with a change in responses of olfactory receptor neurons (ORN) to the imprinted chemical, and therefore that the memory could reside in the sensory cilia (Nevitt et al., 1994). Odor receptor activation in fish can lead to intracellular cAMP and cGMP signaling (Breer et al., 1990; Nakamura and Gold, 1987); compared to naïve adults, imprinted salmon have increased cilia guanylyl cyclase activity to the chemical that they experienced as juveniles, suggesting cGMP modulates ORN sensitivity in olfactory imprinting (Dittman et al., 1997).

Another aspect of imprinting is that early experience can profoundly alter animals' choice of food. Juvenile Sepia cuttlefish prefer prey that they have seen early in life, and this visual experience has a profound effect on subsequent prey choice, even without ingestion and nutritional reward (Darmaillacq et al., 2006). Thus imprinting of food choices may have specialized properties that go beyond classical reward-association paradigm, and may or may not involve different neural circuits.

Nature or nurture? A molecular development example

Imprinting was first introduced by Lorenz as an instinctive behavior, i.e. a complex behavioral sequence that is innately wired, not subjected to environmental influence, and can be elicited "without a learning experience" (Vicedo, 2009). However, during the course of development, animals are never fully deprived of environmental input, and certain "innate traits" may actually be the consequence of environmental influence (Lehrman, 1970). Essentially, the capacity of geese to imprint on humans hints that their critical period offers a unique chance to shape the animals' behavior, to form attachments, and even to override the seemingly "innate" sequences of behavior, such as the formation of attachment with other geese.

The neurodevelopment of vision serves as an example of how the interplay of external environment and innate programs shape neural system function. In the visual system, different types of neurons form connections with one another in a highly specialized manner, following innate mechanisms of neurodevelopment. For example, kitten retinal ganglion cells relay information to the lateral geniculate nucleus (LGN), which projects to visual cortex. During the first months after birth, while these connections are weak and susceptible to external input, visual deprivation through the closure of one eye can lead to irreversible weakening of this eye's input representation in the brain, reflecting a decreased number of visual cortical cells that can be activated by stimuli from the previously deprived eye (Hubel and Wiesel, 1970; Wiesel and Hubel, 1963). In addition, LGN cell death is increased in layers that receive input from the deprived eye. Monocular tetrodotoxin injection creates imbalanced activities of the two eyes, in the absence of vision, and is sufficient to shift ocular dominance in visual cortex

(Chapman et al., 1986). Collectively, these physiological results elucidate a restricted period of active competition between eyes to establish cortical connection for long-term function, the process of which is subject to early activity and environmental modulation.

Activity-dependent developmental refinement is a feature of many circuits in the central nervous system (Kaas et al., 1983; Lichtman and Colman, 2000). In less extreme and non-pathological cases, different environmental inputs during the postnatal critical period can help shape brain structure and define the innate representation of the external world. Freudian theory argues for the existence of a superego, which dictates our social manners and identities within relationships; crucially, it is established during early childhood. This concept obviously fails to identify the physical brain correlates of the superego and how the superego operates to modify human behaviors. But to what extent might Freud be correct? How small a nervous system can incorporate empirical experience gained during early development into long-term behavioral memories?

How long can such memories last? In my thesis, I will discuss the molecular mechanisms and neural circuits for early plasticity in the compact nervous system of the nematode *Caenorhabditis elegans*.

C. elegans **as a model organism for the study of behavior**

Learning is a universal property of the nervous system. Even the nematode worm *C. elegans,* whose nervous system consists of 302 neurons (White et al., 1986), shows modification of its preferences for sensory cues such as temperature, touch, taste, and odor based on experience (Ardiel and Rankin, 2010; Colbert and Bargmann, 1995;

Kimata et al., 2012; Mori and Ohshima, 1995). Living in a complex microbial environment, *C. elegans* is capable of quickly detecting environmental cues and altering its behavioral strategies. In particular, with its chemosensory system composed of more than 30 ciliated neurons, an animal can directly or indirectly detect olfactory and gustatory stimuli from the environment and modify its response accordingly. The simplicity of the C. *elegans* nervous system and the complexity of its behavioral repertoire allow us to examine how a behavior is initiated and modified by the external world.

Experience-dependent plasticity in *C. elegans*

The most extensively characterized form of *C. elegans* plasticity is habituation of the tap-withdrawal response (Rankin et al., 1990). Animals respond to a mechanical tapping by a reversal to move backward. Repetitive tapping leads to decreases in both the reversal amplitude and frequency, hence tap-withdrawal habituation. Similar to the spaced odor conditioning that persists long-term odor memory, animals that receive blocks of tapping spaced by 1-min intervals can maintain the habituation memory for 24 hours (Beck and Rankin, 1995; Rose et al., 2002). Glutamatergic signaling and the vesicular glutamate transporter EAT-4 are required for both short- and long-term habituation (Rankin and Wicks, 2000; Rose et al., 2003), and the expression of a AMPAR glutamate receptor GLR-1 is regulated by and required for only the long-term habituation (Rose et al., 2003; Rose and Rankin, 2006).

C. elegans also shows plasticity in its olfactory behavior. As in other animals, learning and memory in *C. elegans* depend on the training regimen. For example, pairing an odor with bacterial food in a single training session results in a short-term increase in preference for that odor, an effect called odor enhancement (Torayama et al., 2007). A single massed training gives rise to a memory that lasts a few hours, while repeated training with spaced odor-food parings can induce an enduring memory that lasts for 24 hours (Kauffman et al., 2010). Pairing starvation with the same odor can lead to decreased odor preference, known as odor adaptation, suggesting bidirectional modulation of chemotaxis by pairing with either the presence or absence of food (Colbert and Bargmann, 1995). Many different odors have been shown to induce either enhancement, adaptation, or both, including butanone (detected by a sensory neuron AWCon), 2-nonanone (detected by AWB), and diacetyl (detected by AWA), reflecting the flexibility to modify chemotaxis using various stimuli and sensory neurons (Kimura et al., 2010; Morrison and van der Kooy, 2001; Stetak et al., 2009).

Although sensory neurons are crucial for experience-dependent changes in chemotaxis, the phenomenon engages more than just the sensory system. LET-60, a RAS MAP kinase, is required for butanone adaptation through its functioning in first-layer AIY interneurons (Hirotsu and Iino, 2005). AWC sensory neurons express the peptide NLP-1, which signals to AIA interneurons through the peptide receptor NPR-11; AIA interneurons can then send ascending modulation to AWC through another peptide, INS-1 (Chalasani et al., 2010). This peptide-to-peptide neuromodulatory feedback engages and alters calcium dynamics in both sensory neurons and interneurons.

C. elegans adults show enhanced attraction to chemical odors experienced during the first larval stage, a process defined as positive odor imprinting. Odor imprinting requires the orphan G protein-coupled receptor SRA-11 in the AIY interneurons (Remy and Hobert, 2005). The progeny of imprinted animals also show enhanced attraction to the odor, but the molecular mechanisms underlying this effect are not known (Remy, 2010).

Experience-dependent plasticity of dietary choice in *C. elegans*

Animals' survival and fitness depends on their ability to distinguish between nutritious food sources and pathogenic ones that can infect and kill them (Meisel et al., 2014). A substantial component of the pathogen defense in *C. elegans* is behavioral. It is hypothesized that a surveillance system is deployed to detect infections in intestinal and hypodermal tissues and relay the damage signal to the nervous system, which will in turn induce an avoidance response. This does not require an actual pathogen, but only tissue damage. For example, RNA interference (RNAi) knockdown of essential genes in non-neuronal tissues is sufficient to lead to animals' avoidance of bacterial lawn, a process that depends on serotonin signaling (Melo and Ruvkun, 2012).

As an immediate defense, animal can leave a pathogen lawn within hours after infection, in part by modulation of sensory preference by the Toll signaling receptor TOL-1 in BAG sensory neurons (Pujol et al., 2001; Brandt and Ringstad, 2015). *Pseudomonas aeruginosa* virulence factors and the secondary metabolites (phenazine and pyochelin) can be detected by ASJ sensory neurons, which rapidly activate the

transcription of the TGFβ analog DAF-7 within 6 minutes of infection (Meisel et al., 2014). Through the TGFβ receptor DAF-1, these chemicals modulate the RIM interneurons, and subsequently regulate aerotaxis and lawn avoidance (Meisel et al., 2014). The equivalent sequence of other pathogenic infections are mostly not known, but avoidance of pathogen *Serratia marcescens* can be modulated through detection of the bacterial metabolite serrawettin W2 by AWB sensory neurons (Pradel et al., 2007).

On a longer time scale, after six hours of exposure to a bacterial pathogen, *C. elegans* learns to avoid that bacterial odor through associative learning to prevent future encounters. Such behavior resembles conditioned taste aversion, a widespread form of animal learning (Zhang et al., 2005). This associative aversive memory lasts between 12 and 24 hours. Neurons required for naïve bacterial preference as well as learned pathogen aversion have been mapped by laser killing experiments (Ha et al., 2010). Molecules required for adult pathogen aversive learning have been identified in genetic studies and mapped back to the following circuit: first, the neurotransmitter serotonin must be made by ADF sensory neurons; second, its receptor MOD-1 is required in either AIY or AIZ interneurons (Zhang et al., 2005); third, the TGFβ homolog DBL-1, generated by the command interneurons AVA, regulates learning (Zhang and Zhang, 2012); and fourth, two antagonizing neuropeptide pathways – insulin peptide INS-6 from ASI sensory neurons and INS-7 from URX sensory neurons – allow learning by modulating the RIA interneurons through the insulin receptor DAF-2 (Chen et al., 2013). Response to bacterial odors in AWB and AWC sensory neurons, which detect volatile odors, appear to be unchanged by aversive learning (Ha et al., 2010). And the neural correlates of the adult memory remain unknown. It is hypothesized that pathogen infection can modulate

interneuron properties, such as RIA's response to pathogen odors, which when paired with serotonin release causes animals to avoid the experienced bacteria (Ha et al., 2010).

Animals also make food choice among non-pathogens depending on their nutritional value. For example, they are more likely to remain (dwell) on areas with high quality food (HB101), and are more likely to roam from and ultimately leave areas with low quality food (OP50) (Shtonda and Avery, 2006). Interestingly, newly hatched larvae that have experienced high quality food for the first 3 hours of life will establish a higher tendency to leave a low quality lawn later, a memory sustained for ~24 hours. This medium-term dietary choice is defined by past food experience, and the relatively long-lasting change in preference may relate to the early formation of the memory during the L1 developmental stage (Shtonda and Avery, 2006).

The first larval stage is critical to the life cycle of *C. elegans*. In an environment with high population density and limited food, L1 animals can commit to an alternative developmental state called "dauer" to survive stressful conditions (Cassada and Russell, 1975). The dauer is morphologically and behaviorally distinct from other larval stages, with a significant amount of neuronal remodeling. For example, IL2 neurons undergo a tremendous arborization in the dauer state (Schroeder et al., 2013). This cellular remodeling is essential for the nictation behavior, through which dauers can lift up their bodies and increase survival through dispersal (Lee et al., 2012).

The goal of my graduate thesis is to extend our understanding of early plasticity using *C. elegans* as a model organism. I found that exposing newly-hatched larvae to the pathogenic bacterium *Pseudomonas aeruginosa* PA14 can generate an aversive memory of bacterial odors that is sustained into adulthood (4 days). This critical period dependent

associative learning behavior is defined as aversive olfactory imprinting. By contrast, training of adults results in a medium-term memory that lasts for less than a day. Is this learning specific to a particular pathogen, or can animals learn to avoid different kinds of bacteria? Is there a sensitive period in which the animals can learn more efficiently than in other developmental periods, like imprinting in other animal species? In the first half of Chapter 2, I characterize aversive imprinting behavior in C. *elegans* and show that it is a form of associative learning with a critical period in the first larval stage.

The nervous system of the *C. elegans* adult hermaphrodite is composed of 302 neurons, the synaptic connections of which have been fully mapped. In the second half of Chapter 2, taking advantage of the connectome and other powerful genetic tools for *C. elegans*, I examine the neuronal requirements of imprinting by genetic silencing of individual candidate neurons. It is revealed that two distinct circuits are required for memory formation and retrieval.

In Chapter 3, I identify molecules that enable learning and the bridging of memory formation and retrieval circuits, and define molecular signaling mechanisms between these neurons.

A basic but formidable question is how long-term memory is stored in the nervous system, and how detailed information (such as sensory specificity) is encoded. In Chapter 4, I use functional calcium imaging approach to examine the responses of relevant neurons to bacterial stimuli, and ask 1) whether the imprinting-related interneurons acquire any change of properties after learning; 2) how sensory neurons are involved in bacterial recognition and in the learning process.

Finally, in Chapter 5, I will conclude the thesis, present a few possible experiments as future directions for further investigation, and propose conceptual hypotheses that can be tested in the future.

Inspired by classical neuroethology and modern genetics, my work defines the molecular and neural circuit requirements for the ancient behavior of imprinting through a reductionistic approach. The logic and insights gained from these circuits may provide a foundation for further understanding of early learning in other animals.

CHAPTER 2:

Behavioral and circuit characterization of aversive olfactory imprinting in *C. elegans*

INTRODUCTION

Aversive learning and fear conditioning are important behavioral strategies for animals to avoid life-threatening environments. The classical learning paradigm used in the fruit fly *Drosophila* is to pair an aversive unconditioned stimulus, e.g. electrical shock, with a neutral conditioned stimulus, e.g. a chemical odorant that elicits a sensory response without any value. If learning happens, animals change their preferences to avoid the conditioned stimulus associated with the electrical shock. Similarly, mammals can learn to associate an environmental context with an aversive cue such as foot shock in fear conditioning, so that the context alone later can induce freezing or avoidance behavior (Ehrlich et al., 2009). Depending on the training regimen, the memory can last from hours to days.

The neural circuits for learning and memory are studied in many animals. *C. elegans* provides opportunities for high-resolution answers because of its compact nervous system. Is learning in larvae different from learning in adults? How many forms of learning and memory can be encoded by 302 neurons? How do animals alter their behavioral strategies to change odor preferences? With the known connectome as well as powerful genetic tools to test each neuron's contribution, can we dissect the circuit mechanisms of learning and memory?

In this chapter, I describe how pathogen training during the first larval stage results in a long-lasting aversive memory that is maintained into the adult stage. I use genetic silencing of candidate neurons to ask which are required for imprinting. I then use a reversible chemical genetic neuronal silencing tool to determine their timing of action, and characterize two distinct groups of neurons required for the formation and retrieval of

this privileged aversive memory. I also show how these neurons contribute to behavioral strategies that enable animals to avoid the imprinted pathogen in an olfactory chemotaxis environment.

RESULTS

Early pathogen training of *C. elegans* induces long-term aversion

Learned pathogen aversion can be induced by exposing adult *C. elegans* to pathogenic bacteria for 4-24 hours, or by cultivating animals with both pathogenic and non-pathogenic bacteria (Chen et al., 2013; Zhang et al., 2005). In either case, the aversive memory lasts between 12 and 24 hours. I modified the learning assay by hatching *C. elegans* eggs on a uniform lawn of the pathogenic bacterium *Pseudomonas aeruginosa* PA14 (Figure 2.1A) and forcing exposure to the pathogen for 12 hours during the first larval (L1) stage. This treatment establishes an intestinal infection but does not kill the animals (Tan et al., 1999). Antibiotic washes were then performed to clear the infection (Figure 2.1B), and animals were grown on non-pathogenic *Escherichia coli* OP50 until adulthood.

When tested in an olfactory choice assay between PA14 and OP50, animals trained as L1 larvae were significantly more likely to migrate away from PA14 than naïve animals (Figure 2.1C). This shift in preference, measured days after training as a learning index (naïve choice index – trained choice index), resembled the shift in preference of adult animals immediately after training with PA14 (Figure 2.1C). No shift in preference was observed in animals that had been exposed to non-pathogenic *P. aeruginosa*

PA*50E12 (Rahme et al., 1997) or starved for 12 hours as L1 larvae, suggesting that pathogenic infection is required for learning to occur (Figure 2.1D). The progeny of trained animals returned to the naïve preference (Figure 2.1D).

To ask whether this long-lasting aversive memory occurs during a critical period, I exposed animals to PA14 at different developmental stages and tested olfactory choice in mature (second-day) adults. Only exposure in the L1 stage for the full 12 hours resulted in stable learned aversion (Figure 2.2A); 6 hours of treatment either early or late in L1 did not suffice. In agreement with previous work, animals trained with PA14 as first-day adults did not show learned aversion 24 hours later, nor did animals trained as L2, L3, or L4 larvae. This long-lasting behavioral response will be called "imprinted aversion" to emphasize its early formation, long duration, and the existence of an apparent critical period in the L1 stage.

The pathogenicity of PA14 is in part mediated by the toxic translational inhibitor exotoxin A (ToxA) (McEwan et al., 2012; Melo and Ruvkun, 2012). Animals imprinted on an *E. coli* strain expressing ToxA avoided the ToxA strain as adults in an olfactory choice assay with OP50, showing that imprinted aversion can be induced by a second strain with a distinct odor (Figure 2.2B). ToxA-imprinted animals did not avoid PA14, and conversely, PA14-imprinted animals did not avoid ToxA (Figure 2.2B). Thus animals selectively avoid the bacterial odors that they experienced during pathogenic infection, a defining property of associative learning.

Imprinted adults appeared healthy as naïve adults, suggesting that the altered behavior is not a consequence of sustained damage from the bacterial infection or early starvation. Their growth, locomotion patterns, and abilities to perform behavioral tasks

such as chemotaxis and local search were similar to those of naïve animals, although they had subtle changes in quantitative behavioral assays. These included an overall reduction in spontaneous pirouette rates off food, a reduced suppression of basal reorientations by AIY during local search, and a reduced ability of AIB to increase pirouettes upon optogenetic stimulation (Figure 2.3A-C). These results suggest that imprinting induces a subtle but long-lasting reorganization of neural circuits.

Neural circuits: both sensory neurons and interneurons are required for imprinting

Olfactory chemotaxis in *C. elegans* is initiated by sensory neurons that converge on common interneurons including AIB and AIY, which synapse with each other and with downstream neurons including RIM and RIA (White et al., 1986) (Figure 2.4A). Adult learned pathogen aversion requires either AIB or AIY, both RIA and RIM, and several sensory neurons including AWB, AWC, and the serotoninergic neuron ADF (Ha et al., 2010) (Figure 2.4A). To ask whether the same neurons participate in imprinted aversion, I examined strains expressing the tetanus toxin light chain (TeTx), the gain-of-function potassium channel UNC-103(gf), or a cytotoxic mouse caspase from cell-type selective promoters (Petersen et al., 2004; Yoshida et al., 2012) . These experiments indicated that AIB, AIY, RIA and RIM were all required for imprinted aversion (Figure 2.4B). Since our behavioral choice assays were different from those in prior circuit work, I confirmed that the AIB::TeTx strain was proficient in adult learning but impaired in imprinted aversion in this assay, whereas RIM::TeTx was impaired in both forms of learning (Figure 2.4B). Among sensory neurons, AWB and at least one of AWC and ASEL were required both for imprinted aversion as for adult learned aversion (Ha et al.,

2010) (Figure 2.4B). Thus imprinted aversion and adult learned aversion have similar but not identical neuronal requirements.

It should be noted that these experiments have potential caveats. Cells were subjected to different genetic ablation methods, which may lead to different degrees of perturbation in behavioral assays. Transgenes often have leaky or transient expression in other tissues during development, which may not be known. As a first pass, imprinting seemingly involves many sensory neurons and interneurons, whose importance can be confirmed with alternative reagents.

Distinct circuits for memory formation and retrieval

Neurons expressing toxic transgenes or subjected to laser ablations are inactive throughout life. To distinguish the contributions of interneurons in formation and retrieval of the imprinted memory, selected neurons were acutely silenced by expressing the *Drosophila* histamine-gated chloride channel HisCl1 (Pokala et al., 2014) (Figure 2.5A-B). *C. elegans* does not use histamine as an endogenous transmitter, but absorbs exogenous histamine to rapidly and reversibly silence neurons expressing a HisCl1 transgene. Silencing either AIB or RIM during the L1 learning period abolished imprinted aversion in the adult, suggesting that AIB and RIM are required for formation of the imprinted memory (Figure 2.5C). Silencing AIB or RIM neurons in adults during the olfactory choice assay spared imprinted aversion, indicating that AIB and RIM are dispensable for memory retrieval (Figure 2.5C). Conversely, imprinted aversion was robust to silencing AIY or RIA neurons during the L1 learning period, but impaired by silencing AIY or RIA neurons during the olfactory choice assay in adults (Figure 2.5D).

These results identify distinct neurons required during learning and retrieval stages of imprinted aversion.

Changes in locomotion and chemotaxis strategies after imprinting

The behavioral strategies that give rise to imprinted aversion were examined through a quantitative analysis of chemotaxis parameters. *C. elegans* approaches attractive chemicals using a biased random walk, in which the frequency of high-angle turns ("pirouettes") increases when an animal moves down the gradient and decreases when it moves up the gradient (Figure 2.6A) (Pierce-Shimomura et al., 1999). The turning bias is reversed in a gradient of repellent (Yamazoe-Umemoto et al., 2015). I found that naïve animals turned less when approaching PA14 and turned more when leaving PA14, as expected for biased random walk attraction, whereas PA14-trained animals expressed a reversed pirouette bias appropriate to learned aversion (Figure 2.6B). This effect depended on the learned association, as animals imprinted on PA14 did not change their pirouette bias in response to the non-pathogenic bacteria OP50 (Figure 2.6B) or the untrained toxic bacterium ToxA (Figure 2.6C).

Silencing the AIY memory retrieval neurons with HisCl1 during the olfactory choice assay eliminated the PA14 pirouette bias in both naïve and imprinted animals (Figure 2.6D). In addition, imprinting changed the contributions of AIY to basal pirouette regulation, resulting in a stronger AIY effect in chemotaxis assays and a weaker AIY effect during an undirected local search (Figure 2.3A-B). These results indicate that AIY neurons have altered functions after imprinting, which include an acute role in generating the reversed pirouette bias in imprinted aversion.

DISCUSSION

Aversive imprinting: an early-formed long-lasting memory

C. elegans that are exposed to pathogenic bacteria early in life demonstrate aversion to those bacterial odors as adults. Although it has an early critical period and long duration, this imprinted aversion differs from classical olfactory imprinting in its valence. Classical imprinting behaviors are mostly positive bonding, and the aversive olfactory imprinting forms negative avoidance memory. There may be two different kinds of imprinting that both describe behaviors that are markedly affected by experience that occurs within an early developmental stage. On the one hand, imprinting can refer to behavioral modifications that *must* be subjected to a stimulus in a particular time window to have any influence at all, e.g. geese will not form any imprinted bonds once critical periods close; on the other hand, imprinting can also refer to behavioral modifications that can be *most profoundly* influenced by a stimulus encountered during a particular time, e.g. aversive pathogen learning occurs in both larvae and adults, but only larvae can form a long-term memory. Scott uses "critical period" and "optimal period" to discriminate the two scenarios (Scott, 1962). The first kind of imprinting mainly involves positive valence; the second kind of imprinting can be general learning, which can use both positive and negative valences to represent environments that can be either favorable or life-threatening.

Classical positive imprinting and the *C. elegans* aversive olfactory imprinting may deploy different underlying mechanisms. For example, olfactory imprinting in

salmon uses cGMP-based signaling mechanisms, which involve a small subset of olfactory neurons and cause altered odor responses in the olfactory cilia (Dittman et al., 1997; Lema and Nevitt, 2004). In comparison, aversive imprinting in *C. elegans* engages both interneurons and sensory neurons. Even within *C. elegans*, positive and negative imprinting are distinct. *C. elegans* positive imprinting require *sra-11* and is transmitted to the progeny of imprinted animals (Remy, 2010; Remy and Hobert, 2005); but aversive imprinting does not require *sra-11* and is not transgenerational.

In the most conservative terms, imprinted aversion in *C. elegans* may be described as a form of optimal learning occurs during early development that results in a long-term memory. Little is known about general mechanisms of classical imprinting in other species, so as more is learned about the two kinds of imprinting, the mechanisms may diverge or converge.

A neural circuit for imprinted aversion

The circuit requirements for imprinted aversion overlap partly with other forms of olfactory learning such as adult learned aversion and long-term appetitive memory (Figure 2.4A, 4.9, Table 1). The AWB and AWC sensory neurons that detect volatile odorants and regulate chemotaxis are required for both forms of learning. Among the four imprinting-relevant interneurons, RIM and RIA are also required for adult learning, suggesting overlapping circuit requirements. Imprinting has a stronger reliance on the AIB and AIY interneurons, which are individually dispensable for adult learned aversion

(Ha et al., 2010) (Table 1). AIB and AIY are immediate targets for sensory neurons, suggesting that imprinting engages early steps of sensory processing.

The formation and retrieval of the imprinted memory depended on distinct groups of interneurons in a sensory processing circuit (Figure 4.9). These neurons receive input from many sensory neurons that detect both pathogenic and nutritious bacteria. The AWC and AWB neurons, which are required for imprinted aversion and adult learned aversion, detect both *E. coli*- and PA14-conditioned media (Ha et al., 2010). The ASJ neurons detect PA14 secondary metabolites associated with virulence (Meisel et al., 2014), and also detect *E. coli* conditioned media, as is the case with numerous other sensory neurons (Zaslaver et al., 2015). The collective activity of multiple sensory neurons allows discrimination between bacterial odors, providing a substrate for olfactory learning and memory (Harris et al., 2014). The specific role of sensory neurons in imprinting remain elusive. Are they only passively involved in the odor detection, or are they actively engaged in the synthesis of memory, or both? These questions will be further discussed in Chapter 4.

The AIB and RIM neurons are necessary during learning, but dispensable for memory retrieval in the adult. The AIY and RIA neurons, which were required only for memory retrieval, are sites at which the imprinted memory may be expressed. The separation of neurons in learning and memory is also observed in aversive olfactory learning in the fruit fly *Drosophila*. Behavior genetics studies have identified a brain region, the mushroom body, as a key center for *Drosophila* associative learning (Heisenberg, 2003; Keene and Waddell, 2007). The structural architecture of the mushroom body has been extensively mapped: ~2000 Kenyon cells in the mushroom

body, representing sensory stimuli, converge onto 34 mushroom body output neurons that can be categorized into 21 distinct types which are innervated by 8 classes of dopaminergic neurons (Aso et al., 2014; Tanaka et al., 2008). The dopaminergic neurons encode aversive or appetitive stimuli, and are required for only learning but not for memory retrieval (Krashes et al., 2007; Bouzaiane et al., 2015; Owald et al., 2015; Sejourne et al., 2011).

Variability and learning

The AIB and RIM neurons are acutely involved in sensorimotor behaviors, so it was unexpected that they were required only during learning. AIB is a synaptic target of many sensory neurons, and can transmit information from sensory neurons to downstream neurons that drive reversal responses and other reorientation behaviors (Gray et al., 2005). AIB and RIM are also elements of a coupled network of neurons that includes the backward command neuron AVA. Functional calcium imaging of freely moving animals indicates that AIB, RIM and AVA are active during most or all reversals, and less active during forward locomotion (Gordus et al., 2015). In this context, each neuron can be considered as receiving inputs (e.g. sensory stimulation by odorants), sending outputs (reversals and omega turns), and retaining network membership (part of the global reversal pattern).

The role of RIM in learning may be related to its role in generating variability in the naïve sensory responses. Odor can reliably trigger the sensory neuronal response; but the reversal/omega behavior is probabilistic, as are the odor-evoked responses of the

interneurons AIB, AVA, and RIM (Gordus et al., 2015). RIM increases the coupling of AIB to the reversal circuit, and loosens its connection to the sensory input. Effectively, this means that RIM activity causes sensory inputs to be variably transmitted to AIB and the rest of the circuit (Gordus et al., 2015). RIM releases many neurotransmitters such as glutamate and tyramine; however, it is not known which molecule encodes variability. Variability is often considered to be noise in the system, but it can be an active and adaptive element of neural circuits and behavior. For example, trial and error learning requires variation, and high variability at the beginning of training predicts better final performance in human and rat motor learning (Wu et al., 2014).

Analogies can be drawn between imprinted aversion in *C. elegans* and sensorimotor learning in songbirds during the critical period. Juvenile songs are variable, and adult songs much less so; this results from the active generation of variability by the anterior forebrain pathway in young animals, which is used to entrain a motor pathway for song generation. A young bird learns and practices its tutor song using a specialized brain region called LMAN that is not required for adult song performance (Bottjer et al., 1984). The active generation of variability by LMAN is essential for song learning in juveniles, and can be re-engaged in adulthood to permit song plasticity (Kao et al., 2005; Olveczky et al., 2005). The switch from an early learning pathway to a mature retrieval pathway in birdsong can be considered similar to the analogous switch in *C. elegans* aversive imprinting, and the requirement for variability-generating neurons at the time of learning may also be parallel. We speculate that a requirement for variability-generating neurons during memory formation phase may be a general feature for long-term sensorimotor memory.

Learning induced specific and nonspecific behavioral changes

At a behavioral level, aversive imprinting of *C. elegans* gives rise to a specific avoidance of the experienced pathogen through an altered chemotaxis strategy, i.e. imprinted animals have obtained a higher turning rate when approaching the trained bacteria PA14. This turning bias is specific to the imprinting odorant (PA14 smell) and dependent on the AIY memory retrieval neurons (Figure 2.6). Consistent with our end-point chemotaxis measurements, imprinting memory retrieval pathways deploy AIY interneurons for an altered pirouette bias to avoid pathogen.

On the other hand, circuit-behavior examinations have shown that imprinting also gives rise to subtle and nonspecific changes in locomotion patterns. Although imprinted animals are developmentally healthy and capable of performing these tasks, their AIY and AIB interneurons have become less coupled to the pirouette motor output. For example, neuronal silencing of AIY in imprinted animals is less likely to affect pirouette in local search behavior, and optogenetic activation of AIB in imprinted animals is less able to initiate pirouette (Figure 2.3).

These subtle changes of neuronal contribution to behaviors can be the byproduct of imprinted memory due to circuit network effects. *C. elegans* neurons are highly interconnected with a statistical property that is similar to mammal cortex (Varshney et al., 2011). Therefore, even if aversive imprinting only deploys and remodels a small fraction of the nervous system, the rest of the neurons in the network may be affected passively due to their dense connections with learning neurons. In particular, command

interneurons (AVA and AVB) have high centrality in both chemical and electrical synaptic networks (Varshney et al., 2011); therefore, imprinting-elicited changes in other neurons can be passively propagated to command interneurons to affect locomotion. It will be valuable to separate the imprinting-relevant changes from this ripple effect in the neural network. For example, AIB is not required for the memory retrieval stage, and therefore its change of ability in initiating turns seem unlikely to affect imprinted memory.

However, it is also plausible that these nonspecific locomotion changes may be meaningful or even essential for imprinted aversion. For example, AIY after imprinting has seemingly transformed in its sensory drive and repressed its motor output of regulating turns. The activity of AIY is required for memory retrieval, but it is not yet clear that how its input and output have been remodeled to facilitate the retrieval process. Changes in these neuronal properties will be further investigated and discussed in Chapter 4.

Figure 2.1 Aversive imprinting and adult learning in *C. elegans*

(A) Schematic illustration of bacterial choice assay, imprinting protocol, and adult pathogen training protocol.

(B) Antibiotic clearance of pathogen after L1 imprinted aversion. (B_1) Schematic illustration of the pathogenic infection evaluation assay. (B_2) Colony counts of lysate from naïve adults, adults immediately after 6-hour training with PA14, and adults trained as L1s. Each dot represents a single measurement; each bar graph represents population mean and SEM.

(C) Olfactory choice preference index of naïve, PA14-imprinted, and adult-trained animals. Each dot represents a single population assay calculated as shown; each line represents the mean value.

(D) Learning index of animals imprinted on PA14, adult-trained, imprinted on non-pathogenic PA*50E12, starved for 12 hours after hatching, and F1 offspring of PA14-imprinted animals. Boxes represent median and first and third quartiles, and whiskers represent 10^{th}-90^{th} percentiles. *n*, number of independent assays, 100-200 animals/assay. *P* values were generated by ANOVA with the Dunnett correction (*** $P < 0.001$, ** $P < 0.01$, * $P < 0.05$, ns not significant).

Figure 2.1

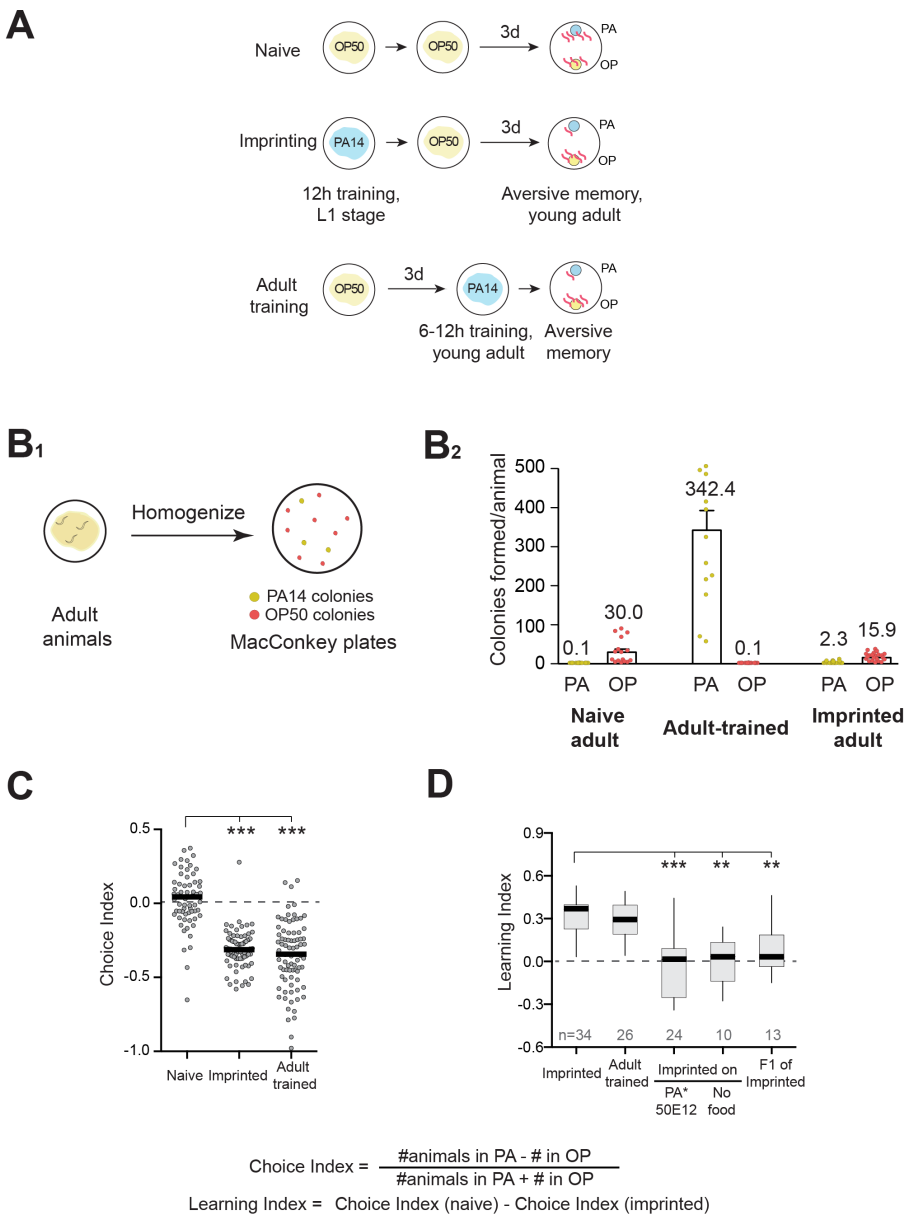

$$\text{Choice Index} = \frac{\#\text{animals in PA} - \#\text{ in OP}}{\#\text{animals in PA} + \#\text{ in OP}}$$

Learning Index = Choice Index (naive) - Choice Index (imprinted)

Figure 2.2 Temporal requirements and sensory specificity of aversive imprinting

(A) Learning index of mature (two-day old) adults after exposure to PA14 at different developmental stages.

(B) Learning index of animals imprinted either on pathogenic PA14 or on an *E. coli* BL21 strain expressing the *Pseudomonas* translational inhibitor ToxA, then tested with choices between PA14/OP50 and ToxA/OP50.

Boxes represent median and first and third quartiles, and whiskers represent 10^{th}-90^{th} percentiles. *n*, number of independent assays, 100-200 animals/assay. *P* values were generated by ANOVA with the Dunnett correction (*** $P < 0.001$, ** $P < 0.01$, * $P < 0.05$, ns not significant).

Figure 2.2

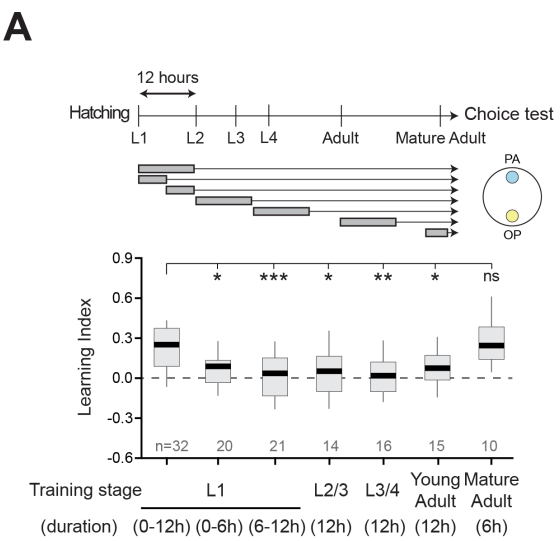
A
12 hours
Hatching
Choice test
L1
L2
L3
L4
Adult
Mature Adult
PA
OP
Learning Index
0.9
0.6
0.3
0.0
-0.3
-0.6
*
***
*
**
*
ns
n=32
20
21
14
16
15
10
Training stage
L1
L2/3
L3/4
Young Adult
Mature Adult
(duration)
(0-12h)
(0-6h)
(6-12h)
(12h)
(12h)
(12h)
(6h)

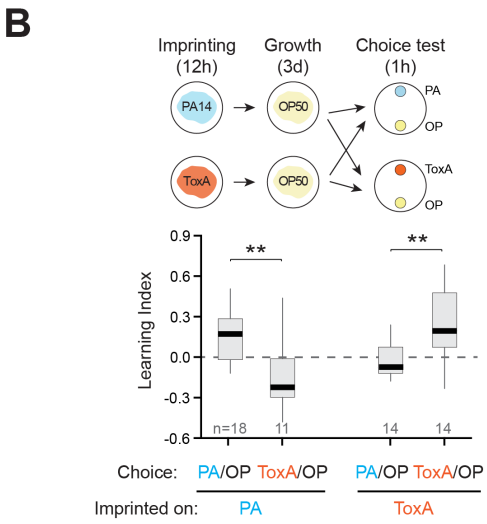
B
Imprinting (12h)
Growth (3d)
Choice test (1h)
PA14
OP50
ToxA
OP50
PA
OP
ToxA
OP
Learning Index
0.9
0.6
0.3
0.0
-0.3
-0.6
**
**
n=18
11
14
14
Choice:
PA/OP
ToxA/OP
PA/OP
ToxA/OP
Imprinted on:
PA
ToxA

Figure 2.3 Locomotion changes in imprinted animals

(A) Normal local search behavior, but a decreased contribution of AIY to pirouette frequencies after aversive imprinting. A pirouette is a reversal followed by a high-angle omega turn. (A_1) Illustration of the local search experiment (Gray et al., 2005). (A_2) Pirouette frequency off food in naïve and imprinted adults, with (green) or without (black) AIY silenced. The reorientation frequency in the absence of bacteria increased when AIY was silenced acutely with HisCl1 in naïve animals but not in imprinted animals. Shaded regions are ±SEM. Averaged from 6 movies (60-84 animals) per condition. Event frequency of the histamine treatment group was compared to the control at indicated time points; *P* values were generated by the nonparametric t-test (** $P < 0.01$, ns not significant).

(B) Imprinted animals have decreased basal pirouette frequencies during the chemotaxis choice test. (B_{1-3}) Average pirouette frequency of naïve (black) and PA14-imprinted (red) animals (B_1) navigating between PA14 and OP50 (average of 5 movies per group); (B_2) navigating between a novel bacterium ToxA and OP50 (average of 3 movies per group); (B_3) navigating between PA14 and OP50 with AIY neurons silenced with HisCl1 (average of 3 movies per group). Compared to the naïve group, animals imprinted on PA14 had a lower basal pirouette frequency, regardless of whether they were responding to PA14 or ToxA; AIY silencing eliminated this effect. In each panel, naïve and imprinted event frequencies were compared and *P* values were generated by ANOVA with Tukey correction (** $P < 0.01$, * $P < 0.05$). Bar graphs represent population mean and error bars represent ±SEM.

(C) Pirouettes induced by optogenetic activation of AIB with ChR2 are decreased after aversive imprinting. (C_1-C_2) Average frequency of (C_1) pirouette reorientations and (C_2) non-pirouette reorientations upon optogenetic activation of AIB in naïve (black) and imprinted (red) animals (grey bar, 20 s light pulse). Shaded regions are ±SEM. Averaged from 6 movies (120-150 animals) per group. The difference in event frequencies 2 sec before and 2 sec after light activation was compared between naïve and imprinted groups; *P* values were generated by two-way ANOVA (** $P < 0.01$, ns not significant).

Figure 2.3

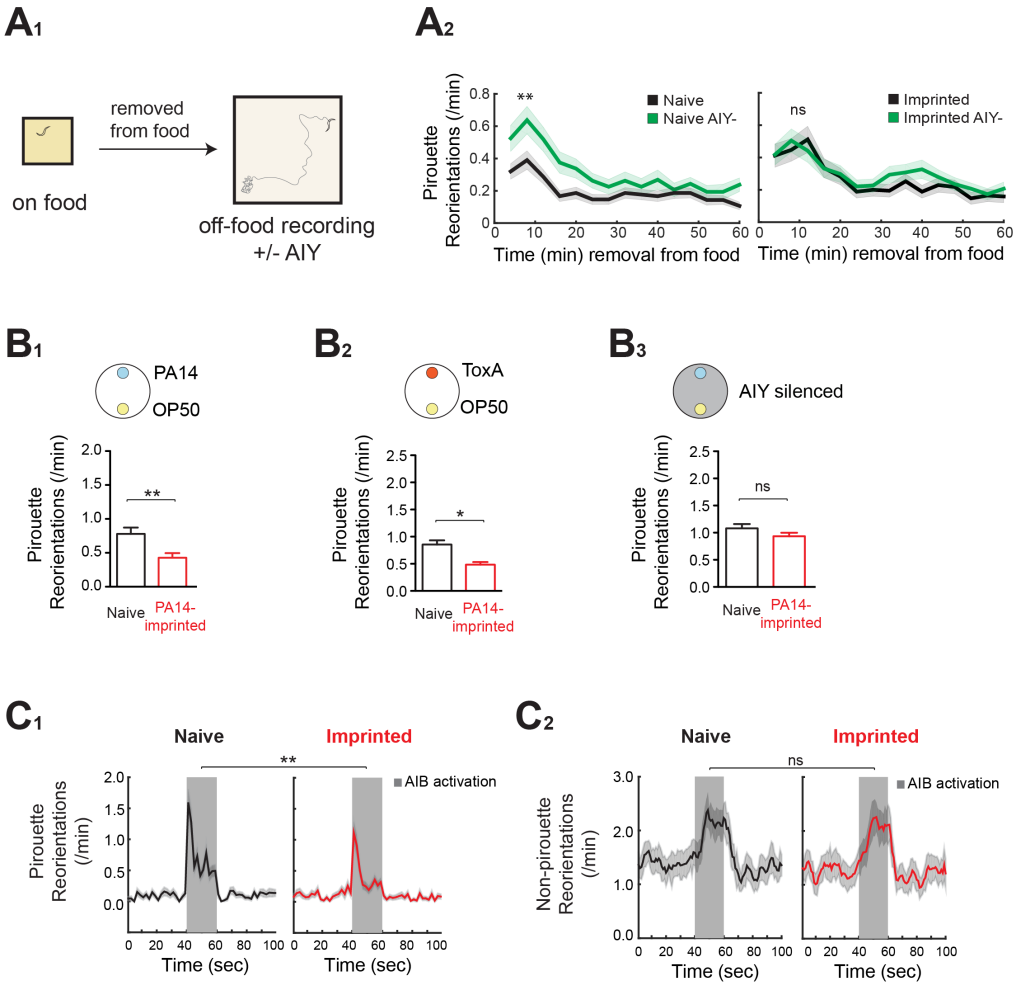
A1
removed
from food
on food
off-food recording
+/- AIY
A2
Pirouette
Reorientations (/min)
**
Naive
Naive AIY-
Time (min) removal from food
ns
Imprinted
Imprinted AIY-
Time (min) removal from food
B1
PA14
OP50
Pirouette
Reorientations (/min)
**
Naive
PA14-
imprinted
B2
ToxA
OP50
Pirouette
Reorientations (/min)
*
Naive
PA14-
imprinted
B3
AIY silenced
Pirouette
Reorientations (/min)
ns
Naive
PA14-
imprinted
C1
Naive
Imprinted
**
AIB activation
Pirouette
Reorientations
(/min)
Time (sec)
Time (sec)
C2
Naive
Imprinted
ns
AIB activation
Non-pirouette
Reorientations
(/min)
Time (sec)
Time (sec)

Figure 2.4 Adult learning circuit diagram and neuronal requirements for both forms of learning

(A) Weighted circuit diagram of adult learned pathogen aversion defined in previous studies (Chen et al., 2013; Ha et al., 2010; Zhang et al., 2005; Zhang and Zhang, 2012). Synaptic weights are based on the number of chemical synapses from www.wormweb.org. The circuit was mapped by killing neurons with a laser, flowing volatile cues from bacterial conditioned medium past individual animals suspended in buffer droplets, and recording body bends characteristic of reorientation as a preference readout. Imprinted aversion in this thesis is characterized using a plate-based population chemotaxis assay, so there may be differences between the two assays that result from odor presentation, motor readout, or behavioral states.

(B) Imprinted aversion and adult learned aversion in strains with genetic inactivation of candidate neurons. *TeTx:* tetanus toxin light chain; *unc-103(gf):* a leaky potassium channel (Petersen et al., 2004); mCasp: murine caspase (Yoshida et al., 2012). Asterisks and red bars mark genotypes and conditions with statistically significant values indicating learning. Because these are chronic manipulations, they do not have the internal controls of the HisCl1 strains in Figure 2.5; the variability here is not unusual for multicopy *C. elegans* transgenes.

Boxes represent median and first and third quartiles, and whiskers represent 10^{th}-90^{th} percentiles. *P* values were generated by Anova with Sidak correction (*** $P<0.001$, ** $P<0.01$, ns not significant). *n*, number of independent assays, 100-200 animals/assay.

Figure 2.4

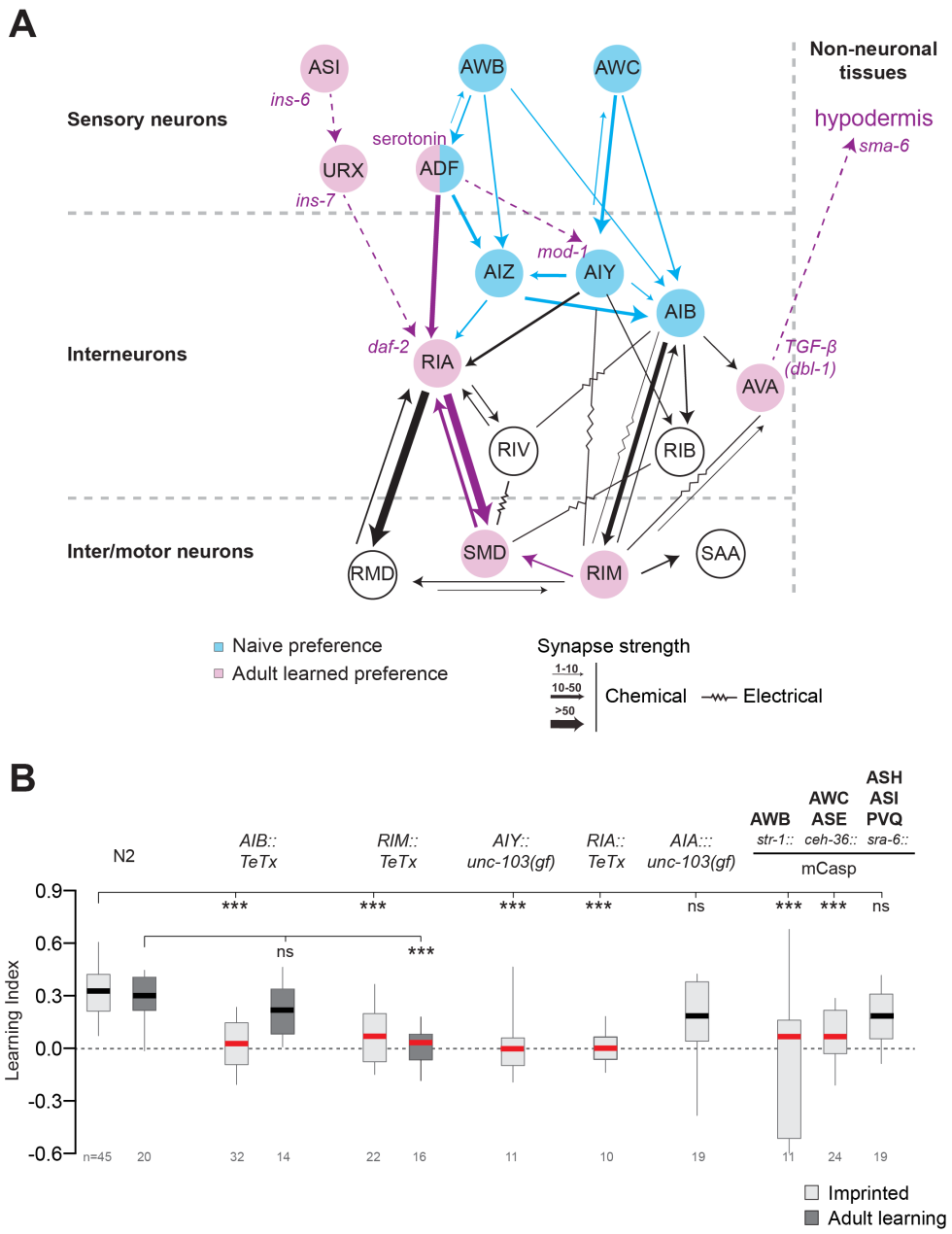
A
Sensory neurons
Interneurons
Inter/motor neurons
Non-neuronal tissues
hypodermis
ASI
AWB
AWC
ins-6
serotonin
URX
ADF
ins-7
sma-6
mod-1
AIZ
AIY
AIB
daf-2
RIA
TGF-β (dbl-1)
AVA
RIV
RIB
SMD
RIM
SAA
RMD
Naive preference
Adult learned preference
Synapse strength
1-10
10-50
>50
Chemical
Electrical
B
N2
AIB:: TeTx
RIM:: TeTx
AIY:: unc-103(gf)
RIA:: TeTx
AIA::: unc-103(gf)
AWB str-1::
AWC ceh-36::
ASH ASI PVQ sra-6::
mCasp
***
ns
Learning Index
0.9
0.6
0.3
0.0
-0.3
-0.6
n=45
20
32
14
22
16
11
10
19
11
24
19
Imprinted
Adult learning

Figure 2.5 Distinct circuits for the formation and retrieval of imprinted memory

(A) Weighted wiring diagram of interneurons implicated in imprinted memory formation and retrieval. Synaptic strength is based on the number of chemical synapses from www.wormweb.org.

(B) Schematic illustration of neuronal silencing either at the memory formation or memory retrieval stage using cell-specific expression of a histamine-gated chloride channel (HisCl1).

(C-D) Neuronal silencing to identify neurons required either during memory formation (C) or during memory retrieval (D).

Boxes represent median and first and third quartiles, and whiskers represent 10^{th}-90^{th} percentiles. *n,* number of independent assays, 100-200 animals/assay. *P* values were generated by ANOVA with the Dunnett correction (** $P < 0.01$, * $P < 0.05$, ns not significant).

Figure 2.5

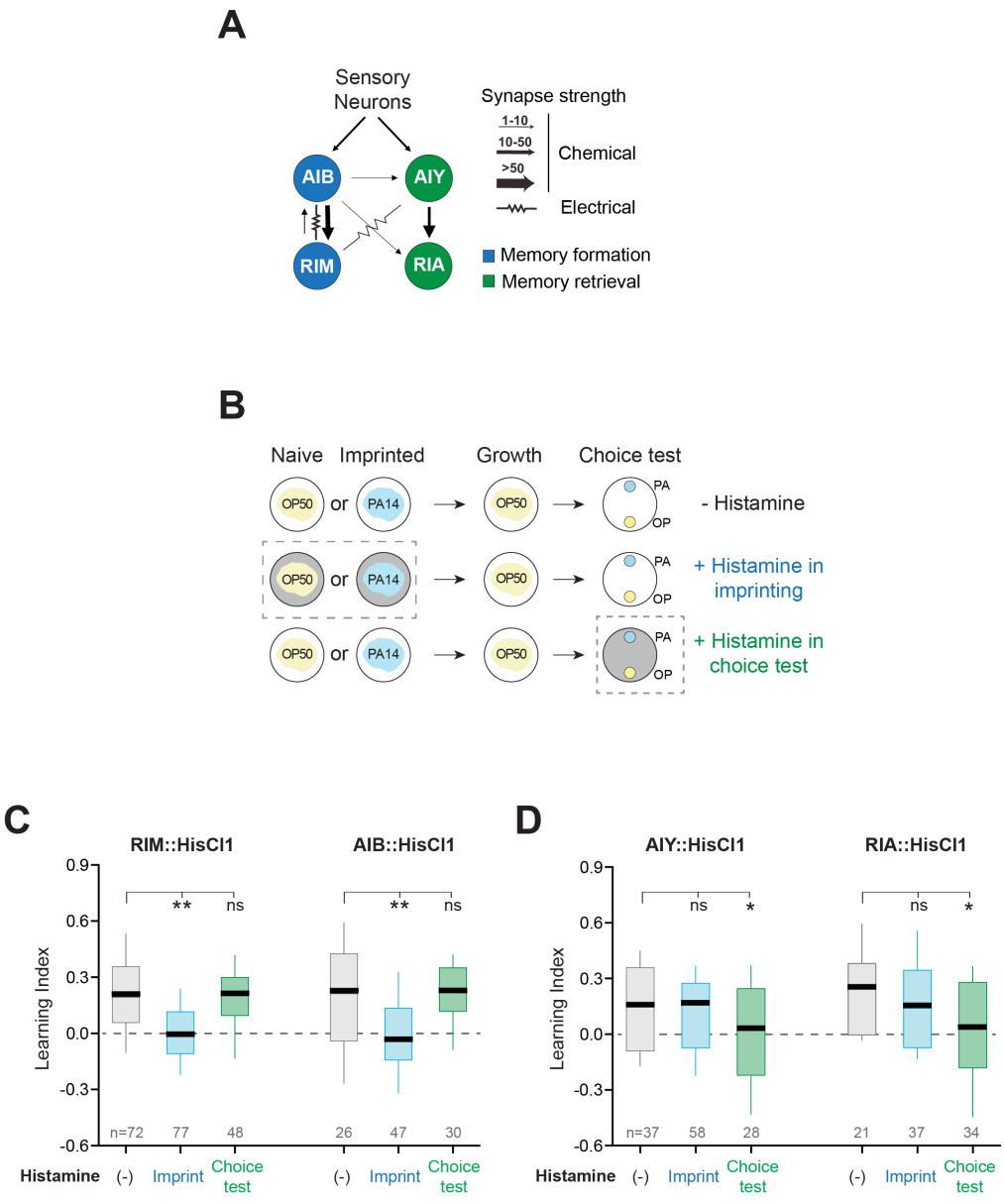
A
Sensory Neurons
AIB
AIY
RIM
RIA
Synapse strength
1-10
10-50
>50
Chemical
Electrical
Memory formation
Memory retrieval
B
Naive
Imprinted
Growth
Choice test
OP50
or
PA14
PA
OP
- Histamine
+ Histamine in imprinting
+ Histamine in choice test
C
RIM::HisCl1
AIB::HisCl1
Learning Index
0.9
0.6
0.3
0.0
-0.3
-0.6
**
ns
n=72
77
48
26
47
30
Histamine
(-)
Imprint
Choice test
D
AIY::HisCl1
RIA::HisCl1
ns
*
n=37
58
28
21
37
34

Figure 2.6 Behavioral strategies allowing imprinted aversion

(A) A pirouette is a reversal coupled to a high-angle turn. The bearing angle θ is the animal's direction of movement with respect to the odor source (here, PA14 lawn) before the pirouette. Each choice assay has two bacterial odor sources, which were examined separately (see Experimental Procedures).

(B) Normalized pirouette frequency of naïve and imprinted animals at different bearing angles with respect to a PA14 lawn (left) or OP50 lawn (right) in the choice assay. Naïve event frequency was compared to imprinted frequency at each bearing angle; *P* values were generated by ANOVA with the Sidak correction (* $P < 0.05$).

(C) Normalized pirouette frequency of naïve and PA14-imprinted animals navigating between a novel toxic bacterium, ToxA, and OP50.

(D) Normalized pirouette frequency of naïve and PA14-imprinted animals navigating between PA14 and OP50 with AIY neurons silenced with HisCl1.

Pirouette rates were calculated from 3-5 movies with 40-50 animals each and normalized to average rates across angles.

Figure 2.6

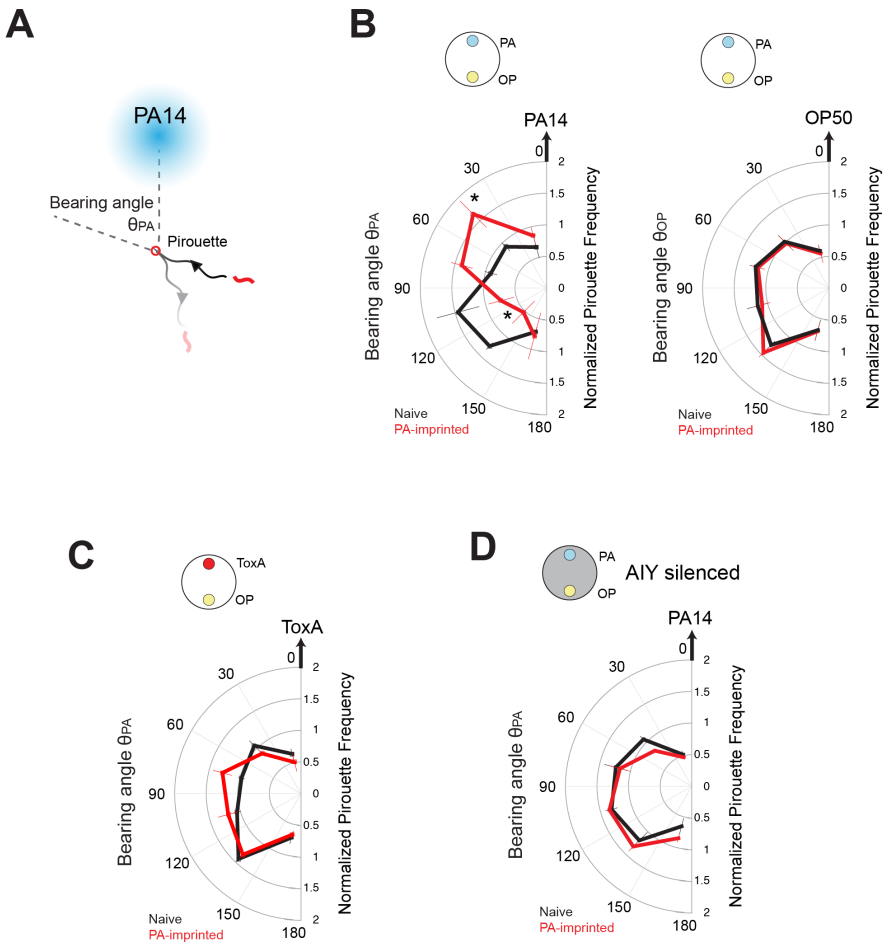
A
PA14
Bearing angle
θPA
Pirouette
B
PA
OP
PA14
OP50
Bearing angle θPA
Bearing angle θOP
Normalized Pirouette Frequency
Naive
PA-imprinted
C
ToxA
OP
D
AIY silenced

Table 1 Differential neuronal requirement for adult learning and imprinting

Neuron	Requirement for adult learning	Requirement for aversive imprinting
AWC	Required for naïve preference (Ha et al., 2010; Harris et al., 2014)	Required (or required with ASE)
AWB	Required for naïve preference (Ha et al., 2010; Harris et al., 2014)	Required
ASI	Required for *ins-6* signaling (Chen et al., 2013)	Not required: mCasp ablation (Figure 2.4B). Should be confirmed with a second inactivation reagent
ADF	Required (Ha et al., 2010; Zhang et al., 2005)	Unknown, but serotonin is required, which is made by ADF
AIB	Required for naïve preference but not learning (Ha et al., 2010)	Required for memory formation
AIY	Required for naïve preference but not learning (Ha et al., 2010)	Required for memory retrieval
AIZ	Required for naïve preference but not learning (Ha et al., 2010)	Unknown
RIA	Required for learned preference (Ha et al., 2010)	Required for memory retrieval
RIM	Required for learned preference (Ha et al., 2010)	Required for memory formation
AVA	Required for TGFβ signaling (Zhang and Zhang, 2012)	Unknown

CHAPTER 3:

Genetic requirements for aversive olfactory imprinting

INTRODUCTION

What molecules and genes allow the nervous system to form, retain, and retrieve a memory? This question has been asked through many approaches over the past decades. Eric Kandel and colleagues pioneered the use of the *Aplysia* gill withdrawal reflex paradigm to study the molecular basis of a behavioral memory (Kandel, 2001; Kandel and Tauc, 1965). Gill withdrawal can be progressively attenuated (habituation) or strengthened (sensitization), depending on training experience. Spaced repetition between training sessions can convert a short-term memory, which lasts minutes, into a long-term form that lasts for days (Brunelli et al., 1976; Pinsker et al., 1973). Through electrophysiology and biochemical characterization, Kandel's team found essential genes and pathways for short- and long-term memory.

For short-term memory, release of the neurotransmitter serotonin can upregulate cAMP signaling in the presynaptic sensory neurons (Brunelli et al., 1976). cAMP activates a protein kinase PKA, which acts on an S-type potassium channel to reduce potassium current, allowing stronger calcium influx, which causes enhanced neurotransmitter release and prolonged withdrawal behavior (Byrne and Kandel, 1996; Castellucci and Kandel, 1976; Klein and Kandel, 1980; Siegelbaum et al., 1982).

Additional molecular pathways are involved in the formation of long-term memory. In the presynaptic neuron, persistent activation of PKA recruits mitogen-activated protein kinase (MAPK) and turns on gene transcription that is dependent on the activity of cAMP response element binding protein (CREB) (Bartsch et al., 1995; Dash et al., 1990; Kandel, 2001). CREB not only inactivates the memory suppressor genes, such as the transcription factor ApCREB-2 (Bartsch et al., 1995), but also turns on immediate-

response genes, such as the activation factor ApAF, to allow synaptic growth for memory (Bartsch et al., 2000).

In the meantime, fly geneticists led by Seymour Benzer investigated learning-related genes using behavior genetic approaches (Quinn et al., 1974; Tully, 1996). Chemical mutagenesis and forward genetic screens led to the discovery of the mutant fly *dunce*, which fails to associate electrical shock with an odor cue in aversive learning (Dudai et al., 1976). The biochemical identity of dunce was found to be a cAMP phosphodiesterase (Byers et al., 1981). Along with the independent discovery of cAMP signaling in *Aplysia* learning, *dunce* strongly implicated this second messenger pathway in associative learning. The molecular mechanisms of learning have proven to be highly conserved from invertebrates to mammals (Barco et al., 2006; Kandel, 2001).

In *C. elegans*, much progress has been focused on characterizing learning genes and mapping them onto the relevant neurons and circuits. Short-term memory, such as odor adaptation, requires various molecules in the sensory neuron AWC (guanylyl cyclase ODR-1 and cGMP dependent protein kinase EGL-4), and the interneurons AIA (neuropeptide Y receptor NPR-11) and AIY (RAS kinase LET-60) (Chalasani et al., 2010; Hirotsu and Iino, 2005; L'Etoile et al., 2002) (Table 2). Long-term memory, such as odor associative spaced training, correlates with large-scale gene expression changes that depend on CREB activity (Lakhina et al., 2015), agreeing with the earlier work from other animal models.

In this chapter, I discuss genes that are essential for aversive imprinting, and compare them to genes required for medium-term adult aversive learning. I map these

genetic requirements onto the imprinting-relevant circuit described in Chapter 2, and suggest explanations for how molecular pathways synthesize the memory.

RESULTS

Genetic requirements for adult learning and imprinting

The overlap between neural circuits for adult learned aversion and imprinted aversion (RIM and RIA) suggests that they might share molecular components. Indeed, the serotonin biosynthesis enzyme TPH-1 and the serotonin receptor MOD-1 required for adult learned aversion were required for imprinted aversion as well (Zhang et al., 2005) (Figure 3.1A).

Glutamate is broadly employed as an excitatory neurotransmitter in vertebrate and invertebrate nervous systems (Luscher and Frerking, 2001; Malinow and Malenka, 2002). Glutamatergic signaling as well as the vesicular glutamate transporter EAT-4 are required for touch habituation in *C. elegans,* among other behaviors (Lee et al., 1999; Rankin and Wicks, 2000; Rose et al., 2003). I found that both adult learned aversion and imprinted aversion required *eat-4,* but glutamate receptors distinguished between the two forms of memory. The glutamate receptor GLR-3, which is expressed in RIA, was required for both adult learned aversion and imprinted aversion. However, the AMPA-type glutamate receptor GLR-1, which is expressed in AIB, RIM, RIA, and other neurons, was required for imprinted aversion but not for adult learned aversion, and the NMDA-type glutamate receptor NMR-1 affected adult learned aversion but not imprinted aversion (Figure 3.1A). Interestingly, introducing a leaky channel with a single nucleotide mutated GLR-1(AT) in

AIB neurons of wild-type animals can lead to an imprinting deficit (Figure 5.2A) (Zheng et al., 1999) (Figure 3.1B).

The cAMP response element-binding protein (CREB) is a transcription factor required for long-term memory in *Aplysia*, *C. elegans*, *Drosophila,* and mice (Kauffman et al., 2010; Silva et al., 1998; Yin et al., 1994). The *C. elegans* CREB homolog *crh-1* was required for imprinted aversion, but not for adult learned aversion (Figure 3.1A). Imprinted aversion did not require SRA-11, a G protein-coupled receptor required for positive odor imprinting (Figure 3.1A) (Remy, 2010; Remy and Hobert, 2005).

I also tested the possibility that learning can occur through RNA interference pathways by examining mutants of dsRNA uptake channel *sid-1*, as well as members of the argonaute protein family *rde-1* and *rde-4* that are required for RNAi (Parrish and Fire, 2001; Tabara et al., 1999). All three mutants showed positive learning in both imprinting and adult learning tests; although the *rde-1* and *rde-4* mutants learned less effectively than the wild-type (Figure 3.1C).

Although much remains to be learned about the timing, neuronal site of action, and specificity of these genes, it appears that imprinted aversion has genetic requirements that overlap partly but not entirely with other forms of learning.

Tyramine is required for imprinting in RIM learning neurons

The RIM neurons release several neurotransmitters, including the monoamine neurotransmitter tyramine (Alkema et al., 2005) (Figure 3.2A). Invertebrate tyramine and octopamine are analogous to vertebrate epinephrine and norepinephrine, neuromodulators

that can act as learning cues (Tully et al., 2007). Synthesis of tyramine and of the related transmitter octopamine requires the tyrosine decarboxylase TDC-1, and we found that *tdc-1* mutants were defective both in imprinted aversion and in adult learned aversion (Figure 3.2B, 3.3B). *tbh-1* mutants, which are deficient in octopamine synthesis, had normal imprinted aversion, suggesting that tyramine is the relevant transmitter (Figure 3.2B). *tdc-1* is expressed in RIM and RIC neurons, and in non-neuronal cells in the gonad (Alkema et al., 2005). Imprinted aversion in *tdc-1* mutants was rescued by expressing a *tdc-1* cDNA from the RIM-specific *gcy-13* promoter, but not from the RIC-specific *tbh-1* promoter, indicating that tyramine synthesized by the RIM neurons is sufficient for imprinting (Figure 3.2B).

Imprinted aversion in *tdc-1* mutants was rescued by exogenous tyramine during the L1 stage, when the RIM neurons were required, but not at later times (Figure 3.2C, left). Direct administration of tyramine during the L1 learning period rescued imprinted aversion when RIM was simultaneously silenced with HisCl1 (Figure 3.2C, right). The requirement for RIM in imprinted aversion is therefore closely associated with tyramine signaling in the L1 stage. However, L1 supplementation with exogenous tyramine and serotonin was not sufficient to induce imprinted aversion to non-pathogenic bacteria (Figure 3.2D).

The tyramine receptor SER-2 is required in AIY memory retrieval neurons

C. elegans senses tyramine through the G-protein coupled receptors TYRA-2, TYRA-3, SER-2, and the tyramine-gated chloride channel LGC-55 (Donnelly et al., 2013; Rex et al., 2005; Tsalik et al., 2003; Wragg et al., 2007). *tyra-2, ser-2,* and *lgc-55* were all

required for imprinted aversion, but *tyra-3* was not (Figure 3.3A). Among these, *ser-2* was required for imprinted aversion but not adult learned aversion (Figure 3.3B).

The *ser-2* gene encodes multiple isoforms from different promoters (Tsalik et al., 2003). In localizing its site of action, we found that a distal promoter fragment (*ser-2p2*) driving a *ser-2e* cDNA rescued imprinted aversion in *ser-2* mutants, but a proximal promoter fragment (*ser-2p1*) did not (Figure 3.3A). Rescuing activity was narrowed down further using an inverted Cre-lox (FLEx) recombination strategy to provide *ser-2* to subsets of *ser-2p2* neurons (Figure 3.3C). Expressing the Cre recombinase only in AIY neurons rescued learned aversion almost as well as full *ser-2p2* expression, whereas expression in other *ser2p2*-expressing neurons (RME, SIA, and AIZ) was ineffective (Figure 3.3C). Thus SER-2 in AIY detects the tyramine produced by RIM, bridging the memory formation and retrieval circuits for imprinted aversion.

DISCUSSION

Neuromodulator as a learning signal

The AIB and RIM neurons are necessary during learning, but dispensable for memory retrieval in the adult. The RIM neurotransmitter tyramine is also necessary for learning during the L1 stage, and tyramine can replace the requirement for RIM activity. These results indicate that the neuromodulator tyramine from RIM is an essential learning cue.

Neuromodulatory systems have essential roles in learning paradigms including the gill withdrawal reflex of *Aplysia* (serotonin), *Drosophila* olfactory learning

(dopamine, octopamine), vertebrate reward learning (dopamine), and vertebrate fear conditioning (norepinephrine and others) (Johansen et al., 2011; Kandel, 2001; Waddell, 2013). Interestingly, *Drosophila* olfactory learning and memory often require a combination of multiple neuromodulators, just as learned pathogen aversion in *C. elegans* requires tyramine, serotonin, and, in adult learning, insulin and TGF-beta peptides (Table 2). Structurally, olfactory inputs into the mushroom bodies are transmitted in parallel to different lobes, each of which is innervated by a few dopaminergic neurons that represent positive or negative contexts (Aso et al., 2014). Dopamine is the direct learning input into the *Drosophila* mushroom body to shape the output synapses and functions (Cohn et al., 2015; Hige et al., 2015; Waddell, 2013); other neuromodulators such as octopamine can also modulate dopamine signaling (Burke et al., 2012; Cassenaer and Laurent, 2012; Schroll et al., 2006).

These examples provide a framework for considering modulators in imprinted aversion as well. Combinations of neuromodulators (serotonin, tyramine and neuropeptides) could encode pathogenic infection and the recovery from infection, or chains of modulators might transmit this information to sensory circuits to allow their modification. Serotonin is transcriptionally elevated by PA14 infection, and serotonin supplementation can make adult learning more effective (Zhang et al., 2005). Although serotonin and tyramine may relay information about pathogenic infection, they probably do not encode the aversive unconditioned stimulus directly, as certain dopaminergic neurons do in *Drosophila* olfactory learning (Aso et al., 2014; Hige et al., 2015). Exogenous serotonin and tyramine are not sufficient to make animals aversively imprint

on a nonpathogenic *Pseudomonas* PA50E12, suggesting there are other cues required for learning.

Differential genes required in short- and long-term memory

Imprinted aversion shares features with other kinds of learning in *C. elegans* and other animals. The neuronal circuits for imprinted aversion and learned adult aversion are overlapping, but not identical. At a genetic level, both imprinted aversion and adult learned aversion require serotonin and the MOD-1 serotonin receptor, tyramine and tyramine receptors TYRA-3 and LGC-55, and vesicular glutamate transporter EAT-4 and glutamate receptor GLR-3. The common genetic requirements suggesting that short and long-term memory can share similar genetic components. These shared genes are key molecules involved in neuronal signaling and circuit function, and emerged from a candidate screen; more genes would surely be uncovered from a broader and unbiased approach, so this represents only a limited view of the genetics of aversive imprinting.

Both imprinted aversion and adult learned aversion require two tyramine receptors, LGC-55 and TYRA-2. LGC-55 is expressed in the forward command neuron AVB and in head motor neurons, and TYRA-2 is expressed in head sensory neurons, suggesting that these neurons could also contribute to aversive memory (Pirri et al., 2009; Rex et al., 2005). SER-2 was required only for imprinted aversion and not for learned adult aversion. Acting in the AIY memory retrieval neurons in imprinted aversion, SER-2 provides a molecular bridge between the neurons involved in memory formation (RIM) and memory retrieval (AIY), two processes that occur three days apart. Tyramine, as a

monoamine modulator, operates at a slow time scale to influence circuit functions (Marder et al., 2014) and its mutant can be rescued by chemical supplementation. Exogenous tyramine provided only at the L1 stage can rescue a tyramine-deficient mutant, suggesting that tyramine has a restricted time of action during learning. These results suggest that acute tyramine action *via* SER-2 initiates long-term changes in AIY that drive imprinted aversion. In motor neurons, SER-2 signals through $G_{\alpha o}$ to inhibit neurotransmitter release (Donnelly et al., 2013); how it functions in AIY to affect imprinted memory is unknown. It is possible that it functions through transcriptional regulations to encode long-term changes, which will be discussed in Chapter 4 and 5.

The requirements for the AMPA-type glutamate receptor GLR-1, tyramine receptor SER-2, and the CREB in imprinted aversion, but not adult learned aversion, echo requirements in long-term versus short-term learning in other *C. elegans* learning paradigms (Table 2). Both GLR-1 and CREB are also crucial for 24-hour memory of touch habituation, but not for habituation memory that lasts 12 hours or less (Rose et al., 2003; Timbers and Rankin, 2011). These two genes are present throughout life, although it is unknown how their expression and activity in different neurons varies at early larval stages from adulthood.

It is plausible that the basis of the early critical period that gives rise to long-lasting imprinted aversion could be a change of CREB-dependent gene expression in the relevant neurons. CREB is required for long-term appetitive olfactory learning that lasts for 24 hours, but not for short-term appetitive learning (Kauffman et al., 2010). Although expressed ubiquitously, CREB is required in different neurons for different functions: in AIM interneurons for long-term appetitive olfactory memory (Lakhina et al., 2015), in

RIC interneurons for detecting starvation states (Suo et al., 2006); and in AFD sensory neurons for thermotaxis (Nishida et al., 2011). In long-term appetitive olfactory training, CREB drives induction of over 700 genes detectable by whole-animal RNA sequencing (Lakhina et al., 2015). On the one hand, these global effects emphasize that the strong unconditioned stimuli of food, starvation, and pathogenic infection act on the whole animal, not just single synapses; on the other hand, the global transcriptional effects need to be refined to specific circuits and neurons to unveil the causal mechanisms.

Figure 3.1 Genetic requirements for aversive imprinting

(A) Imprinted aversion and adult learned aversion in mutants for the serotonin biosynthetic enzyme TPH-1, the serotonin receptor MOD-1, the vesicular glutamate transporter EAT-4, the glutamate receptors GLR-1, GLR-3 and NMR-1, the CREB homolog CRH-1 (two alleles), and the orphan G-protein coupled receptor SRA-11. Red bars mark assays with a significant learning deficit. Boxes represent median and first and third quartiles, and whiskers represent 10^{th}-90^{th} percentiles.

(B) Imprinted and adult learned aversion in strains with abnormal glutamate receptor *glr-1* signaling. *glr-1(AT)* is a leaky channel with a single nucleotide mutation (Zheng et al., 1999), which when expressed in AIB interneurons can disrupt aversive imprinting. Each bar graph represents population mean and SEM.

(C) Imprinted and adult learned aversion in strains with defects in RNA interference (RNAi) signaling. Each bar graph represents population mean and SEM.

n, number of independent assays, 100-200 animals/assay. *P* values were generated by ANOVA with the Dunnett correction. (*** $P < 0.001$, ** $P < 0.01$, * $P < 0.05$, ns not significant).

Figure 3.1

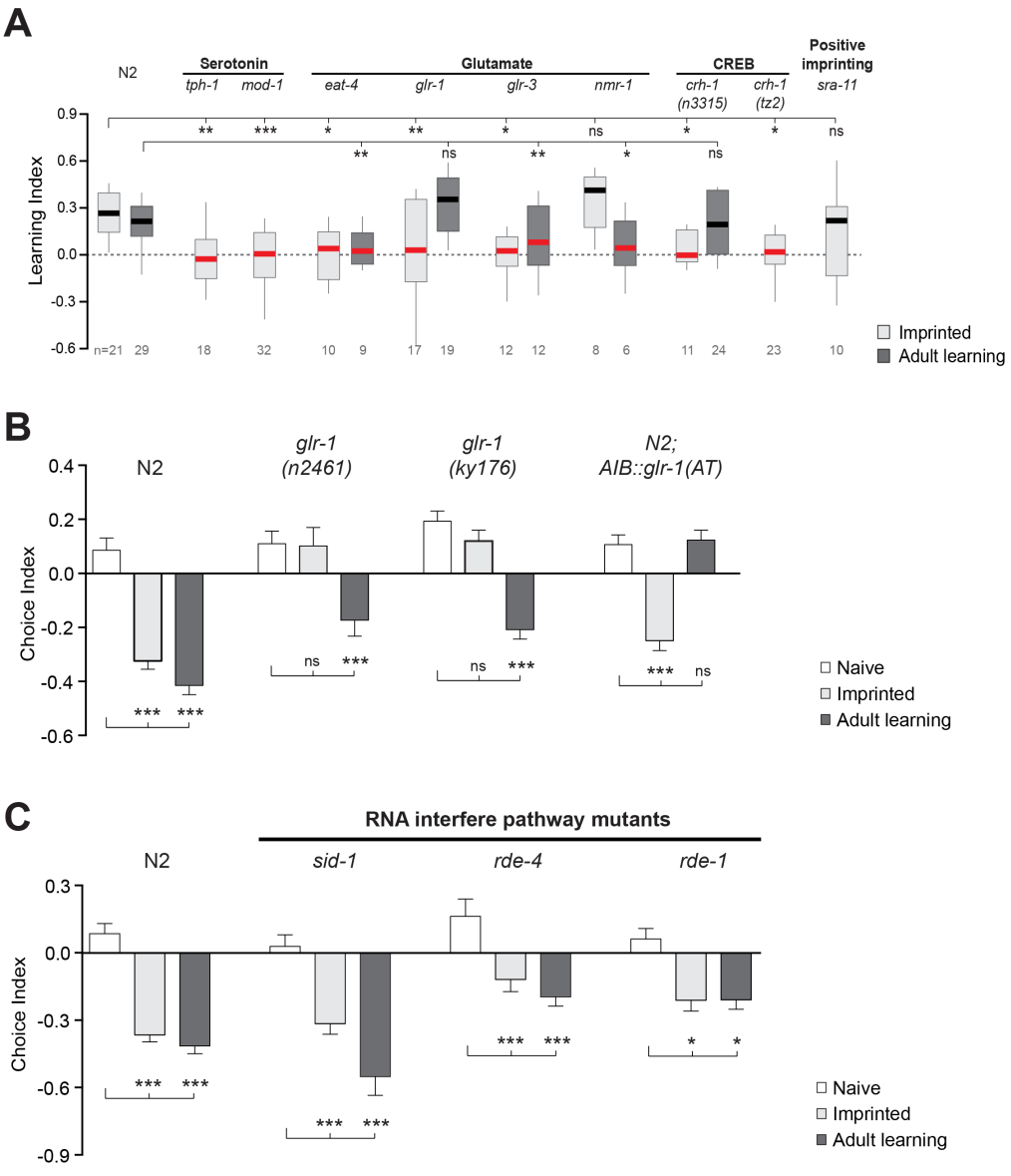
A
N2
Serotonin
tph-1
mod-1
Glutamate
eat-4
glr-1
glr-3
nmr-1
CREB
crh-1 (n3315)
crh-1 (tz2)
Positive imprinting
sra-11
Learning Index
0.9
0.6
0.3
0.0
-0.3
-0.6
n=21 29 18 32 10 9 17 19 12 12 8 6 11 24 23 10
Imprinted
Adult learning
B
N2
glr-1 (n2461)
glr-1 (ky176)
N2; AIB::glr-1(AT)
Choice Index
0.4
0.2
0.0
-0.2
-0.4
-0.6
Naive
Imprinted
Adult learning
C
RNA interfere pathway mutants
N2
sid-1
rde-4
rde-1
Choice Index
0.3
0.0
-0.3
-0.6
-0.9
Naive
Imprinted
Adult learning

Figure 3.2 Tyramine is required for aversive imprinting

(A) Biosynthetic pathways for tyramine (produced in RIM and RIC neurons) and octopamine (produced in RIC neurons). Cells of the somatic gonad also make tyramine and octopamine.

(B) Learning index of tyramine/octopamine mutants and rescued strains.

(C) Learning index after exogenous tyramine or histamine administration to *tdc-1* mutants and RIM::HisCl1 strains.

(D) Tyramine and serotonin administration during L1 stage fails to induce imprinted aversion to the non-pathogenic *Pseudomonas* strain PA50E12.

Boxes represent median and first and third quartiles, and whiskers represent 10^{th}-90^{th} percentiles. *n*, number of independent assays, 100-200 animals/assay. *P* values were generated by ANOVA with the Dunnett correction. (*** $P < 0.001$, ** $P < 0.01$, * $P < 0.05$, ns not significant).

Figure 3.2

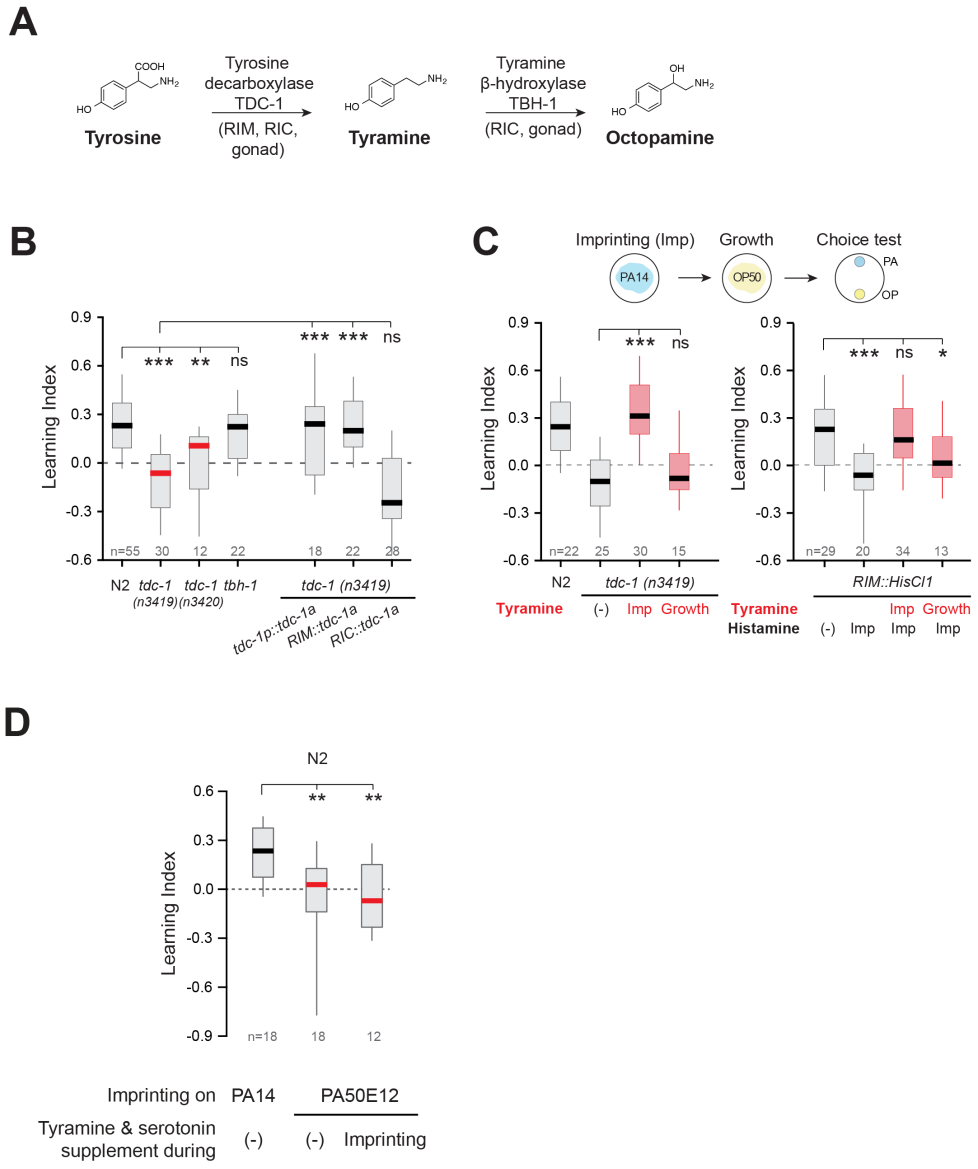
A
Tyrosine
Tyrosine decarboxylase TDC-1
(RIM, RIC, gonad)
Tyramine
Tyramine β-hydroxylase TBH-1
(RIC, gonad)
Octopamine
B
Learning Index
N2
tdc-1 (n3419)
tdc-1 (n3420)
tbh-1
tdc-1 (n3419)
tdc-1p::tdc-1a
RIM::tdc-1a
RIC::tdc-1a
C
Imprinting (Imp)
Growth
Choice test
PA14
OP50
PA
OP
Tyramine
Histamine
RIM::HisCl1
D
N2
Imprinting on
PA14
PA50E12
Tyramine & serotonin supplement during
(-)
Imprinting

Figure 3.3

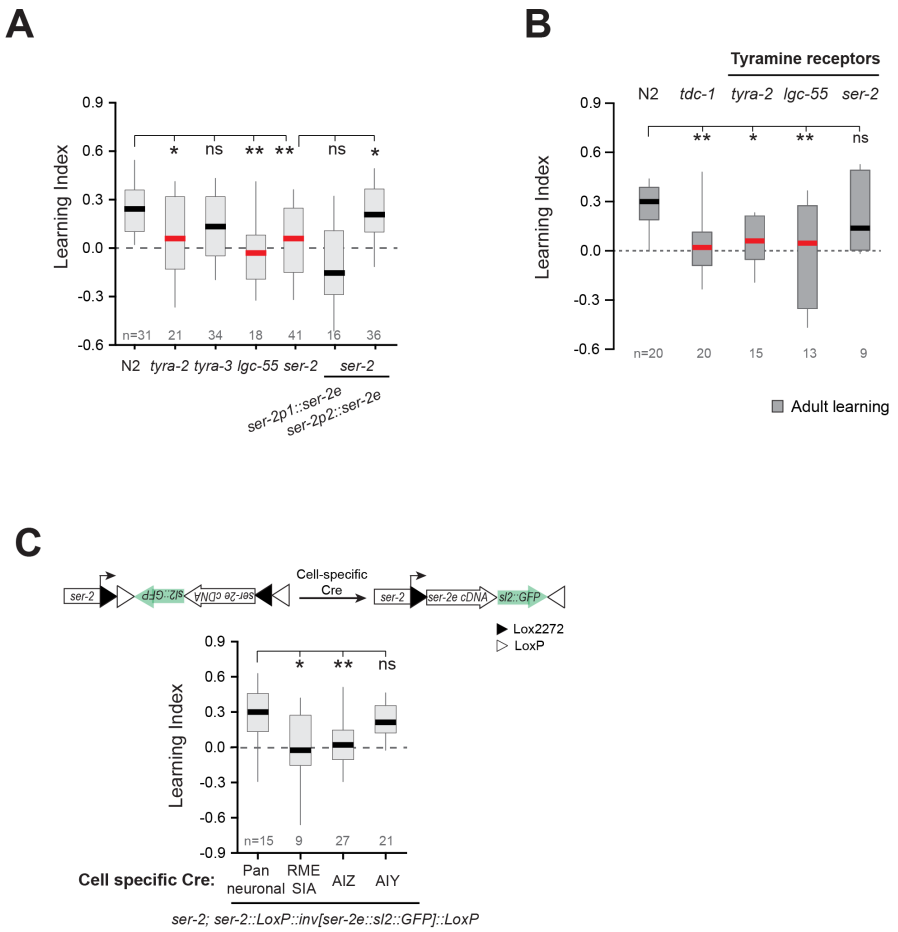

Figure 3.3 Tyramine receptors SER-2 is required for aversive imprinting

(A) Learning index of tyramine receptor mutants and rescued strains.

(B) Adult learned aversion in tyramine deficient mutant *tdc-1* and tyramine receptor mutants *tyra-2*, *lgc-55* and *ser-2*.

(C) Cell-specific rescue of *ser-2* using intersectional promoters. Cre expression and inversion allows *ser-2* expression in subsets of *ser-2p2*-expressing cells.

Boxes represent median and first and third quartiles, and whiskers represent 10th-90th percentiles. *n*, number of independent assays, 100-200 animals/assay. *P* values were generated by ANOVA with the Dunnett correction. (*** P <0.001, ** P <0.01, * P <0.05, ns not significant).

Table 2 Plasticity genes in *C. elegans*

Gene	Plasticity	Encoded protein and function sites	Reference
egl-4	Olfactory learning	cGMP-dependent kinase in AWCon	(L'Etoile et al., 2002)
odr-1	Olfactory learning	Guanylyl cyclase in AWCon	(L'Etoile and Bargmann, 2000; Morrison and van der Kooy, 2001)
let-60	Olfactory learning	RAS-GTPase in AIY	(Hirotsu and Iino, 2005)
npr-11	Olfactory learning	Neuropeptide Y receptor in AIA	(Chalasani et al., 2010)
nlp-1	Olfactory learning	Neuropeptide in AWC	(Chalasani et al., 2010)
ins-1	Olfactory and gustatory learning	Neuropeptide in AIA and ASI	(Chalasani et al., 2010; Tomioka et al., 2006)
crh-1	Olfactory learning, touch habituation and aversive imprinting	CREB, ubiquitous	(Amano and Maruyama, 2011; Kauffman et al., 2010; Timbers and Rankin, 2011)
eat-4	Touch habituation and pathogen learning	Vesicular glutamate transporter	(Rankin and Wicks, 2000; Rose et al., 2002)
glr-1	Olfactory learning, touch habituation and aversive imprinting	AMPA receptor	(Rose et al., 2003; Stetak et al., 2009)
nmr-1	Gustatory learning	NMDA receptor	(Kano et al., 2008)

Table 2 continued

Gene	Plasticity	Encoded protein and function sites	Reference
tph-1	Pathogen learning	Serotonin synthesis in ADF	(Zhang et al., 2005)
mod-1	Pathogen learning	Serotonin receptor in AIY and AIZ	(Zhang et al., 2005)
dbl-1	Pathogen learning	TGFβ in AVA	(Zhang and Zhang, 2012)
ins-6	Pathogen learning	Neuropeptide in ASI	(Chen et al., 2013)
ins-7	Pathogen learning	Neuropeptide in URX	(Chen et al., 2013)
daf-2	Gustatory and pathogen learning	Neuropeptide receptor in RIA	(Chen et al., 2013; Kauffman et al., 2010; Ohno et al., 2014)

CHAPTER 4:

Functional neuronal changes after aversive olfactory imprinting

INTRODUCTION

Developmental plasticity can lead to long-term and sometimes irreversible changes in the nervous system that modulate behavior. One of the most striking examples comes from studying the neural basis of sensorimotor wiring in barn owls (Pena and Gutfreund, 2014). To localize the source of a sound, animals measure both auditory and visual cues to estimate its physical location in space. This sensory-spatial map, e.g. the precise relationship between visual-auditory measurements and a location in space, can be modulated by early experience. After wearing prisms that systematically shift visual cues by a few degrees, young barn owls can learn to adjust their orienting perceptions by taking into account the optical displacement from the prism, and successfully learn to localize the object with a shifted visual field (Knudsen and Knudsen, 1989a, b). Chronic visual displacement by prism irreversibly changes the sensorimotor map, resulting in a systematic error in orienting tasks. However, prism removal in youth (<200 days old) can allow the animal to recalibrate its sensorimotor map and acquire normal orienting ability (Brainard and Knudsen, 1993; Knudsen and Knudsen, 1990). The ability to adjust to a shifted visual field and relearn the sensorimotor association is lost after the close of the sensitive period.

The neural correlates of this orienting task have been rigorously examined by electrophysiological studies. In the prism-reared animals, neural circuits in the midbrain inferior colliculus change their tuning properties to respond more strongly to the stimuli from the shifted visual field, and less strongly to the normal stimuli without the optic displacement (Brainard and Knudsen, 1998; Feldman and Knudsen, 1997). This shift of neural responses after an early optical shift experience is proposed to be a representation

of memory, and the midbrain region inferior colliculus that allows this experience-dependent recalibration is proposed to be the storage site of the memory.

Similarly, I speculate that aversive imprinting in *C. elegans*, which also occurs during early development, may lead to changes in neural circuits that can store the olfactory memory and later allow animals to avoid the experienced pathogen. If so, where are those sites of memory? Does this neural correlate of memory actually result from a change in the synapses? Are these effects correlated to or even essential for the aversive behavior? As discussed in an earlier chapter, early stress experience in *C. elegans* can induce developmental reprogramming into the alternative larval stage, dauer. Dauer behaviors are distinct from those of normal developmental larvae (Hu, 2007): dauer larvae lose sensitivity to gustatory signals and behave poorly in salt chemotaxis, become more resistant to noxious thermal signals, display much reduced locomotion activity for energy preservation, and gain the nictation behavior to sway the body in the air and achieve maximal dispersal (Cassada and Russell, 1975). These changes of behavior are correlated with drastic changes of neuronal structures, including the enlarged tip of the inner labial neurons, increased winglike structures and enhanced innervation with body wall, as well as changes of relative positions of the amphidial neurons (Albert and Riddle, 1983). In this chapter, to assess changes in functional activity, I examine neuronal responses to bacterial odors in animals expressing genetically encoded calcium indicators in the learning-related interneurons AIB, RIM, AIY, and RIA.

Besides the aforementioned four key interneurons, can learning happen at the sensory level? Sensory neuronal ablation raises a concern that the loss of learning may be an indirect result of the loss of primary detection. I take a functional approach to record

sensory responses to pathogens in both naïve and imprinted animals, in the hope of understanding how the bacterial smell is represented in the animals' brains, and how experience can change this representation. At the end of this chapter, I will report work in progress using a multi-focal microscope that allows real-time volumetric recording of 12 pairs of sensory neurons, to ask how naïve and imprinted animals encode pathogen smell by their neuronal representations.

RESULTS

Imprinting does not qualitatively alter AIY-RIA synaptic structures

Because both aversive imprinting and dauer formation occur while the nervous system is still developing, we speculate that imprinting, similarly, may have led to neuronal structure changes. The four interneurons required for imprinting have been examined and shown to have similar morphologies in the naïve and imprinted animals, suggesting that the early pathogen experience did not drastically alter the cell fate or development.

To examine whether the subcellular structures are altered after imprinting, I first examined AIB, RIM, AIY and RIA interneurons. Each neuron appeared superficially normal in somatic and axonal morphology. I then focused on the two memory retrieval neurons, AIY and RIA, and examined their synaptic marker expression in both naïve and imprinted animals. AIY-RIA synaptic structure can be visualized by the colocalization of two tagged proteins: the presynaptic synaptic vesicle associated protein RAB-3 (fused with mCherry) in AIY neurons and the postsynaptic glutamate receptor GLR-1 (fused

with GFP) in RIA neurons (Shao et al., 2013). Measured by the co-localized voxel number, AIY-RIA synapses appeared superficially similar between naïve and imprinted adults, suggesting that imprinting did not lead to major structural changes in AIY-RIA neurons (Figure 4.1).

Functional changes in the learning neurons AIB and RIM

The lack of developmental and structural changes to neurons after imprinting does not preclude the possibility of functional changes in these neurons. Because aversive imprinting makes animals avoid the pathogen that naïve animals were attracted to, I examined neuronal responses to alternating bacterial odors of animals expressing the genetically-encoded calcium indicator GCaMP in specific cell types (Tian et al., 2009). AIB, RIM, AIY, and RIA have all been shown to respond to chemical odors with calcium increases or decreases (Gordus et al., 2015; Hendricks et al., 2012; Larsch et al., 2013), and these calcium signals are likely to correlate with their activity, albeit with low temporal resolution (Larsch et al., 2015). Each neuron was examined in naïve and imprinted animals presented with alternating streams of OP50- and PA14-conditioned medium to imitate the sensory experience associated with a choice between bacterial odors in the memory retrieval context (Ha et al., 2010).

The memory formation neurons AIB and RIM are synaptic targets of many sensory neurons and are acutely involved in sensorimotor behaviors (Figure 4.9) – they are elements of a coupled network of neurons that is active during most or all reversals (Gordus et al., 2015; White et al., 1986). AIB and RIM neurons were visualized from the same animal simultaneously, and their calcium responses were strongly correlated under

all conditions. Calcium responses from both neurons in naïve animals fell acutely after a transition from OP50- to PA14-conditioned medium and increased slowly after a reciprocal transition from PA14 to OP50 (Figure 4.2A-B). Calcium transients were similar in naïve and imprinted adult animals, albeit with a slightly albeit significantly stronger AIB response after imprinting (Figure 4.2A-B). Thus, after imprinting, AIB and RIM remained responsive to OP50 and PA14 bacterial odors, although they contribute little to the aversive memory retrieval.

The subtle changes in AIB functions after imprinting were examined further. AIB and RIM have bistable calcium states and variable responses to odor stimulation (Figure 4.2C-E). In the trials of which these neurons were in a high calcium state before PA14 odor stimulation (Figure 4.2D-E, top row), AIB in naïve animals responded to PA14 with a sharp calcium suppression, soon followed by reactivation. Imprinted animals showed a more sustained calcium suppression and longer durations at the low-calcium states throughout the PA14 episode window (Figure 4.2F-G). This effect was not observed in a comparison of naïve and imprinted RIM responses. Moreover, as previously described, AIB is still capable of driving reversal behaviors by optogenetic activation; however, this ability to drive turns is was attenuated in the imprinted animals (Figure 2.3C). These subtle effects collectively hint at AIB's stronger engagement in sensory detection and weaker involvement in motor initiation after imprinting.

Functional changes in the AIY memory retrieval neurons

In the AIY memory retrieval neurons, calcium increased after a transition from OP50- to PA14-conditioned medium and fell after the reciprocal transition (Figure 4.3A-

B). The average response in AIY was significantly stronger in the imprinted adults, reflected in ~15% increase of response after imprinting in the cumulative distribution (Figure 4.3C).

Like AIB and RIM, AIY is involved in locomotion, but unlike them it suppresses turns while active (Gray et al., 2005). Silencing AIY elicits an increased turning rate in naïve animals, which is less prominent in imprinted animals (Figure 2.3A). AIY's enhanced calcium response to pathogens and its dampened ability to suppress turns in the imprinted group resemble AIB in that imprinting causes a stronger sensory engagement and weakened coupling with motor circuit.

Among AIB, RIM, and AIY, only AIY activity is essential in adults at the time of memory retrieval (Figure 2.5). To ask whether the change in AIY activity is central to imprinted memory, I examined AIY activity in animals whose RIM interneurons were silenced during L1, precluding imprinting (Figure 4.4). These animals had the same increased AIY responses to bacterial odors as control imprinted animals, despite showing the behavioral preferences of naïve animals. Thus the changes in AIY calcium responses after exposure to PA14 in the L1 stage are not sufficient for imprinted aversion.

Functional changes in the memory retrieval neurons RIA

RIA interneurons have the most numerous neuronal (non-muscle) synapses among all the *C. elegans* neurons (Sasakura, 2013; White et al., 1986). Accordingly, they have complex responses that integrate sensory input and motor feedback. RIA axons have compartmentalized calcium responses in dorsal (nrD) and ventral (nrV) regions that are generated by reciprocal connections with dorsal and ventral head motor neurons,

respectively. Due to the alternation of dorsal and ventral motor activity, this component of the response is often anti-correlated in nrD and nrV (Hendricks et al., 2012) (Figure 4.5A-B). Administration of bacterial conditioned medium can acutely synchronize the activities of nrD and nrV, a second pattern of activity, which will be discussed later (Hendricks et al., 2012) (Figure 4.7). To enable the detection of sensory inputs, I delivered alternating streams of bacterial conditioned media in 10-second pulses, a timescale slower than the dominant timescale of spontaneous nrD/nrV activity, and examined both average responses across many animals and trials and the correlation of nrD/nrV responses within individual trials.

In naïve animals, average calcium levels transiently increased in both nrD and nrV compartments each time bacterial streams were exchanged, rising immediately after a switch from OP50 to PA14 and immediately after a switch from PA14 to OP50 and falling within two seconds (Figure 4.5C,E). This response was notably different from that of AIB, RIM, and AIY, which responded asymmetrically to the conditioned bacteria at baseline. By contrast, the average calcium levels in imprinted animals fell in both nrD and nrV immediately after a switch from OP50 to PA14 (Figure 4.5C,E), and their average increase after a switch from PA14 to OP50 was considerably stronger than that in naïve animals. This alteration in RIA activity appeared specific to the choice context, as RIA neurons in naïve and imprinted animals had comparable responses to alternative pulses of buffer and conditioned medium from OP50 or PA14 (Figure 4.6A-B).

To better understand the shift in response in OP-PA alternations, I aligned individual traces to the reciprocal odor transitions and ranked them based on the rise or fall in calcium levels at the transition (Figure 4.5D,F). Both visual inspection and

quantitative analysis demonstrated a systematic shift across the entire distribution of responses between the responses of naïve and imprinted animals: after imprinting, fewer animals/trials responded to PA14 with a calcium increase, and more animals/trials responded to OP50 with a calcium increase. Imprinted animals had reciprocal changes in the fraction of responses that decreased (Figure 4.5D,F).

Sensory cues such as bacterial conditioned medium increase the frequency at which nrD and nrV become synchronized, so that both compartments experience simultaneous calcium influx or efflux (Hendricks et al., 2012). Indeed, naïve animal had more synchronized calcium events at odor transitions than other times; imprinted animals showed an even more enhanced synchrony at transitions (Figure 4.7A-B). Raster plots of individual synchronized calcium influx (in red) and efflux (in blue) events show significant increases of stimuli-triggered synchrony in the imprinted group (Figure 4.7A-B). Among trials in which nrD and nrV calcium fluctuations were synchronized, the calcium in these compartments increased after either PA14 or OP50 addition in naïve animals (Figure 4.7A). In imprinted animals, the synchronized calcium signals decreased upon PA14 addition, and increased upon OP50 addition, matching the responses measured in each compartment separately (Figure 4.7A).

The calcium changes in RIA were specific to the bacteria experienced during training; RIA neurons in naïve and PA14-imprinted animals did not respond differently to conditioned medium from a novel toxic bacterium, ToxA, when it was presented in alternation with OP50 (Figure 4.6C, 4.7C).

Finally, I examined RIA calcium dynamics in animals in which the RIM interneurons were acutely silenced with HisCl1 during L1 exposure to PA14, precluding

imprinting. RIA calcium responses in these adult animals were indistinguishable from those of naïve controls with respect to compartmentalized dynamics in nrD, nrV, or synchronous activity (Figure 4.7D). In summary, the circuit requirements, choice-specificity, and stimulus-specificity for changes in RIA calcium dynamics all correlate with imprinted behavioral memory.

Probing circuits and synaptic functions in imprinting-relevant neurons

The AIY and RIA memory retrieval neurons are synaptically connected and both present functional calcium changes after imprinting. Do AIY-RIA synapses have any change of function after imprinting? To address this question, I presynaptically activated AIY using a red-shifted channelrhodopsin variant (Chrimson), and post-synaptically recorded neuron activities from RIA using GCaMP (Klapoetke et al., 2014) (Figure 4.8A). 2-second pulses of AIY activations resulted in suppression of RIA calcium responses in both axonal compartments and its synchronized activity (Figure 5.1B,D). Moreover, this inhibitory synapse may be enhanced in the imprinted animals (Figure 5.1C). In the preliminary optogenetic experiment, I identified an inhibitory synaptic connection between AIY and RIA. In the future, it will be interesting to ask: 1) which neurotransmitter(s) and receptor(s) operate at this inhibitory synapse; 2) what the activity relationship is between AIY and RIA; 3) whether this synapse, and the subtle change of its synaptic strength, are relevant to learning. This approach can be extended to other neurons to probe circuit properties at high resolution and to understand how the input-output relationships of relevant neurons are altered by learning.

Multi-neuronal recording of sensory response to bacteria

Aversive imprinting is a form of associative learning that contains sensory specificity of the imprinted bacteria. To understand how animals differentiate bacterial species and how the sensory specificity of aversive imprinting is achieved, I have initiated a functional approach to record and compare the sensory neuronal responses to different bacterial stimuli, and correlate those with or without imprinting.

Using a nuclear-localized calcium indicator GCaMP6s expressed by a broadly active sensory neuron promoter *che-2* (Figure 4.9A) (Fujiwara et al., 1999; Tian et al., 2009), and a multi-focal microscope (MFM) to capture multiple neurons from 9 focal planes (with 2 μm z-steps) in one snapshot (Figure 4.9B) (Abrahamsson et al., 2013), I delivered a 30-second pulse of PA14-conditioned media to the nose of the worm and recorded the neuronal activities of the worm in a microfluidic chip (Chronis et al., 2007). Multiple neurons from 9 focal planes, each 2 μm apart, were captured simultaneously on the camera, from left to right, top to bottom (Figure 4.9B). About a dozen neurons are recorded: AWB and AWC are detectors of attractive and repulsive volatile odors (Bargmann et al., 1993; Troemel et al., 1997); ADF is the serotonergic neuron that is crucial for adult aversive learning, imprinting, detecting *Pseudomonas* infection, and also contributes to chemotaxis (Bargmann and Horvitz, 1991; Jafari et al., 2011; Melo and Ruvkun, 2012; Zhang et al., 2005); ASJ has been reported to detect the *Pseudomonas* viral factor, signals infection through TGF-β pathways, and aids lawn-leaving behavior (Meisel et al., 2014); AFD is the major thermosensor to regulate temperature preference and is innervated by other sensory neurons such as ASE (Mori and Ohshima, 1995; Satterlee et al., 2004); ADL and ASK are both involved in detecting pheromones and

repulsive cues, and can further modulate other neurons' chemotaxis responses (Chao et al., 2004; Hukema et al., 2006; Jang et al., 2012; Macosko et al., 2009).

Recording sensory responses from the same animal to different bacterial species can elucidate how different bacteria species are recognized and differentiated by such a compact nervous system. In a preliminary experiment, I applied 30-second alternations between OP50 and PA14, as well as OP50 and ToxA, to a naïve animal and imaged the sensory responses (Figure 4.9C). Fluorescent pixel values were recorded and normalized, in this case without any deconvolution (see Experimental Procedures). Each odor exchange was associated with an enhancement or suppression of neuronal calcium response.

For example, the cell A (tentatively identified as ADF) was activated by PA14 or ToxA smells, but the cell B (tentatively identified as AFD) was suppressed by PA14 and activated by ToxA (Figure 4.8C-D). More neurons had informative changes in OP-PA alternation than in OP-ToxA alternation, consistent with the fact that OP50 and ToxA are both *E. coli* strains and may produce similar chemical metabolites.

In the future, this approach can be used to compare sensory response profiles between naïve and imprinted animals. I hope to extend the use of MFM to further investigate how imprinting encodes memory specificity, which will be discussed in Chapter 5.

DISCUSSION

Retrieval of the imprinted memory

Compared to the medium-term memory formed by adult learning, the four-day long imprinted memory engages more neurons (AIB and AIY, see Table 1). By studying calcium response to bacterial odors, I found that the activity of AIY and RIA neurons, which are required only for memory retrieval, was altered after imprinting. AIY and RIA have common synaptic inputs, and AIY provides synaptic input to RIA, so these functional changes may be linked (Figure 4.10).

The first-layer AIY interneurons integrate contextual information from multiple sensory neurons (Larsch et al., 2015), and coordinate motor output to direct the turning bias for pathogen aversion (Gray et al., 2005; Li et al., 2014). AIY receives tyramine modulation from RIM learning neurons through the GPCR SER-2 (Figure 4.9). Functional changes in AIY activity were observed after exposure to PA14, but these changes did not require the RIM learning neurons, and imprinted aversion did. These results suggest that the change in AIY response is not sufficient for altered behavior in the choice assay. The calcium changes may reflect either the sensory experience of PA14 in L1, or pathogen infection physiology through serotonin receptor MOD-1 in AIY (Zhang et al., 2005), or both. Any of these can be necessary, but not sufficient elements for learning to occur.

By contrast, imprinting established a polarity change and increased synchrony of RIA response to the trained pathogen, but not the untrained stimuli. This change is RIM-dependent, like imprinting behavior. Both AIY and RIA have experience-dependent

calcium response alterations, but only changes in RIA were correlated with the behavioral outcome.

RIA is a major integrating interneuron with direct and indirect inputs from multiple neurons required for aversive learning and memory (Figure 4.9). It is activated by sensory signals and by feedback from motor neurons that guide head movements (Hendricks et al., 2012). One possible model for memory is that RIA receives both excitatory and inhibitory inputs from bacterial odors, and that imprinting changes the relative weights of excitation and inhibition based on odors that are present when RIM is active and tyramine is released. Many neurons required for learning form both direct connections with the RIA neurons (ADF, AWB, AWC, AIB), and indirect connections through AIY and other integrating neurons. Better understanding of these sensory neurons and their functional changes after imprinting may provide context and specificity for the neuronal correlates of imprinted memory. Certainly, the convergence of these signals in RIA is a potential site for the representation of the imprinted memory.

In *Drosophila*, similarly, the mushroom bodies receive input from olfactory projection neurons that represent sensory stimuli through the Kenyon cells (Aso et al., 2014; Caron et al., 2013; Turner et al., 2008) and are densely innervated with dopaminergic axons that represent unconditioned stimuli (Schroll et al., 2006; Schwaerzel et al., 2003). Selective silencing of subsets of mushroom body output neurons impairs both short- and long-term memory retrieval, arguing that the stable form of memory resides in mushroom bodies (Isabel et al., 2004; Krashes et al., 2007). Calcium imaging has revealed learning related changes in both Kenyon cells and mushroom body output neurons (Akalal et al., 2011; Yu et al., 2004; Owald et al., 2015; Sejourne et al.,

2011). Despite the small number of neurons and projections in the nematode nervous system, the properties of RIM in generating variability and memory synthesis, the requirement for AIY in memory retrieval, and the change of RIA response after learning, collectively represent a information that is central to learning and memory.

Figure 4.1

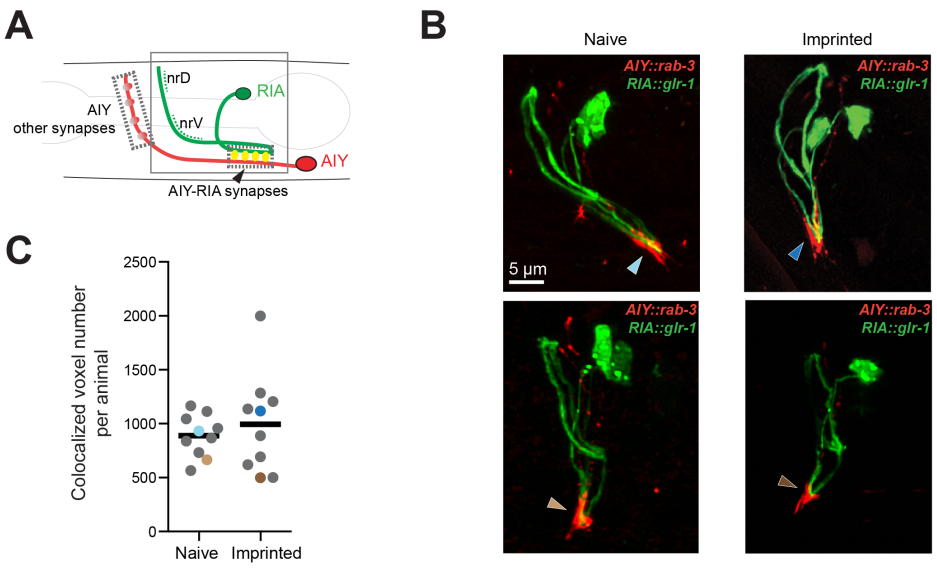

Figure 4.1 AIY-RIA synaptic structures after imprinting

(A) Illustration of AIY (red) and RIA (green) neurons, showing the nrD and nrV compartments of RIA and regions where AIY forms synapses with RIA (yellow). (B) Representative images of synaptic markers in naïve and imprinted animals. mCherry::RAB-3 was expressed in AIY to mark presynaptic vesicles and the glutamate receptor GLR-1::GFP was expressed in RIA to mark postsynaptic regions. Arrowheads mark the regions of AIY-RIA synapses; orientation is as in (A). For each condition, two images show animals with moderate (top) or low (bottom) colocalization. (C) Colocalization of RAB-3 and GLR-1 in naïve and imprinted adults. Each dot represents the number of colocalized voxels in one animal, and bar represents population mean. Colored arrowheads in (B) correspond to similarly colored dots in (C).

Figure 4.2 Responses of memory formation neurons AIB and RIM after imprinting

(A-B) Average (A) AIB and (B) RIM calcium responses to 60 s alternations between OP50- and PA14-conditioned medium in naïve (black) and imprinted (red) animals. Average differences before and after odor transitions were compared in naïve and imprinted animals; *P* values were generated by two-way ANOVA with the Bonferroni correction (** $P < 0.01$, ns not significant).

(C) AIB and RIM have bistable activity states in naïve and imprinted animals. Trials were classified into low activity state ($dF/F < 0.5$, light grey) or high activity state ($dF/F > 0.5$, dark grey) prior to PA14 addition (Gordus et al., 2015). A fraction of animals did not respond in any trial; this fraction was comparable in naive (5/19) and imprinted (7/24) animals.

(D-E) Heatmaps of individual trials at high (top) or low (bottom) calcium states for (D) AIB and (E) RIM. Heatmaps show GCaMP responses to 60 s alternations between OP50- and PA14-conditioned medium.

(F) Schematic illustration of the off state duration.

(G) Cumulative distribution of the durations of the first OFF response after PA addition in AIB and RIM in naïve and imprinted animals. *P* values comparing distributions were generated by nonparametric Kolmogorov-Smirnov test (** $P < 0.01$).

Calcium traces were normalized on a 0-1 scale, see Experimental Procedures. Shaded regions around traces are ±SEM. Blue background: PA14-conditioned medium; yellow: OP50-conditioned medium. AIB and RIM: naïve, n=14 animals (excluding 5 non-responders); imprinted, n=17 animals (excluding 7 non-responders), Each animal was subjected to 4 trials during a 9 minute recording.

Figure 4.2

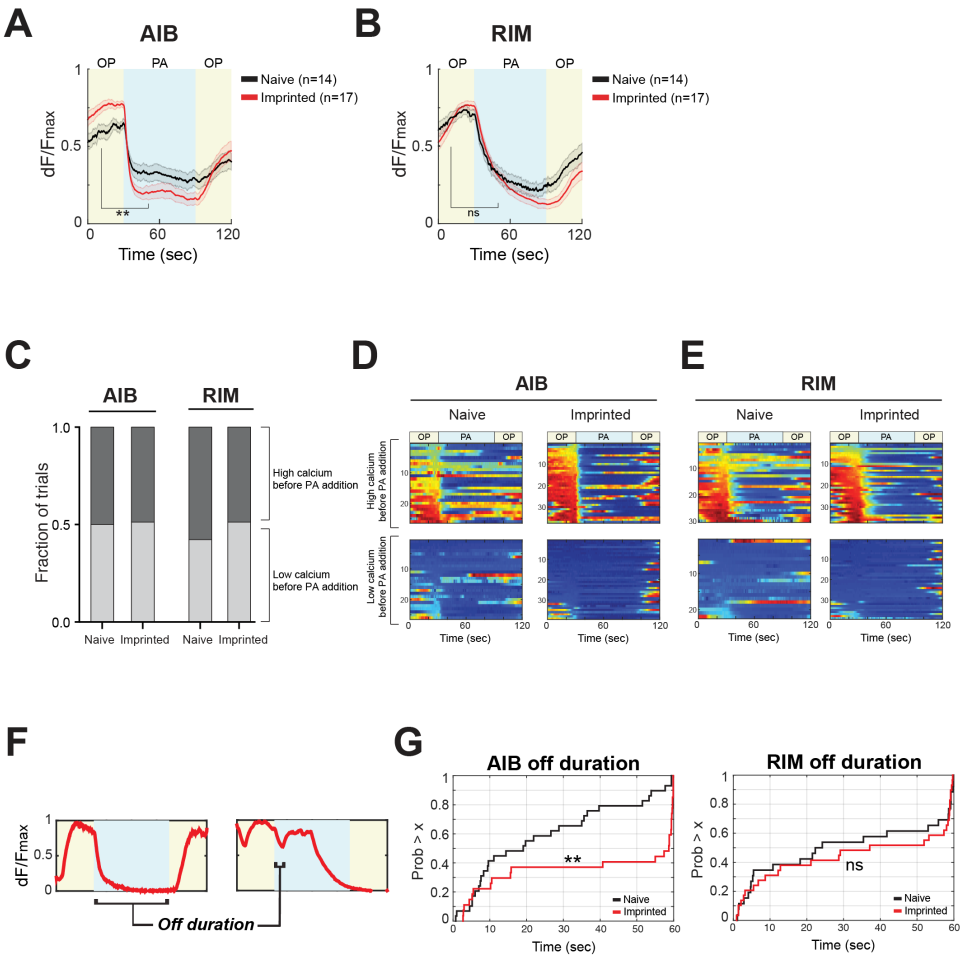
A
AIB
OP
PA
OP
Naive (n=14)
Imprinted (n=17)
dF/Fmax
**
Time (sec)
B
RIM
ns
C
AIB
RIM
Fraction of trials
High calcium before PA addition
Low calcium before PA addition
Naive
Imprinted
D
AIB
E
RIM
Time (sec)
F
dF/Fmax
Off duration
G
AIB off duration
RIM off duration
Prob > x
Time (sec)

Figure 4.3

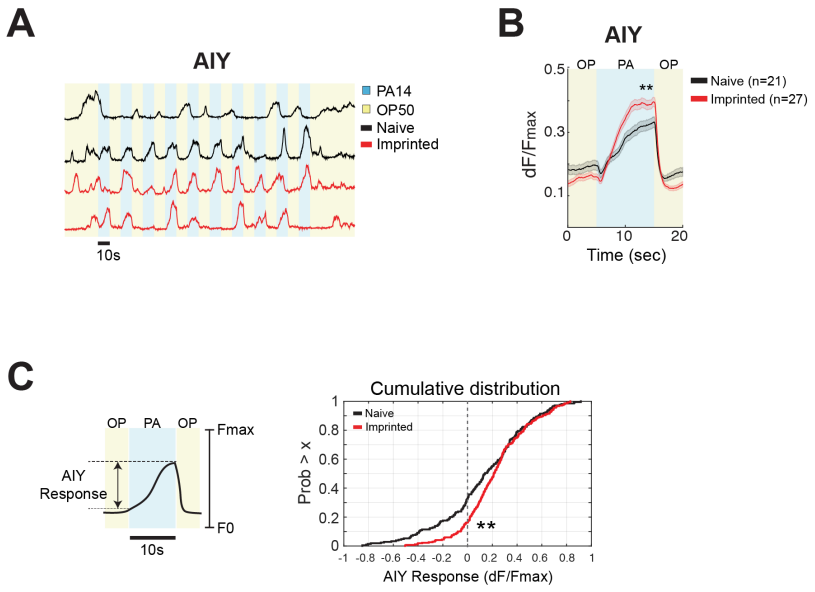

Figure 4.3 Responses of memory retrieval neurons AIY after imprinting

(A) Representative traces of AIY axonal GCaMP5A response to 10s alternations of OP50- and PA14-conditioned medium in naïve (black) and imprinted (red) animals. AIY does not respond in all trials but does respond in all animals.

(B) Average AIY calcium responses to 10 s alternations between OP50- and PA14-conditioned medium in naïve (black) and imprinted (red) animals. Average differences before and after odor transitions were compared in naïve and imprinted animals; *P* values were generated by two-way ANOVA with the Bonferroni correction (** $P < 0.01$).

(C) Cumulative distribution of AIY responses. Left, illustration of AIY response to bacterial alternations. Each response to PA14 was normalized to the peak F_{max} over 10 trials. Right, cumulative distribution of the calcium responses of naïve (n=27) and imprinted (n=29) animals. *P* values comparing distributions were generated by nonparametric Kolmogorov-Smirnov test (**$P < 0.01$).

Figure 4.4

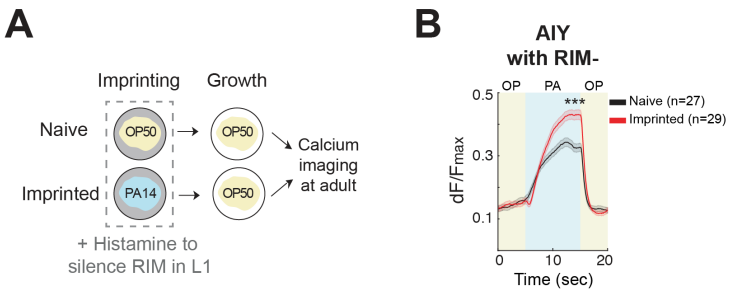

Figure 4.4 AIY calcium response precluding imprinting

(A) Illustration of the experiment.

(B) Average AIY calcium responses to 10 s alternations between OP50- and PA14-conditioned medium in naïve (black) and imprinted (red) animals of which their RIM neurons were silenced during L1, compared to Figure 4.3B. Average differences before and after odor transitions were compared in naïve and imprinted animals; *P* values were generated by two-way ANOVA with the Bonferroni correction (*** $P < 0.001$).

Figure 4.5 Responses of memory retrieval neurons RIA after imprinting

(A) Schematic illustration of RIA neuron showing nrD and nrV axonal compartments.

(B) Representative traces of RIA nrD (blue) and nrV (green) calcium in naïve animal responding to 10s alternations between OP50- and PA14-conditioned medium, showing synchronous and anti-synchronous events.

(C-F) RIA responses to pathogen stimuli. (C and E) Average GCaMP response to 10s alternations between OP50- and PA14-conditioned medium in RIA axonal compartments (C) nrV or (E) nrD of naïve (black) and imprinted (red) animals. Shaded regions are ±SEM. Blue shading: PA14-conditioned medium; yellow shading: OP50-conditioned medium. Naïve, n=41 animals; imprinted, n=55 animals. The average difference in calcium for 1 sec before and 1 sec after odor transitions was compared between naïve and imprinted animals; *P* values were generated by two-way ANOVA with Tukey's correction (*** $P<0.001$). (D and F) Calcium dynamics heatmap of RIA axonal compartment (D) nrV or (F) nrD during odor transitions, from PA14 to OP50 or OP50 to PA14, respectively. Traces were ordered according to the time derivatives of response at odor addition (time = 0). Arrowhead indicates calcium activation ($dF/dt>0.01$ $\%s^{-1}$), suppression response ($dF/dt<-0.01$ $\%s^{-1}$), or no response.

Figure 4.5

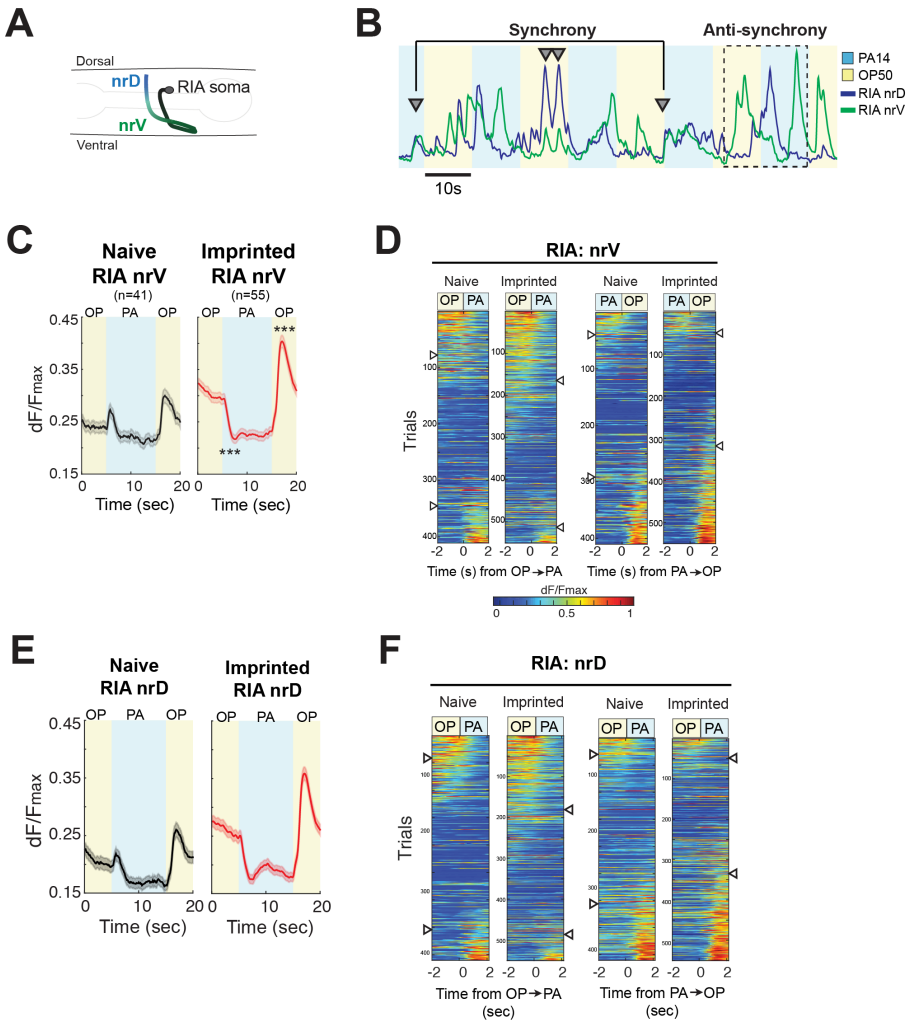
A
Dorsal
nrD
RIA soma
nrV
Ventral
B
Synchrony
Anti-synchrony
PA14
OP50
RIA nrD
RIA nrV
10s
C
Naive
RIA nrV
(n=41)
Imprinted
RIA nrV
(n=55)
OP PA OP
dF/Fmax
Time (sec)
***
D
RIA: nrV
Naive
Imprinted
Trials
Time (s) from OP→PA
Time (s) from PA→OP
dF/Fmax
E
Naive
RIA nrD
Imprinted
RIA nrD
F
RIA: nrD
Time from OP→PA (sec)
Time from PA→OP (sec)

Figure 4.6

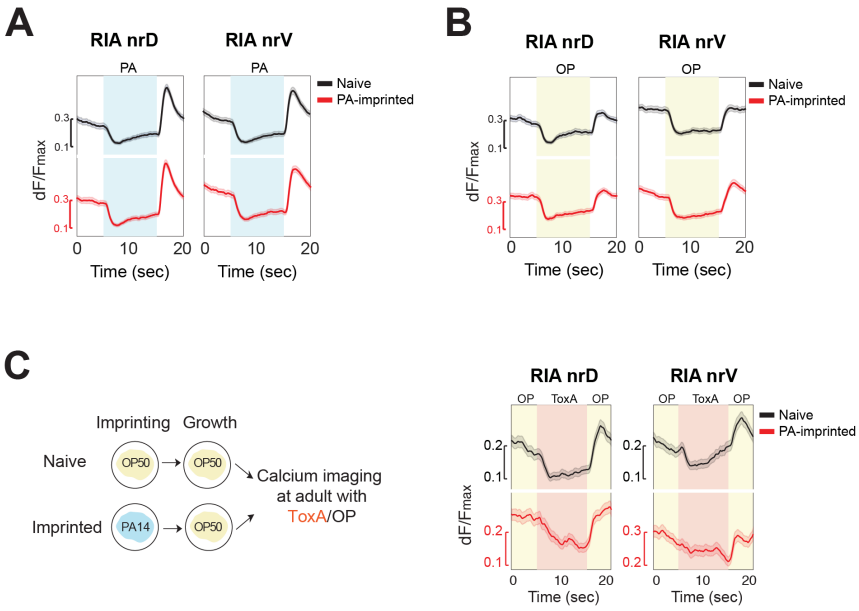

Figure 4.6 Responses of memory retrieval neurons RIA in other context

(A-B) Naïve (black) and imprinted (red) RIA compartmental calcium response to alternating (A) PA14- or (B) OP50-conditioned medium and buffer. Shaded regions are ±SEM. Naïve in PA, n=11 animals, imprinted in PA, n=11 animals; naïve in OP, n=11 animals; imprinted in OP, n=13 animals.

(C) RIA calcium responses of naïve and PA14-imprinted animals to alternating OP50- and ToxA-conditioned medium. Left: schematic illustration of the experiment. Right: average RIA axonal responses of naïve (black) and PA14-imprinted (red) animal. Shaded regions are ±SEM. Pink shading: ToxA-conditioned medium; yellow shading: OP50-conditioned medium.

Figure 4.7 Synchronized activities of RIA after imprinting

(A) Average synchronous calcium flux rate of nrD and nrV compartments of RIA neurons.

(B) Raster plot of synchronous nrD and nrV calcium influx (red) or efflux (blue) in naïve and PA14-imprinted animals, with alternating OP50- and PA14-conditioned medium.

(C) Average RIA synchronous calcium flux rate of naïve and PA14-imprinted animals, with alternating OP50- and ToxA-conditioned medium

(D) Average RIA synchronous calcium flux rate and raster plots of synchronized events from naïve and PA14-imprinted animals with RIM silenced during L1, with alternating OP50- and PA14-conditioned medium.

RIA Calcium dynamics synchrony was defined as previously described: both compartments have time derivative (dF/dt) > 0.005 ($\%s^{-1}$) (influx) or < -0.005 ($\%s^{-1}$) (efflux) were captured as synchronous events (Hendricks et al., 2012, also see Experimental Procedures).

Figure 4.7

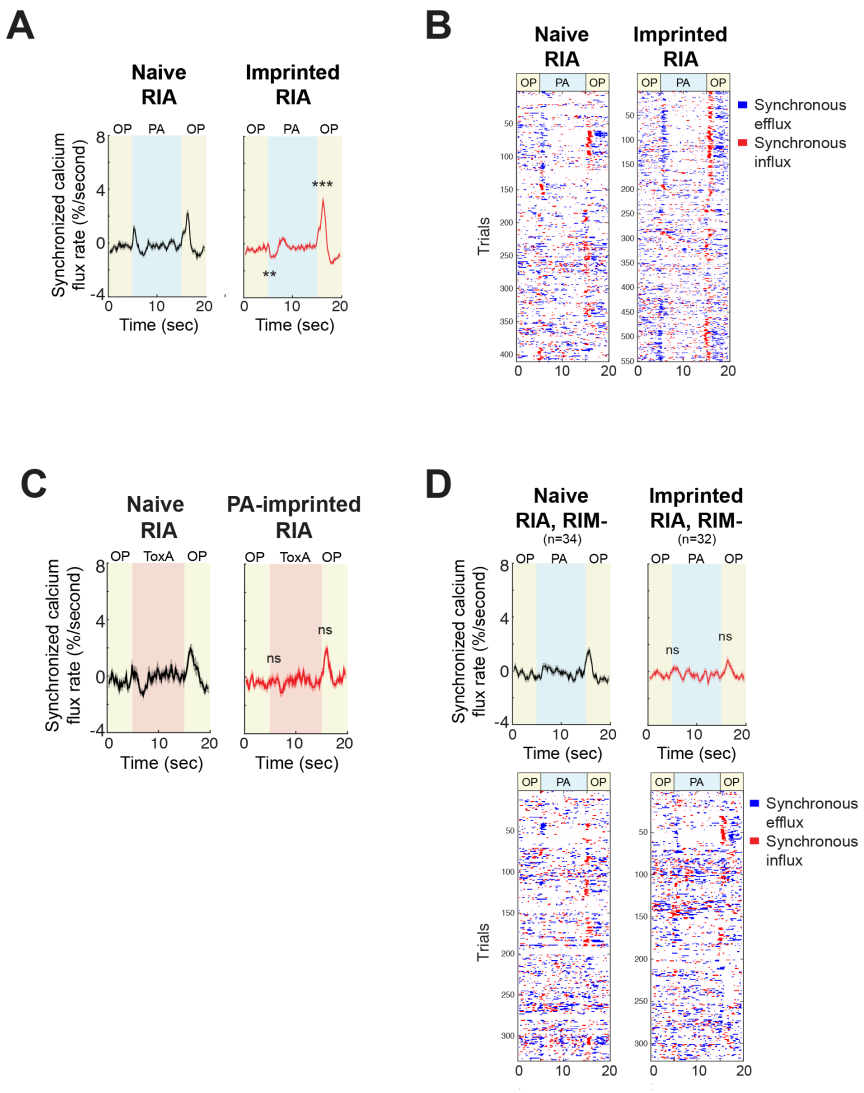
A
Naive RIA
Imprinted RIA
OP PA OP
Synchronized calcium flux rate (%/second)
Time (sec)
**
***
B
Naive RIA
Imprinted RIA
Trials
Synchronous efflux
Synchronous influx
C
Naive RIA
PA-imprinted RIA
OP ToxA OP
ns
D
Naive RIA, RIM- (n=34)
Imprinted RIA, RIM- (n=32)

Figure 4.8

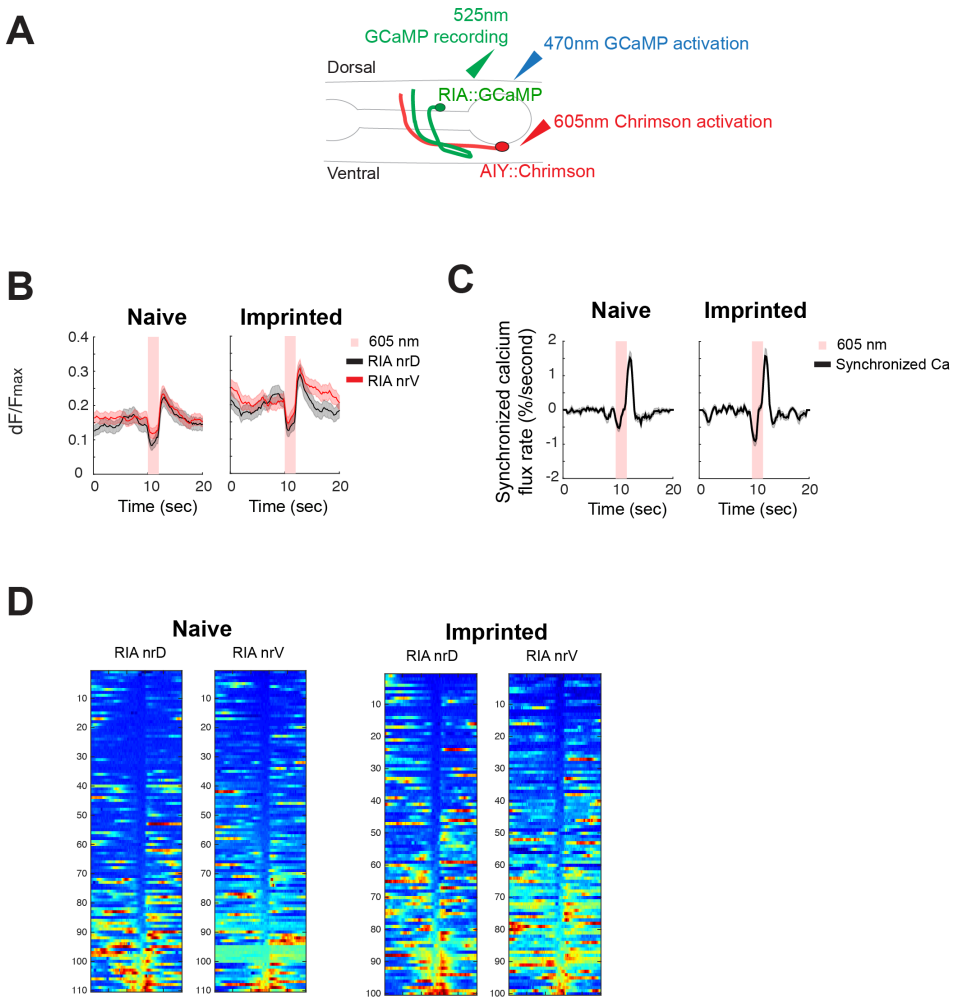

Figure 4.8 Characterization of AIY-RIA synapses

(A) Schematic illustration of the experiment.

(B) RIA averaged compartmental dynamics, (C) synchronized calcium activity, and (D) heatmaps of the compartmental activity in all trials, following 2-second optogenetic activation of AIY neurons. This experiment was performed in the absence of sensory stimulation. Pink shading: Chrimson activation.

Figure 4.9 Multi-neuron calcium imaging with a multi-focal microscope (MFM)

(A) Schematic illustration of the widespread sensory neuronal expression of the nuclear-localized calcium indicator *che-2::GCaMP6_nls*.

(B) A single-frame MFM snapshot of the neurons from both the left side (first three focal planes) and the right side (last three focal planes) of a single animal.

(C-D) (C) Schematic illustration of two cells. (D) A naïve animal's response to 30 s alternations of bacterial conditioned medium, in cell A and B (blue shading: PA14-conditioned media; yellow shading: OP50-conditioned media).

Figure 4.9

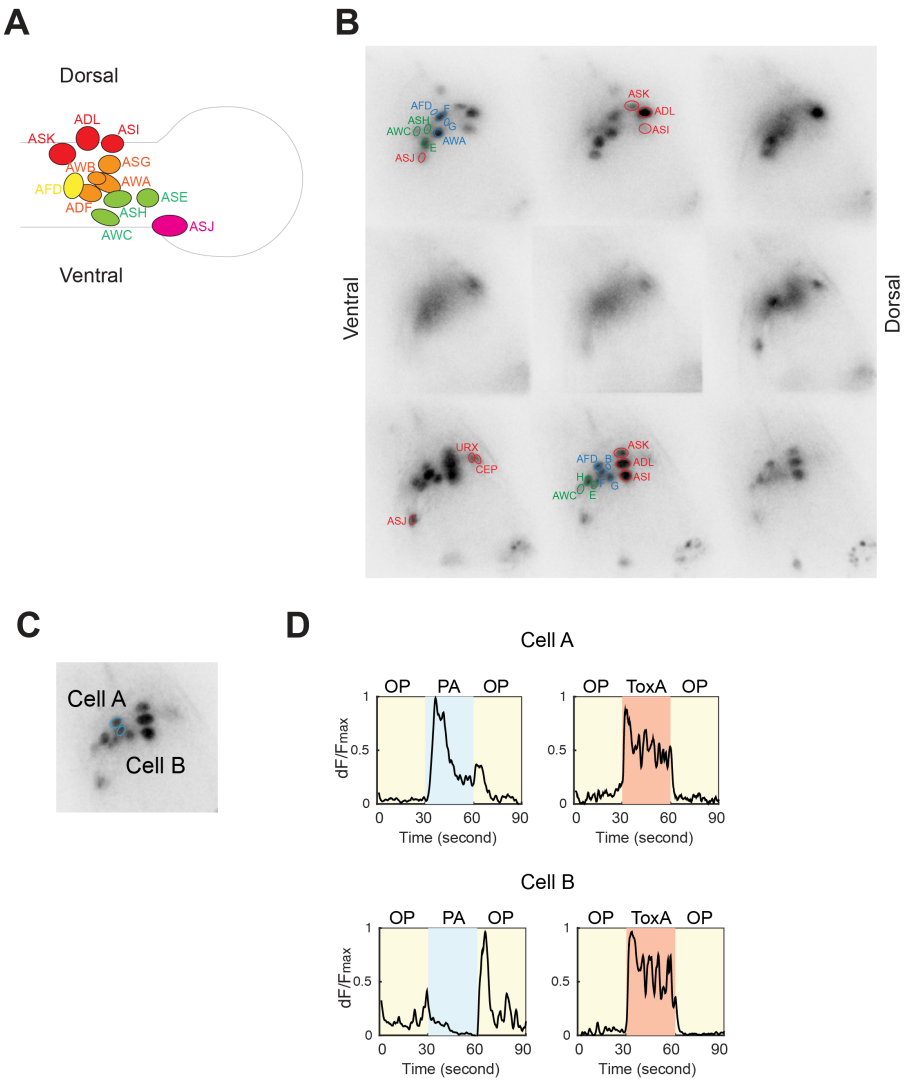
A
Dorsal
ADL
ASI
ASK
ASG
AWB
AWA
AFD
ASE
ADF
ASH
ASJ
AWC
Ventral
B
Ventral
Dorsal
ASK
ADL
ASI
AWA
ASJ
URX
CEP
C
Cell A
Cell B
D
Cell A
OP
PA
OP
ToxA
dF/Fmax
Time (second)
Cell B

Figure 4.10

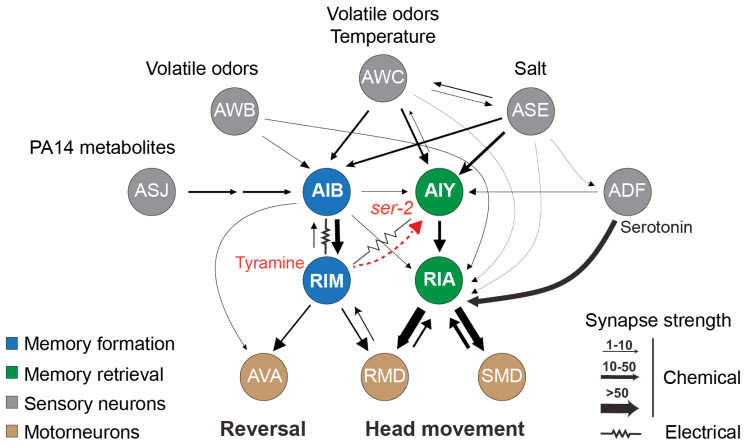

Figure 4.10 A circuit for aversive imprinting

Synaptic strengths are based on the number of chemical synapses from www.wormweb.org. The four imprinting interneurons receive input from many sensory neurons (in grey) that represent different sensory modalities, and send output to motorneurons (in brown) to produce behaviors. Many additional neurons are synaptically connected to this network (Figure 2.4A, Table 1) (White et al., 1986). Adult learning requires either AIB or AIY neurons, whereas aversive imprinting requires both AIB and AIY. Both adult learning and aversive imprinting appear to require AWC, AWB, ADF, RIM, and RIA neurons. Among the neurons shown, AWC, AIB, RIM, and RIA are glutamatergic; AIY, SMD, and RMD are cholinergic; ADF is serotonergic, RIM is tyraminergic, and all neurons express one or more neuropeptides. The SRA-11 receptor required for positive imprinting is required in AIY.

CHAPTER 5:

Conclusions and future experiments

C. elegans that are exposed to pathogenic bacteria in the first larval stage form an associative learned aversion to the bacterial odors that is maintained in mature adults. Imprinted aversion differs from classical olfactory imprinting in its valence. Classical olfactory imprinting drives positive approaching that is often social behavior – homing to the natal stream for salmon (Nevitt et al., 1994), bonding between mammals and their young (Hudson, 1993; Lorenz, 1935), and kin recognition in zebrafish (Gerlach et al., 2008). In contrast, the imprinted aversion in *C. elegans* may be a form of optimal learning (Scott, 1962), forming long-term aversive memory to avoid life-threatening scenarios.

What is the essence and physical substrate of memory? Santiago Ramon y Cajal first proposed in 1894 that memory storage can be achieved by the growth of neural connections (Cajal, 1894). Early genetic studies have characterized crucial molecules, like cAMP and CREB, that allow synaptic plasticity and long-term memory (Brunelli et al., 1976; Cedar et al., 1972). However, it still remains a question at the circuit level how a fixed neural circuit converts naïve attraction to aversion behavior after an early experience – is the aversive pathway simply dormant in the network, or does learning resynthesize the naïve pathway to give it a new valence? Our data suggest that imprinted memory is generated by neuromodulation and represented as changes of network properties. Memory formation and retrieval require two distinct circuits, which are bridged by tyramine and its receptor SER-2. These four interneurons appear to participate and respond to odors in both naïve and imprinted animals, although their functions and ways of deployment have changed after the learning experience. What learning has generated appeared to be neither a single change at a single neuron to impact a single

behavioral output, nor simply activation of a dormant avoidance circuit; it induces reorganization and changes in many neurons, some of which are associated with the aversive memory. The most interesting change among those we have identified is the sign change of RIA response to bacteria, which correlates with a sign change of behavioral preference.

Future directions of study include identifying other relevant sites of the imprinted memory: the requirement of AIY and RIA neurons for memory retrieval has hinted that the memory could reside in these two neurons or in their upstream circuits. Further genetic investigations to map the molecular requirements onto the relevant neural circuits at the relevant times will help to understand how neural dynamics and molecular substrates orchestrate the behavioral memory.

Identifying other neurons and changes that are relevant to aversive imprinting

We investigated four interneurons AIB, RIM, AIY and RIA, due to their known roles in chemotaxis tasks as well as their genetic accessibility. However, there is still much to be learned about other neurons' functions in aversive imprinting. For example, the interneuron AIZ is strongly interconnected with the two key memory neurons AIY and RIA, and AIZ regulates adult learning through serotonin receptor MOD-1 (Zhang et al., 2005). Optogenetic activation of AIZ drives an escape behavior, including a sharp reversal (Li et al., 2014). Is AIZ required for aversive imprinting, and if so, is it required during memory formation or retrieval? Is it possible that the reversed turning bias after imprinting (Figure 2.6) is primarily driven by AIZ? What is AIZ's neuronal response to

pathogens after imprinting? These are unanswered questions that can be addressed with optogenetic and chemogenetic reagents that are specific to AIZ.

Sensory neurons are another class of important circuit elements that are understudied in this dissertation. Chronic ablation of candidate sensory neurons, such as caspase expressions in AWC neurons, lead to both learning defects and chemotaxis defects, making it difficult to separate the effect of sensory detection from contributions to learning (Figure 2.4). Functional imaging may provide useful insights into how imprinting engages different groups of sensory neurons. Pan-sensory neuronal recordings in naïve and PA14-imprinted animals can be used to test their response: either OP-PA (imprinted pathogen) alternation or OP-ToxA (novel pathogen) alternation. Comparing naïve and imprinted animals' profiles to OP-PA alternation should reveal changes induced by learning. Comparing imprinted animals' response to OP-PA and OP-ToxA alternations should reveal how the sensory neurons encode the specificity of the aversive imprinted memory.

Identifying transcriptional changes in imprinting-relevant neurons

One remaining mystery is how neurons encode an enduring memory that lasts days. AIY is the site of convergence of sensory input, tyramine and serotonin modulation, as well as one of the memory retrieval sites. AIY's role in memory retrieval depends on SER-2, a G protein-coupled receptor. I suspect that SER-2 activation leads to changes of gene expressions and transcriptional regulation. Examining transcriptional changes in AIY after imprinting may shed light on the molecular mechanisms of long-term memory.

To compare the transcriptome from a single pair of AIY neurons in naïve and imprinted animals, one may use translational ribosomal affinity purification (TRAP) combined with RNA sequencing (Heiman et al., 2014; Heiman et al., 2008; Flavell, personal communications). Tissue-specific expression of the ribosomal subunit protein RPL-22 fused with an HA tag will allow purifications of AIY-specific mRNA through immunoprecipitation against HA tag from both naïve and imprinted animals, respectively, for RNA sequencing analysis.

Changes of gene expression between naïve and imprinted animals may be due to the memory, or the history of infection, or both. To control for the changes that are not learning specific, one can in parallel perform a TRAP profiling experiment to compare naïve and imprinted animals in *ser-2* null background. Transcriptional changes between naïve and imprinted animals present only in wild-type comparisons, but absent in *ser-2* comparisons, would be more closely linked with learning-related activity.

Compared to the candidate genetic approach that we have been focused on, this experiment will unbiasedly profile transcriptional changes associated with learning, and provide novel insights in the genetic substrates of learning.

Mapping genetic requirements onto the relevant learning circuits

Aversive imprinting requires many genes that express in many different neurons, and their site of functioning can be further investigated. For example, the glutamate AMPAR receptor GLR-1 is required for aversive imprinting but not for adult learning, suggesting that glutamate signaling through the AMPAR receptor may have specific roles

for synthesis of long-term but not medium-term memory (Figure 3.1B) (Table 2). GLR-1 is expressed in about a dozen inter- and motor-neurons (Brockie et al., 2001; Maricq et al., 1995) and its site(s) of function can be narrowed down. Interestingly, introducing a leaky channel with a single nucleotide mutated GLR-1(AT) in AIB neurons of wild-type animals can lead to an imprinting deficit (Figure 3.1B) (Zheng et al., 1999). These results indicate that normal glutamate signaling through GLR-1 is necessary for imprinting, and the loss of its function in AIB is sufficient to disrupt learning. Like GLR-1, AIB interneurons are not required for adult learning but are crucial for aversive imprinting. Further investigating the role of AIB and glutamate signaling, the timing of their action, and the downstream signaling effects may elucidate the differences between adult learning and imprinting.

Another gene that is required for imprinting but not adult learning is CRH-1, the cAMP response element binding (CREB) protein that is required for long-term but not short-term memory in many animal models. CRH-1 is expressed in many neuronal and non-neuronal tissues, and is also required for thermotaxis and longevity (Mair et al., 2011; Rose and Rankin, 2006). To map its action sites, I suggest the following experiments. First, a CREB reporter strain, in which CRH-1 binding leads to GFP expression, can shed light on neurons with enhanced CREB activities during memory formation, consolidation, or retrieval, to uncover the potential sites and timing of CRH-1 action. Second, selective knockout or rescue of CRH-1 in these sites will confirm whether CREB in those neurons is required for aversive imprinting. Third, since CREB is a transcription factor, performing RNA sequencing of the neuronal sites of action of CREB, in the presence and

absence of imprinting and the presence and absence of the *crh-1* gene, can elucidate CREB-induced changes of gene expression specific to imprinting.

C. elegans double-stranded RNA (dsRNA) can silence genes in a systemic way – if formed in one cell, dsRNA can modulate gene expressions across tissues (Feinberg and Hunter, 2003). Since very little is known about how the pathogen infection signal from the intestine or hypodermis relays to the nervous system, it is plausible that the gut cells, which recognize pathogen infection and odor specificity, can trigger systemic RNAi specific to the chemoreceptors that match the pathogen smells to form a memory. The several tested RNAi pathways are not critical for aversive imprinting; however, other argonaute protein candidates can be tested in the future.

Behavioral characterization and exploration

I characterized aversive imprinting as a form of associative learning that occurs during a critical period, which has partial but not complete overlap of genetic and neural circuit requirements with adult learning. However, it is not yet fully known how many different forms of memory an animal can preserve and recall with such a compact nervous system. For example, can animals aversively imprinted on the pathogen PA14 learn to avoid another pathogen, ToxA, during adult training? To what degree do the imprinted memory and adult learned memory share the same formation or retrieval pathway, and can both forms of memory co-exist? If not, which memory would prevail – the earlier formed, enduring imprinted memory, or the recently acquired adult-trained

memory? Answering each of these questions can lead to a better understanding of the neural basis of both forms of memory and their interrelationships.

EXPERIMENTAL PROCEDURES

Nematode growth and molecular biology

All strains were maintained at room temperature (22-23°C) on nematode growth medium (NGM) plate, seeded with *E. coli* OP50 bacteria as a food source (Brenner, 1974). Wild-type animals were the Bristol strain N2. Standard molecular biology methods were used.

Bacterial preparation for imprinting

For PA14, a single colony was inoculated into 2 mL LB and grown at 26°C overnight (OD_{600} 2~3). For the BL21 strain expressing ToxA from the T7 promoter, a single colony was inoculated into 2 mL LB containing antibiotics (100 μg/mL carbenicillin) and grown at 37°C overnight (OD_{600} 2~3), diluted to OD_{600} ~ 1, and induced with 10 mM IPTG for 30 min. 30 μL of the bacterial culture were seeded onto NGM plates with IPTG and incubated at room temperature (22°C) for 24-48 hours before use.

Imprinting training

Eggs from young adult hermaphrodites were obtained by bleaching (Stiernagle, 2006), placed on an NGM plate with pathogen or control OP50 bacteria, and incubated at room temperature (22°C). Eggs hatched after ~7 hour, and after 19 hours (12 hours of post-hatching training), both naïve and imprinted L1 larvae were washed off the plate with 200 nM neomycin (Tan et al., 1999) in M9 buffer, rinsed three times, transferred to an OP50-seeded plate, washed again with neomycin solution after 24 hours, and transferred to a second OP50-seeded plate where they were grown at room temperature (22°C).

Food choice assay (modified from (Zhang et al., 2005))

Fresh overnight bacterial cultures were diluted to OD_{600} = 1, and 20 μL of each bacteria suspension was seeded on a round NGM plate (radius = 5 cm) and incubated at room temperature (22°C) for <2 hours. After this relatively short incubation, chemotaxis is dominated by olfactory cues rather than slowly-diffusing water-soluble cues. To start the assay, young adult hermaphrodites were washed from their growth plate with M9 buffer, rinsed twice, and 100-200 animals were placed in the middle of the assay plate, equidistant from the bacterial lawns. Assays were incubated at room temperature for 60 minutes before being placed in 4°C to end the assay. To test animals bearing transgenic extrachromosomal arrays, a COPAS large particle flow cytometry sorter (Union Biometrica) was used to collect the L4 stage animals that expressed the transgenic array one day prior to the food choice assay.

Choice index, learning index, and statistical analysis.

The chemotaxis choice index was calculated as fraction of the animals in PA14 lawn minus the fraction of animals in OP50 lawn; a choice index of zero represents an equal preference for both bacteria. Each learning index was calculated from a random pair of naïve and imprinted assays on the same day by subtracting the naïve choice index from the imprinted choice index; a learning index of zero represents no change of preference after imprinting. Box-and-whisker plots were generated by Prism (GraphPad Software). The median is marked; box represents the first and third quartiles, and whiskers represent

the 10^{th}-90^{th} percentiles. Most statistical comparisons were done either by ANOVA with the Dunnett correction for multiple comparisons or by the nonparametric Mann-Whitney test, as noted in the figure legends.

Post-imprinting evaluation of neuronal survival

To assess effects of imprinting on neuronal health and survival, the four neuron classes AIB, RIM, AIY, and RIA were examined using the cell-specific SL2::GFP markers that accompanied the HisCl1 transgenes, in animals that were not treated with histamine. Similar expression was observed in naïve and imprinted adults, suggesting that the integrity of the cells was maintained after early pathogen exposure.

Histamine and tyramine supplementation (Pokala et al., 2014)

1 M histamine-dihydrochloride (Sigma-Aldrich) or tyramine hydrochloride (Sigma-Aldrich) stocks were made with distilled water, sterile filtered, and diluted into NGM agar that had cooled to 55°C at 10 mM. NGM agar plates were stored at 4°C and used within 1 week.

Chemotaxis recordings and analysis

40-50 animals were placed on a standard food choice assay plate (radius = 5 cm), and a 40-minute movie was recorded at 3 frames per second with Streampix software and a 6.6 MP PL-B781F CMOS camera (Pixelink). Animals' trajectories were extracted by a

custom Matlab (MathWorks) script. A pirouette event was defined as a reversal coupled with an omega turn, and identified as a sharp change in angular speed (≥75 degree/s), followed by a sharp reorientation (body-enclosing ellipse eccentricity ≤0.875, filtered by an angular speed threshold ≥60 degree/s), as previously described (Pokala et al., 2014). Pirouette frequency was calculated by binning the events with respect to the incoming angle toward the stimuli (PA14 lawn) before the reorientation, in 30° intervals. The normalized pirouette frequency for each assay was calculated by dividing the pirouette frequency at each angle bin by the average pirouette frequency of the assay, as previously described (Tsunozaki et al., 2008).

Calcium imaging and data analysis

Bacteria-conditioned medium was prepared on the day of the experiment by filtering a fresh overnight bacterial culture in NGM buffer (with peptone) with a sterile bottle top filter (Nalgene) into amber glass vials (EssVials Inc).

Young transgenic adults expressing GCaMP calcium sensors (Tian et al., 2009) were transferred to a fresh NGM plate, starved for 5 minute, then loaded into a custom PDMS chamber which restrained the animal to allow precise odor stimulation, as previously described (Chalasani et al., 2007). The acetylcholine agonist (-)-tetramisole hydrochloride (Sigma-Aldrich, L9756) at 1 mM was used only during transfer of animals into the chip, but not during imaging, to paralyze body wall muscles and keep animals stationary. Alternating bacteria-conditioned media stimuli were delivered every 60 seconds (AIB, RIM), 10 seconds (AIY, RIA), or 30 seconds (pan-sensory neurons). 60-

second alternation was used in AIB and RIM imaging to capture their slow calcium dynamics (Gordus et al., 2015).

Fluorescent recording protocols were modified from (Gordus et al., 2015). For all the interneurons: calcium signals were recorded at 10 frame per second using a 40x objective (regular imaging in Chapter 4), or 5 frame per second using a 40x objective with 10-millisecond pulse illumination every 100 milliseconds (Chrimson-GCaMP imaging in Chapter 4); experiments were performed on an upright Axioskop 2 microscope (Zeiss), with Metamorph software (Molecular Devices) and an iXon3 DU-897 EMCCD camera (Andor). For the multi-neuronal imaging (Chapter 4): calcium signals were recorded at 5 frame per second using a 60x objective on a custom made MFM microscope (Abrahamsson et al., 2013), with Metamorph software (Molecular Devices) and an iXon3 EMCCD camera (Andor).

Imaging data were analyzed using custom scripts (ImageJ). MATLAB (MathWorks) was used for subsequent data analysis and display as previously described (Gordus et al., 2015; Larsch et al., 2013). GCaMP fluorescence was divided by the lowest 5% as a baseline value, and then divided by the maximal value in the trace to obtain the normalized calcium response dF/F_{max} on a 0-1 scale for each animal. Each animal was normalized only once for data taken throughout a full experiment with many trials. Responses from multiple trials were averaged to obtain a mean population response and SEM. Because of the bimodal responses of AIB and RIM, only the trials in which neurons were in high activity states before PA addition were averaged. RIA calcium synchrony was calculated as previously described as events in which both axon

compartments had time derivatives > 0.005 (% s^{-1}) (influx) or < -0.005 (% s^{-1}) (efflux) (Hendricks et al., 2012).

Pathogenic infection evaluation assay

To evaluate the persistent infection of animals, 4-5 adults were washed quickly in a droplet of M9 buffer with 50 μM neomycin to remove external bacteria, followed by washes in a droplet of M9 buffer without antibiotics, then transferred to an Eppendorf tube and homogenized. 10 μL of the lysate was plated onto a fresh MacConkey plate at 30°C overnight, and the number of PA14 and OP50 colonies was scored the following day.

Foraging assay and analysis

10-12 adult hermaphrodites were conditioned for an hour on an NGM plate with a uniform OP50 lawn. After quickly transferring them to an empty NGM plate to remove the excessive food, animals were transferred to the assay NGM plate with a filter paper barrier (Whatman) saturated with 20 mM $CuCl_2$ (radius = 5 cm) to restrict them to the recorded area. Recording of the assay plate (with the lid on) began 3 min after the food removal at 3 frames per second for 60 minutes, with Streampix software and a 15 MP PL-D7715 CMOS camera (Pixelink). Animals' trajectories were extracted by a custom Matlab (MathWorks) script, and the frequency of pirouette (reversal coupled with a high-angle turn) was binned every four minutes.

Optogenetic stimulation behavioral assay

L4 animals expressing an AIB::Channelrhodopsin2(H134R) array were raised overnight on a NGM plate freshly seeded with OP50 containing 50 μM all-*trans* retinal (Sigma-Aldrich). On the next day, 20-25 adult hermaphrodites were first transferred to an empty NGM plate to starve for 15 minutes, then transferred to the assay NGM plate with a filter paper barrier (Whatman) saturated with 20 mM $CuCl_2$ (radius = 2 cm) to restrict them to the recorded area. After 15 minutes of conditioning, videos were recorded for 20 minutes at 3 frames per second, with Streampix software and a 1.3 MP PL-A741 camera (Pixelink). Blue light pulses were delivered with an LED (455 nm, ~20 $\mu W/mm^2$, Mightex) that was controlled with a custom Matlab (MathWorks) script. Animals were exposed to repeated blue light stimulation for 20 seconds, followed by 100 seconds of dark recovery. Animals' trajectories were extracted by a custom Matlab (MathWorks) script. Reorientation events were aligned to light illumination, and event frequency was binned every 5 sec.

Confocal microscopy and image analysis

Adult hermaphrodites were mounted on 1% agarose pads with 10 mM sodium azide in M9 solution. Images were acquired on an Inverted Axio Observer Z1 LSM 780 laser scanning confocal microscope with a 63x objective (Zeiss), processed by ImageJ, and quantified by Imaris (Bitplane).

Strain List

Strain	Genotype	Comment
CX16632	*kyIs693[pNP502(tdc-1::HisCl1::sl2::mcherry)]*	*RIM/RIC::HisCl1*
CX15758	*kyIs631[pNP472(inx-1::HisCl1::sl2::gfp)]*	*AIB::HisCl1*
CX16880	*kyEx5847[pNP501(ttx-3::HisCl1::sl2::gfp)]*	*AIY::HisCl1*
CX15141	*kyEx5063[pNP443(glr-3::HisCl1::sl2::mcherry)]*	*RIA::HisCl1*
MT15434	*tph-1(mg280) II*	Separated from *cam-1* mutation
MT9668	*mod-1(ok103) V*	
CX13503	*eat-4(ky5) III* (outcrossed 10x)	
KP4	*glr-1(n2461) III* (outcrossed 4x)	
VM1846	*glr-3(ak57) I*	
VW4509	*nmr-1(ak4) II* (outcrossed 12x)	
MT9973	*crh-1(n3315) III* (outcrossed 8x)	
YT17	*crh-1(tz2) II* (outcrossed 6x*)*	
CX13778	*sra-11(ok630) II* (outcrossed 3x*)*	
MT13113	*tdc-1(n3419) II* (outcrossed 11x)	
MT10548	*tdc-1(n3420) II*	
MT9455	*tbh-1(n3247) X* (outcrossed 8x)	
CX16258	*tdc-1(n3419) II; kyEx5551[pXJ23(tdc-1::tdc-1a::sl2::gfp)]*	RIM/RIC rescue
CX16355	*tdc-1(n3419) II; kyEx5578[pXJ08(gcy-13::tdc-1a::sl2::gfp)]*	RIM rescue
CX16257	*tdc-1(n3419) II; kyEx5550[pXJ30(tbh-1::tdc-1a::sl2::gfp)]*	RIC rescue
CX13485	*tyra-2(tm1846) X* (outcrossed 2x)	
CX11839	*tyra-3(ok325) X* (outcrossed 4x)	
CX11501	*lgc-55(tm2913) V* (outcrossed 4x)	
OH313	*ser-2(pk1357) X* (outcrossed 4x)	
CX16924	*ser-2(pk1357) X; kyEx5880[pXJ05(ser-2p1::ser-2e::sl2::gfp)]*	*ser2p1* rescue
CX16516	*ser-2(pk1357) X; kyEx5634 [pXJ14(ser-2p2::ser-2e::sl2::gfp)]*	*ser2p2* rescue

CX16788	*ser-2(pk1357) X; kyEx5785[pXJ29(ser-2p2::inv[ser-2e::sl2::gfp])]; kyEx5786[pSF11(tag-168::nCre)]*	Pan-neuronal Cre rescue
CX16789	*ser-2(pk1357) X; kyEx5785[pXJ29(ser-2p2::inv[ser-2e::sl2::gfp])]; kyEx5787[pXJ27(unc-47::nCre);pSF177(ceh-17::nCre)]*	RME, SIA Cre rescue
CX16790	*ser-2(pk1357) X; kyEx5785[pXJ29(ser-2p2::inv[ser-2e::sl2::gfp])]; kyEx5788[pSF144(odr-2b::nCre)]*	AIZ Cre rescue
CX16962	*ser-2(pk1357) X; kyEx5785[pXJ29(ser-2p2::inv[ser-2e::sl2::gfp])]; kyEx5900[pXJ28(flp-18::nCre)]*	AIY Cre rescue
CX14996	*kyEx4965[pAG03(inx-1::GCaMP3), pAG02(tdc-1::GCaMP3), pAG01(rig-3::GCaMP3)]*	*AIB,RIM,AVA:: GCaMP*
CX16891	*kyEx4857[pSF167(mod-1::GCaMP5A)]; kyEx5846[pXJ07(gcy-13::HisCl1::sl2::mcherry)]*	*AIY::GCaMP; RIM::HisCl1*
CX16662	*kyIs640[pXJ25(glr-3::GCaMP5A(PCR product))]; kyIs693[pNP502(tdc-1::HisCl1::sl2::cherry)]*	*RIA::GCaMP; RIM/RIC::HisCl1*
CX16164	*kyIs644[pXJ33(che-2::GCaMP6s_nls::sl2::mcherry)]*	*Pan-sensory GCaMP*
CX16995	*kyIs640[pXJ25(glr-3::GCaMP5A(PCR product))]; kyEx5907[pXJ34(ttx-3::Chrimson::sl2::cherry)]*	*RIA::GCaMP; AIY::Chrimson*
CX13210	*kyEx3838[pNP325(inx-1::ChR2(H134R)GFP)]*	*AIB::ChR2*
CX13432	*kyEx4010[pGL66(inx-1::TetanusToxinLC::mcherry)]*	*AIB::TeTx*
CX14993	*kyEx4962[pNP302(tdc-1::TetanusToxinLC::mcherry)]*	*RIM::TeTx*
CX14284	*kyEx4533[pSF238(ttx-3::unc-103(gf)::sl2::gfp)]*	*AIY::unc-103(gf)*
CX9308	*kyEx1917[pNP155(glr-3:TetanusToxinLC::mCherry)]*	*RIA::TeTx*
CX14597	*kyEx4745[pJL29(gcy-28d::unc-103(gf)::sl2::mCherry)]*	*AIA::unc-103(gf)*
	Is[str-1p::mCasp1], a gift from Yoshida et al. (2012).	*AWB::mCasp*
	Is[ceh-36p::mCasp1], a gift from Yoshida et al. (2012).	*AWC/ASE::mCasp*

	Is[sra-6p::mCasp1], a gift from Yoshida et al. (2012).	*ASH/ASI/PVQ::mCasp*
DCR1410	*wyIs45[ttx-3::GFP::rab-3]; olaEx480[glr-3::mCherry]*	*AIY::gfp, RIA::mCherry*
VM4314	*glr-1(ky176) III*	
CX13444	*kyEx4022[inx-1::glr-1(AT)::sl2::GFP]*	*AIB::glr-1(AT)*
CX14844	*sid-1(pk3321) V* (outcrossed 4x)	
WM49	*rde-4(ne301) III* (outcrossed 4x)	
CX14872	*rde-1(ne219) V* (outcrossed 2x)	

REFERENCES

Abrahamsson, S., Chen, J., Hajj, B., Stallinga, S., Katsov, A.Y., Wisniewski, J., Mizuguchi, G., Soule, P., Mueller, F., Dugast Darzacq, C.*, et al.* (2013). Fast multicolor 3D imaging using aberration-corrected multifocus microscopy. Nature methods *10*, 60-63.

Akalal, D.B., Yu, D., and Davis, R.L. (2011). The long-term memory trace formed in the *Drosophila* alpha/beta mushroom body neurons is abolished in long-term memory mutants. The Journal of neuroscience *31*, 5643-5647.

Albert, P.S., and Riddle, D.L. (1983). Developmental alterations in sensory neuroanatomy of the *Caenorhabditis elegans* dauer larva. The Journal of comparative neurology *219*, 461-481.

Alkema, M.J., Hunter-Ensor, M., Ringstad, N., and Horvitz, H.R. (2005). Tyramine functions independently of octopamine in the *Caenorhabditis elegans* nervous system. Neuron *46*, 247-260.

Amano, H., and Maruyama, I.N. (2011). Aversive olfactory learning and associative long-term memory in *Caenorhabditis elegans*. Learn Mem *18*, 654-665.

Ardiel, E.L., and Rankin, C.H. (2010). An elegant mind: learning and memory in *Caenorhabditis elegans*. Learn Mem *17*, 191-201.

Aso, Y., Hattori, D., Yu, Y., Johnston, R.M., Iyer, N.A., Ngo, T.T., Dionne, H., Abbott, L.F., Axel, R., Tanimoto, H.*, et al.* (2014). The neuronal architecture of the mushroom body provides a logic for associative learning. eLife *3*, e04577.

Barco, A., Bailey, C.H., and Kandel, E.R. (2006). Common molecular mechanisms in explicit and implicit memory. Journal of neurochemistry *97*, 1520-1533.

Bargmann, C.I. (2006). Chemosensation in *C. elegans* (October 25, 2006), *WormBook*, ed. The *C. elegans* Research Community, WormBook, doi/10.1895/wormbook.1.123.1, http://www.wormbook.org

Bargmann, C.I., Hartwieg, E., and Horvitz, H.R. (1993). Odorant-selective genes and neurons mediate olfaction in *C. elegans*. Cell *74*, 515-527.

Bargmann, C.I., and Horvitz, H.R. (1991). Chemosensory neurons with overlapping functions direct chemotaxis to multiple chemicals in *C. elegans*. Neuron *7*, 729-742.

Bartsch, D., Ghirardi, M., Casadio, A., Giustetto, M., Karl, K.A., Zhu, H., and Kandel, E.R. (2000). Enhancement of memory-related long-term facilitation by ApAF, a novel transcription factor that acts downstream from both CREB1 and CREB2. Cell *103*, 595-608.

Bartsch, D., Ghirardi, M., Skehel, P.A., Karl, K.A., Herder, S.P., Chen, M., Bailey, C.H., and Kandel, E.R. (1995). *Aplysia* CREB2 represses long-term facilitation: relief of repression converts transient facilitation into long-term functional and structural change. Cell *83*, 979-992.

Beck, C.D., and Rankin, C.H. (1995). Heat shock disrupts long-term memory consolidation in *Caenorhabditis elegans*. Learn Mem *2*, 161-177.

Bottjer, S.W., Miesner, E.A., and Arnold, A.P. (1984). Forebrain lesions disrupt development but not maintenance of song in passerine birds. Science *224*, 901-903.

Bouzaiane, E., Trannoy, S., Scheunemann, L., Placais, P.Y., and Preat, T. (2015). Two independent mushroom body output circuits retrieve the six discrete components of *Drosophila* aversive memory. Cell reports *11*, 1280-1292.

Brandt, J.P., and Ringstad, N. (2015). Toll-like receptor signaling promotes development and function of sensory neurons required for a *C. elegans* pathogen-avoidance behavior. Current Biology *25*, 2228-2237

Brainard, M.S., and Knudsen, E.I. (1993). Experience-dependent plasticity in the inferior colliculus: a site for visual calibration of the neural representation of auditory space in the barn owl. The Journal of neuroscience *13*, 4589-4608.

Brainard, M.S., and Knudsen, E.I. (1998). Sensitive periods for visual calibration of the auditory space map in the barn owl optic tectum. The Journal of neuroscience *18*, 3929-3942.

Breer, H., Boekhoff, I., and Tareilus, E. (1990). Rapid kinetics of second messenger formation in olfactory transduction. Nature *345*, 65-68.

Brenner, S. (1974). The genetics of *Caenorhabditis elegans*. Genetics *77*, 71-94.

Brockie, P.J., Madsen, D.M., Zheng, Y., Mellem, J., and Maricq, A.V. (2001). Differential expression of glutamate receptor subunits in the nervous system of Caenorhabditis elegans and their regulation by the homeodomain protein UNC-42. The Journal of neuroscience *21*, 1510-1522.

Brunelli, M., Castellucci, V., and Kandel, E.R. (1976). Synaptic facilitation and behavioral sensitization in *Aplysia*: possible role of serotonin and cyclic AMP. Science *194*, 1178-1181.

Burke, C.J., Huetteroth, W., Owald, D., Perisse, E., Krashes, M.J., Das, G., Gohl, D., Silies, M., Certel, S., and Waddell, S. (2012). Layered reward signalling through octopamine and dopamine in *Drosophila*. Nature *492*, 433-437.

Byers, D., Davis, R.L., and Kiger, J.A., Jr. (1981). Defect in cyclic AMP phosphodiesterase due to the dunce mutation of learning in *Drosophila* melanogaster. Nature *289*, 79-81.

Byrne, J.H., and Kandel, E.R. (1996). Presynaptic facilitation revisited: state and time dependence. The Journal of neuroscience *16*, 425-435.

Cajal, S.R.Y. (1894). The Croonian Lecture: La Fine Structure des Centres Nerveux. Proceedings of the Royal Society of London *55*, 444-468.

Caron, S.J., Ruta, V., Abbott, L.F., and Axel, R. (2013). Random convergence of olfactory inputs in the *Drosophila* mushroom body. Nature *497*, 113-117.

Cassada, R.C., and Russell, R.L. (1975). The dauerlarva, a post-embryonic developmental variant of the nematode *Caenorhabditis elegans*. Developmental biology *46*, 326-342.

Cassenaer, S., and Laurent, G. (2012). Conditional modulation of spike-timing-dependent plasticity for olfactory learning. Nature *482*, 47-52.

Castellucci, V., and Kandel, E.R. (1976). Presynaptic facilitation as a mechanism for behavioral sensitization in *Aplysia*. Science *194*, 1176-1178.

Cedar, H., Kandel, E.R., and Schwartz, J.H. (1972). Cyclic adenosine monophosphate in the nervous system of *Aplysia californica*. I. Increased synthesis in response to synaptic stimulation. J Gen Physiol *60*, 558-569.

Chalasani, S.H., Kato, S., Albrecht, D.R., Nakagawa, T., Abbott, L.F., and Bargmann, C.I. (2010). Neuropeptide feedback modifies odor-evoked dynamics in *Caenorhabditis elegans* olfactory neurons. Nat Neurosci *13*, 615-621.

Chao, M.Y., Komatsu, H., Fukuto, H.S., Dionne, H.M., and Hart, A.C. (2004). Feeding status and serotonin rapidly and reversibly modulate a *Caenorhabditis elegans* chemosensory circuit. Proceedings of the National Academy of Sciences of the United States of America *101*, 15512-15517.

Chapman, B., Jacobson, M.D., Reiter, H.O., and Stryker, M.P. (1986). Ocular dominance shift in kitten visual cortex caused by imbalance in retinal electrical activity. Nature *324*, 154-156.

Chen, Z., Hendricks, M., Cornils, A., Maier, W., Alcedo, J., and Zhang, Y. (2013). Two insulin-like peptides antagonistically regulate aversive olfactory learning in *C. elegans*. Neuron *77*, 572-585.

Chronis, N., Zimmer, M., and Bargmann, C.I. (2007). Microfluidics for in vivo imaging of neuronal and behavioral activity in *Caenorhabditis elegans*. Nature methods *4*, 727-731.

Cohn, R., Morantte, I., and Ruta, V. (2015). Coordinated and Compartmentalized Neuromodulation Shapes Sensory Processing in *Drosophila*. Cell *163*, 1742-1755.

Colbert, H.A., and Bargmann, C.I. (1995). Odorant-specific adaptation pathways generate olfactory plasticity in *C. elegans*. Neuron *14*, 803-812.

Darmaillacq, A.S., Chichery, R., and Dickel, L. (2006). Food imprinting, new evidence from the cuttlefish *Sepia officinalis*. Biol Lett *2*, 345-347.

Dash, P.K., Hochner, B., and Kandel, E.R. (1990). Injection of the cAMP-responsive element into the nucleus of *Aplysia* sensory neurons blocks long-term facilitation. Nature *345*, 718-721.

Dittman, A.H., Quinn, T.P., Nevitt, G.A., Hacker, B., and Storm, D.R. (1997). Sensitization of olfactory guanylyl cyclase to a specific imprinted odorant in coho salmon. Neuron *19*, 381-389.

Donnelly, J.L., Clark, C.M., Leifer, A.M., Pirri, J.K., Haburcak, M., Francis, M.M., Samuel, A.D., and Alkema, M.J. (2013). Monoaminergic orchestration of motor programs in a complex *C. elegans* behavior. PLoS Biol *11*, e1001529.

Dudai, Y., Jan, Y.N., Byers, D., Quinn, W.G., and Benzer, S. (1976). *dunce*, a mutant of *Drosophila* deficient in learning. Proceedings of the National Academy of Sciences of the United States of America *73*, 1684-1688.

Ehrlich, I., Humeau, Y., Grenier, F., Ciocchi, S., Herry, C., and Luthi, A. (2009). Amygdala inhibitory circuits and the control of fear memory. Neuron *62*, 757-771.

Feinberg, E.H., and Hunter, C.P. (2003). Transport of dsRNA into cells by the transmembrane protein SID-1. Science *301*, 1545-1547.

Feldman, D.E., and Knudsen, E.I. (1997). An anatomical basis for visual calibration of the auditory space map in the barn owl's midbrain. The Journal of neuroscience *17*, 6820-6837.

Fujiwara, M., Ishihara, T., and Katsura, I. (1999). A novel WD40 protein, CHE-2, acts cell-autonomously in the formation of *C. elegans* sensory cilia. Development *126*, 4839-4848.

Gerlach, G., Hodgins-Davis, A., Avolio, C., and Schunter, C. (2008). Kin recognition in zebrafish: a 24-hour window for olfactory imprinting. Proc Biol Sci *275*, 2165-2170.

Gordus, A., Pokala, N., Levy, S., Flavell, S.W., and Bargmann, C.I. (2015). Feedback from network states generates variability in a probabilistic olfactory circuit. Cell *161*, 215-227.

Gray, J.M., Hill, J.J., and Bargmann, C.I. (2005). A circuit for navigation in *Caenorhabditis elegans*. Proceedings of the National Academy of Sciences of the United States of America *102*, 3184-3191.

Ha, H.I., Hendricks, M., Shen, Y., Gabel, C.V., Fang-Yen, C., Qin, Y., Colon-Ramos, D., Shen, K., Samuel, A.D., and Zhang, Y. (2010). Functional organization of a neural network for aversive olfactory learning in *Caenorhabditis elegans*. Neuron *68*, 1173-1186.

Harris, G., Shen, Y., Ha, H., Donato, A., Wallis, S., Zhang, X., and Zhang, Y. (2014). Dissecting the signaling mechanisms underlying recognition and preference of food odors. The Journal of neuroscience *34*, 9389-9403.

Hasler, A.D., and Cooper, J.C. (1976). Chemical cues for homing salmon. Experientia *32*, 1091-1093.

Heiman, M., Kulicke, R., Fenster, R.J., Greengard, P., and Heintz, N. (2014). Cell type-specific mRNA purification by translating ribosome affinity purification (TRAP). Nature protocols *9*, 1282-1291.

Heiman, M., Schaefer, A., Gong, S., Peterson, J.D., Day, M., Ramsey, K.E., Suarez-Farinas, M., Schwarz, C., Stephan, D.A., Surmeier, D.J*., et al.* (2008). A translational profiling approach for the molecular characterization of CNS cell types. Cell *135*, 738-748.

Heisenberg, M. (2003). Mushroom body memoir: from maps to models. Nature reviews Neuroscience *4*, 266-275.

Hendricks, M., Ha, H., Maffey, N., and Zhang, Y. (2012). Compartmentalized calcium dynamics in a *C. elegans* interneuron encode head movement. Nature *487*, 99-103.

Hensch, T.K. (2005). Critical period plasticity in local cortical circuits. Nature reviews Neuroscience *6*, 877-888.

Hige, T., Aso, Y., Modi, M.N., Rubin, G.M., and Turner, G.C. (2015). Heterosynaptic Plasticity Underlies Aversive Olfactory Learning in *Drosophila*. Neuron *88*, 985-998.

Hirotsu, T., and Iino, Y. (2005). Neural circuit-dependent odor adaptation in *C. elegans* is regulated by the Ras-MAPK pathway. Genes Cells *10*, 517-530.

Hu, P.J. (2007). Dauer (August 08, 2007), *WormBook*, ed. The *C. elegans* Research Community, WormBook, doi/10.1895/wormbook.1.144.1, http://www.wormbook.org.

Hubel, D.H., and Wiesel, T.N. (1970). The period of susceptibility to the physiological effects of unilateral eye closure in kittens. The Journal of physiology *206*, 419-436.

Hudson, R. (1993). Olfactory imprinting. Current opinion in neurobiology *3*, 548-552.

Hukema, R.K., Rademakers, S., Dekkers, M.P., Burghoorn, J., and Jansen, G. (2006). Antagonistic sensory cues generate gustatory plasticity in *Caenorhabditis elegans*. The EMBO journal *25*, 312-322.

Iino, Y., and Yoshida, K. (2009). Parallel use of two behavioral mechanisms for chemotaxis in *Caenorhabditis elegans*. The Journal of neuroscience *29*, 5370-5380.

Isabel, G., Pascual, A., and Preat, T. (2004). Exclusive consolidated memory phases in Drosophila. Science *304*, 1024-1027.

Jafari, G., Xie, Y., Kullyev, A., Liang, B., and Sze, J.Y. (2011). Regulation of extrasynaptic 5-HT by serotonin reuptake transporter function in 5-HT-absorbing neurons

underscores adaptation behavior in *Caenorhabditis elegans*. The Journal of neuroscience *31*, 8948-8957.

Jang, H., Kim, K., Neal, S.J., Macosko, E., Kim, D., Butcher, R.A., Zeiger, D.M., Bargmann, C.I., and Sengupta, P. (2012). Neuromodulatory state and sex specify alternative behaviors through antagonistic synaptic pathways in *C. elegans*. Neuron *75*, 585-592.

Johansen, J.P., Cain, C.K., Ostroff, L.E., and LeDoux, J.E. (2011). Molecular mechanisms of fear learning and memory. Cell *147*, 509-524.

Kaas, J.H., Merzenich, M.M., and Killackey, H.P. (1983). The reorganization of somatosensory cortex following peripheral nerve damage in adult and developing mammals. Annual review of neuroscience *6*, 325-356.

Kandel, E.R. (2001). The molecular biology of memory storage: a dialogue between genes and synapses. Science *294*, 1030-1038.

Kandel, E.R., and Tauc, L. (1965). Heterosynaptic facilitation in neurones of the abdominal ganglion of *Aplysia depilans*. The Journal of physiology *181*, 1-27.

Kano, T., Brockie, P.J., Sassa, T., Fujimoto, H., Kawahara, Y., Iino, Y., Mellem, J.E., Madsen, D.M., Hosono, R., and Maricq, A.V. (2008). Memory in *Caenorhabditis elegans* is mediated by NMDA-type ionotropic glutamate receptors. Current biology *18*, 1010-1015.

Kao, M.H., Doupe, A.J., and Brainard, M.S. (2005). Contributions of an avian basal ganglia-forebrain circuit to real-time modulation of song. Nature *433*, 638-643.

Kauffman, A.L., Ashraf, J.M., Corces-Zimmerman, M.R., Landis, J.N., and Murphy, C.T. (2010). Insulin signaling and dietary restriction differentially influence the decline of learning and memory with age. PLoS Biol *8*, e1000372.

Keene, A.C., and Waddell, S. (2007). *Drosophila* olfactory memory: single genes to complex neural circuits. Nature reviews Neuroscience *8*, 341-354.

Kimata, T., Sasakura, H., Ohnishi, N., Nishio, N., and Mori, I. (2012). Thermotaxis of *C. elegans* as a model for temperature perception, neural information processing and neural plasticity. Worm *1*, 31-41.

Kimura, K.D., Fujita, K., and Katsura, I. (2010). Enhancement of odor avoidance regulated by dopamine signaling in *Caenorhabditis elegans*. The Journal of neuroscience *30*, 16365-16375.

Klapoetke, N.C., Murata, Y., Kim, S.S., Pulver, S.R., Birdsey-Benson, A., Cho, Y.K., Morimoto, T.K., Chuong, A.S., Carpenter, E.J., Tian, Z.*, et al.* (2014). Independent optical excitation of distinct neural populations. Nature methods *11*, 338-346.

Klein, M., and Kandel, E.R. (1980). Mechanism of calcium current modulation underlying presynaptic facilitation and behavioral sensitization in *Aplysia*. Proceedings of the National Academy of Sciences of the United States of America *77*, 6912-6916.

Knudsen, E.I., and Knudsen, P.F. (1989a). Vision calibrates sound localization in developing barn owls. The Journal of neuroscience *9*, 3306-3313.

Knudsen, E.I., and Knudsen, P.F. (1989b). Visuomotor adaptation to displacing prisms by adult and baby barn owls. The Journal of neuroscience *9*, 3297-3305.

Knudsen, E.I., and Knudsen, P.F. (1990). Sensitive and critical periods for visual calibration of sound localization by barn owls. The Journal of neuroscience *10*, 222-232.

Krashes, M.J., Keene, A.C., Leung, B., Armstrong, J.D., and Waddell, S. (2007). Sequential use of mushroom body neuron subsets during *Drosophila* odor memory processing. Neuron *53*, 103-115.

L'Etoile, N.D., and Bargmann, C.I. (2000). Olfaction and odor discrimination are mediated by the *C. elegans* guanylyl cyclase ODR-1. Neuron *25*, 575-586.

L'Etoile, N.D., Coburn, C.M., Eastham, J., Kistler, A., Gallegos, G., and Bargmann, C.I. (2002). The cyclic GMP-dependent protein kinase EGL-4 regulates olfactory adaptation in *C. elegans*. Neuron *36*, 1079-1089.

Lakhina, V., Arey, R.N., Kaletsky, R., Kauffman, A., Stein, G., Keyes, W., Xu, D., and Murphy, C.T. (2015). Genome-wide functional analysis of CREB/long-term memory-dependent transcription reveals distinct basal and memory gene expression programs. Neuron *85*, 330-345.

Landers, M.S., and Sullivan, R.M. (2012). The development and neurobiology of infant attachment and fear. Dev Neurosci *34*, 101-114.

Larsch, J., Flavell, S.W., Liu, Q., Gordus, A., Albrecht, D.R., and Bargmann, C.I. (2015). A circuit for gradient climbing in *C. elegans* chemotaxis. Cell reports *12*, 1748-1760.

Larsch, J., Ventimiglia, D., Bargmann, C.I., and Albrecht, D.R. (2013). High-throughput imaging of neuronal activity in *Caenorhabditis elegans*. Proceedings of the National Academy of Sciences of the United States of America *110*, E4266-4273.

Lee, H., Choi, M.K., Lee, D., Kim, H.S., Hwang, H., Kim, H., Park, S., Paik, Y.K., and Lee, J. (2012). Nictation, a dispersal behavior of the nematode *Caenorhabditis elegans*, is regulated by IL2 neurons. Nat Neurosci *15*, 107-112.

Lee, R.Y., Sawin, E.R., Chalfie, M., Horvitz, H.R., and Avery, L. (1999). EAT-4, a homolog of a mammalian sodium-dependent inorganic phosphate cotransporter, is necessary for glutamatergic neurotransmission in *Caenorhabditis elegans*. The Journal of neuroscience *19*, 159-167.

Lehrman, D.S. (1970). Semantic and conceptual issues in the nature-nurture problem. In Development and Evolution of Behavior, L.D.S. Aronson L.R., Tobach E., Rosenblatt J.S., ed. (W. H. Freeman; San Francisco), pp. 17-52.

Lema, S.C., and Nevitt, G.A. (2004). Evidence that thyroid hormone induces olfactory cellular proliferation in salmon during a sensitive period for imprinting. The Journal of experimental biology *207*, 3317-3327.

Leon, M. (1992). The neurobiology of filial learning. Annu Rev Psychol *43*, 377-398.

Li, Z., Liu, J., Zheng, M., and Xu, X.Z. (2014). Encoding of both analog- and digital-like behavioral outputs by one *C. elegans* interneuron. Cell *159*, 751-765.

Lichtman, J.W., and Balice-Gordon, R.J. (1990). Understanding synaptic competition in theory and in practice. Journal of neurobiology *21*, 99-106.

Lichtman, J.W., and Colman, H. (2000). Synapse elimination and indelible memory. Neuron *25*, 269-278.

Lorenz, K. (1935). Der Kumpan in der Umwelt des Vogels. Journal für Ornithologie *83*, 137-213.

Lorenz, K. (1979). The year of the greylag goose, 1st American edn (New York: Harcourt Brace Jovanovich).

Luscher, C., and Frerking, M. (2001). Restless AMPA receptors: implications for synaptic transmission and plasticity. Trends in neurosciences *24*, 665-670.

Macosko, E.Z., Pokala, N., Feinberg, E.H., Chalasani, S.H., Butcher, R.A., Clardy, J., and Bargmann, C.I. (2009). A hub-and-spoke circuit drives pheromone attraction and social behaviour in *C. elegans*. Nature *458*, 1171-1175.

Mair, W., Morantte, I., Rodrigues, A.P., Manning, G., Montminy, M., Shaw, R.J., and Dillin, A. (2011). Lifespan extension induced by AMPK and calcineurin is mediated by CRTC-1 and CREB. Nature *470*, 404-408.

Malinow, R., and Malenka, R.C. (2002). AMPA receptor trafficking and synaptic plasticity. Annual review of neuroscience *25*, 103-126.

Marder, E., O'Leary, T., and Shruti, S. (2014). Neuromodulation of circuits with variable parameters: single neurons and small circuits reveal principles of state-dependent and robust neuromodulation. Annual review of neuroscience *37*, 329-346.

Maricq, A.V., Peckol, E., Driscoll, M., and Bargmann, C.I. (1995). Mechanosensory signalling in *C. elegans* mediated by the GLR-1 glutamate receptor. Nature *378*, 78-81.

McEwan, D.L., Kirienko, N.V., and Ausubel, F.M. (2012). Host translational inhibition by *Pseudomonas aeruginosa* Exotoxin A Triggers an immune response in *Caenorhabditis elegans*. Cell Host Microbe *11*, 364-374.

Meisel, J.D., Panda, O., Mahanti, P., Schroeder, F.C., and Kim, D.H. (2014). Chemosensation of bacterial secondary metabolites modulates neuroendocrine signaling and behavior of *C. elegans*. Cell *159*, 267-280.

Melo, J.A., and Ruvkun, G. (2012). Inactivation of conserved *C. elegans* genes engages pathogen- and xenobiotic-associated defenses. Cell *149*, 452-466.

Mori, I., and Ohshima, Y. (1995). Neural regulation of thermotaxis in *Caenorhabditis elegans*. Nature *376*, 344-348.

Morrison, G.E., and van der Kooy, D. (2001). A mutation in the AMPA-type glutamate receptor, *glr-1*, blocks olfactory associative and nonassociative learning in *Caenorhabditis elegans*. Behavioral neuroscience *115*, 640-649.

Nakamori, T., Maekawa, F., Sato, K., Tanaka, K., and Ohki-Hamazaki, H. (2013). Neural basis of imprinting behavior in chicks. Dev Growth Differ *55*, 198-206.

Nakamura, T., and Gold, G.H. (1987). A cyclic nucleotide-gated conductance in olfactory receptor cilia. Nature *325*, 442-444.

Nevitt, G.A., Dittman, A.H., Quinn, T.P., and Moody, W.J., Jr. (1994). Evidence for a peripheral olfactory memory in imprinted salmon. Proceedings of the National Academy of Sciences of the United States of America *91*, 4288-4292.

Nishida, Y., Sugi, T., Nonomura, M., and Mori, I. (2011). Identification of the AFD neuron as the site of action of the CREB protein in *Caenorhabditis elegans* thermotaxis. EMBO Rep *12*, 855-862.

Ohno, H., Kato, S., Naito, Y., Kunitomo, H., Tomioka, M., and Iino, Y. (2014). Role of synaptic phosphatidylinositol 3-kinase in a behavioral learning response in *C. elegans*. Science *345*, 313-317.

Olveczky, B.P., Andalman, A.S., and Fee, M.S. (2005). Vocal experimentation in the juvenile songbird requires a basal ganglia circuit. PLoS Biol *3*, e153.

Owald, D., Felsenberg, J., Talbot, C.B., Das, G., Perisse, E., Huetteroth, W., and Waddell, S. (2015). Activity of defined mushroom body output neurons underlies learned olfactory behavior in *Drosophila*. Neuron *86*, 417-427.

Parrish, S., and Fire, A. (2001). Distinct roles for RDE-1 and RDE-4 during RNA interference in *Caenorhabditis elegans*. RNA *7*, 1397-1402.

Pena, J.L., and Gutfreund, Y. (2014). New perspectives on the owl's map of auditory space. Current opinion in neurobiology *24*, 55-62.

Petersen, C.I., McFarland, T.R., Stepanovic, S.Z., Yang, P., Reiner, D.J., Hayashi, K., George, A.L., Roden, D.M., Thomas, J.H., and Balser, J.R. (2004). *In vivo* identification of genes that modify ether-a-go-go-related gene activity in *Caenorhabditis elegans* may also affect human cardiac arrhythmia. Proc Natl Acad Sci U S A *101*, 11773-11778.

Pierce-Shimomura, J.T., Morse, T.M., and Lockery, S.R. (1999). The fundamental role of pirouettes in *Caenorhabditis elegans* chemotaxis. The Journal of neuroscience *19*, 9557-9569.

Pinsker, H.M., Hening, W.A., Carew, T.J., and Kandel, E.R. (1973). Long-term sensitization of a defensive withdrawal reflex in *Aplysia*. Science *182*, 1039-1042.

Pirri, J.K., McPherson, A.D., Donnelly, J.L., Francis, M.M., and Alkema, M.J. (2009). A tyramine-gated chloride channel coordinates distinct motor programs of a *Caenorhabditis elegans* escape response. Neuron *62*, 526-538.

Pokala, N., Liu, Q., Gordus, A., and Bargmann, C.I. (2014). Inducible and titratable silencing of *Caenorhabditis elegans* neurons in vivo with histamine-gated chloride channels. Proceedings of the National Academy of Sciences of the United States of America *111*, 2770-2775.

Pradel, E., Zhang, Y., Pujol, N., Matsuyama, T., Bargmann, C.I., and Ewbank, J.J. (2007). Detection and avoidance of a natural product from the pathogenic bacterium *Serratia marcescens* by *Caenorhabditis elegans*. Proceedings of the National Academy of Sciences of the United States of America *104*, 2295-2300.

Pujol, N., Link, E.M., Liu, L.X., Kurz, C.L., Alloing, G., Tan, M.W., Ray, K.P., Solari, R., Johnson, C.D., and Ewbank, J.J. (2001). A reverse genetic analysis of components of the Toll signaling pathway in *Caenorhabditis elegans*. Current biology : CB *11*, 809-821.

Quinn, W.G., Harris, W.A., and Benzer, S. (1974). Conditioned behavior in *Drosophila melanogaster*. Proceedings of the National Academy of Sciences of the United States of America *71*, 708-712.

Rahme, L.G., Tan, M.W., Le, L., Wong, S.M., Tompkins, R.G., Calderwood, S.B., and Ausubel, F.M. (1997). Use of model plant hosts to identify *Pseudomonas aeruginosa* virulence factors. Proceedings of the National Academy of Sciences of the United States of America *94*, 13245-13250.

Rankin, C.H., Beck, C.D., and Chiba, C.M. (1990). *Caenorhabditis elegans*: a new model system for the study of learning and memory. Behav Brain Res *37*, 89-92.

Rankin, C.H., and Wicks, S.R. (2000). Mutations of the *Caenorhabditis elegans* brain-specific inorganic phosphate transporter *eat-4* affect habituation of the tap-withdrawal response without affecting the response itself. The Journal of neuroscience : the official journal of the Society for Neuroscience *20*, 4337-4344.

Remy, J.J. (2010). Stable inheritance of an acquired behavior in *Caenorhabditis elegans*. Current biology *20*, R877-878.

Remy, J.J., and Hobert, O. (2005). An interneuronal chemoreceptor required for olfactory imprinting in *C. elegans*. Science *309*, 787-790.

Rex, E., Hapiak, V., Hobson, R., Smith, K., Xiao, H., and Komuniecki, R. (2005). TYRA-2 (F01E11.5): a *Caenorhabditis elegans* tyramine receptor expressed in the MC and NSM pharyngeal neurons. Journal of neurochemistry *94*, 181-191.

Rose, J.K., Kaun, K.R., Chen, S.H., and Rankin, C.H. (2003). GLR-1, a non-NMDA glutamate receptor homolog, is critical for long-term memory in *Caenorhabditis elegans*. The Journal of neuroscience *23*, 9595-9599.

Rose, J.K., Kaun, K.R., and Rankin, C.H. (2002). A new group-training procedure for habituation demonstrates that presynaptic glutamate release contributes to long-term memory in *Caenorhabditis elegans*. Learn Mem *9*, 130-137.

Rose, J.K., and Rankin, C.H. (2006). Blocking memory reconsolidation reverses memory-associated changes in glutamate receptor expression. The Journal of neuroscience *26*, 11582-11587.

Sanes, J.R., and Lichtman, J.W. (1999). Development of the vertebrate neuromuscular junction. Annual review of neuroscience *22*, 389-442.

Sasakura, H., Mori, I. (2013). Thermosensory Learning in *Caenorhabditis elegans*. Invertebrate Learning and Memory *22*, 124-139.

Satterlee, J.S., Ryu, W.S., and Sengupta, P. (2004). The CMK-1 CaMKI and the TAX-4 Cyclic nucleotide-gated channel regulate thermosensory neuron gene expression and function in *C. elegans*. Current biology *14*, 62-68.

Scholz, A.T., Horrall, R.M., Cooper, J.C., and Hasler, A.D. (1976). Imprinting to chemical cues: the basis for home stream selection in salmon. Science *192*, 1247-1249.

Schroeder, N.E., Androwski, R.J., Rashid, A., Lee, H., Lee, J., and Barr, M.M. (2013). Dauer-specific dendrite arborization in *C. elegans* is regulated by KPC-1/Furin. Current biology *23*, 1527-1535.

Schroll, C., Riemensperger, T., Bucher, D., Ehmer, J., Voller, T., Erbguth, K., Gerber, B., Hendel, T., Nagel, G., Buchner, E.*, et al.* (2006). Light-induced activation of distinct modulatory neurons triggers appetitive or aversive learning in *Drosophila* larvae. Current biology *16*, 1741-1747.

Schwaerzel, M., Monastirioti, M., Scholz, H., Friggi-Grelin, F., Birman, S., and Heisenberg, M. (2003). Dopamine and octopamine differentiate between aversive and appetitive olfactory memories in *Drosophila*. The Journal of neuroscience *23*, 10495-10502.

Scott, J.P. (1962). Critical periods in behavioral development. Science *138*, 949-958.

Sejourne, J., Placais, P.Y., Aso, Y., Siwanowicz, I., Trannoy, S., Thoma, V., Tedjakumala, S.R., Rubin, G.M., Tchenio, P., Ito, K.*, et al.* (2011). Mushroom body efferent neurons responsible for aversive olfactory memory retrieval in *Drosophila*. Nat Neurosci *14*, 903-910.

Semke, E., Distel, H., and Hudson, R. (1995). Specific enhancement of olfactory receptor sensitivity associated with foetal learning of food odors in the rabbit. Die Naturwissenschaften *82*, 148-149.

Shao, Z., Watanabe, S., Christensen, R., Jorgensen, E.M., and Colon-Ramos, D.A. (2013). Synapse location during growth depends on glia location. Cell *154*, 337-350.

Shtonda, B.B., and Avery, L. (2006). Dietary choice behavior in *Caenorhabditis elegans*. The Journal of experimental biology *209*, 89-102.

Siegelbaum, S.A., Camardo, J.S., and Kandel, E.R. (1982). Serotonin and cyclic AMP close single K+ channels in *Aplysia* sensory neurones. Nature *299*, 413-417.

Silva, A.J., Kogan, J.H., Frankland, P.W., and Kida, S. (1998). CREB and memory. Annual review of neuroscience *21*, 127-148.

Stetak, A., Horndli, F., Maricq, A.V., van den Heuvel, S., and Hajnal, A. (2009). Neuron-specific regulation of associative learning and memory by MAGI-1 in *C. elegans*. PLoS One *4*, e6019.

Stiernagle, T. (2006). Maintenance of *C. elegans* (February 11, 2006), *WormBook*, ed. The *C. elegans* Research Community, WormBook, doi/10.1895/wormbook.1.101.1,http://www.wormbook.org.

Suo, S., Kimura, Y., and Van Tol, H.H. (2006). Starvation induces cAMP response element-binding protein-dependent gene expression through octopamine-Gq signaling in *Caenorhabditis elegans*. The Journal of neuroscience *26*, 10082-10090.

Tabara, H., Sarkissian, M., Kelly, W.G., Fleenor, J., Grishok, A., Timmons, L., Fire, A., and Mello, C.C. (1999). The *rde-1* gene, RNA interference, and transposon silencing in *C. elegans*. Cell *99*, 123-132.

Tan, M.W., Mahajan-Miklos, S., and Ausubel, F.M. (1999). Killing of *Caenorhabditis elegans* by *Pseudomonas aeruginosa* used to model mammalian bacterial pathogenesis. Proceedings of the National Academy of Sciences of the United States of America *96*, 715-720.

Tanaka, N.K., Tanimoto, H., and Ito, K. (2008). Neuronal assemblies of the *Drosophila* mushroom body. The Journal of comparative neurology *508*, 711-755.

Tian, L., Hires, S.A., Mao, T., Huber, D., Chiappe, M.E., Chalasani, S.H., Petreanu, L., Akerboom, J., McKinney, S.A., Schreiter, E.R.*, et al.* (2009). Imaging neural activity in worms, flies and mice with improved GCaMP calcium indicators. Nature methods *6*, 875-881.

Timbers, T.A., and Rankin, C.H. (2011). Tap withdrawal circuit interneurons require CREB for long-term habituation in *Caenorhabditis elegans*. Behavioral neuroscience *125*, 560-566.

Tomioka, M., Adachi, T., Suzuki, H., Kunitomo, H., Schafer, W.R., and Iino, Y. (2006). The insulin/PI 3-kinase pathway regulates salt chemotaxis learning in *Caenorhabditis elegans*. Neuron *51*, 613-625.

Torayama, I., Ishihara, T., and Katsura, I. (2007). Caenorhabditis elegans integrates the signals of butanone and food to enhance chemotaxis to butanone. The Journal of neuroscience *27*, 741-750.

Troemel, E.R., Kimmel, B.E., and Bargmann, C.I. (1997). Reprogramming chemotaxis responses: sensory neurons define olfactory preferences in *C. elegans*. Cell *91*, 161-169.

Tsalik, E.L., Niacaris, T., Wenick, A.S., Pau, K., Avery, L., and Hobert, O. (2003). LIM homeobox gene-dependent expression of biogenic amine receptors in restricted regions of the *C. elegans* nervous system. Developmental biology *263*, 81-102.

Tsunozaki, M., Chalasani, S.H., and Bargmann, C.I. (2008). A behavioral switch: cGMP and PKC signaling in olfactory neurons reverses odor preference in *C. elegans*. Neuron *59*, 959-971.

Tully, K., Li, Y., Tsvetkov, E., and Bolshakov, V.Y. (2007). Norepinephrine enables the induction of associative long-term potentiation at thalamo-amygdala synapses. Proceedings of the National Academy of Sciences of the United States of America *104*, 14146-14150.

Tully, T. (1996). Discovery of genes involved with learning and memory: an experimental synthesis of Hirschian and Benzerian perspectives. Proceedings of the National Academy of Sciences of the United States of America *93*, 13460-13467.

Turner, G.C., Bazhenov, M., and Laurent, G. (2008). Olfactory representations by *Drosophila* mushroom body neurons. Journal of neurophysiology *99*, 734-746.

Varshney, L.R., Chen, B.L., Paniagua, E., Hall, D.H., and Chklovskii, D.B. (2011). Structural properties of the *Caenorhabditis elegans* neuronal network. PLoS Comput Biol *7*, e1001066.

Vicedo, M. (2009). The father of ethology and the foster mother of ducks: Konrad Lorenz as expert on motherhood. Isis *100*, 263-291.

Waddell, S. (2013). Reinforcement signalling in *Drosophila*; dopamine does it all after all. Current opinion in neurobiology *23*, 324-329.

White, J.G., Southgate, E., Thomson, J.N., and Brenner, S. (1986). The structure of the nervous system of the nematode *Caenorhabditis elegans*. Philos Trans R Soc Lond B Biol Sci *314*, 1-340.

Wiesel, T.N., and Hubel, D.H. (1963). Effects of visual deprivation on morphology and physiology of cells in the cats lateral geniculate body. Journal of neurophysiology *26*, 978-993.

Wragg, R.T., Hapiak, V., Miller, S.B., Harris, G.P., Gray, J., Komuniecki, P.R., and Komuniecki, R.W. (2007). Tyramine and octopamine independently inhibit serotonin-stimulated aversive behaviors in *Caenorhabditis elegans* through two novel amine receptors. The Journal of neuroscience *27*, 13402-13412.

Wu, H.G., Miyamoto, Y.R., Gonzalez Castro, L.N., Olveczky, B.P., and Smith, M.A. (2014). Temporal structure of motor variability is dynamically regulated and predicts motor learning ability. Nat Neurosci *17*, 312-321.

Yamazoe-Umemoto, A., Fujita, K., Iino, Y., Iwasaki, Y., and Kimura, K.D. (2015). Modulation of different behavioral components by neuropeptide and dopamine signalings in non-associative odor learning of Caenorhabditis elegans. Neurosci Res. *99*, 22-33.

Yin, J.C., Wallach, J.S., Del Vecchio, M., Wilder, E.L., Zhou, H., Quinn, W.G., and Tully, T. (1994). Induction of a dominant negative CREB transgene specifically blocks long-term memory in *Drosophila*. Cell *79*, 49-58.

Yu, D., Ponomarev, A., and Davis, R.L. (2004). Altered representation of the spatial code for odors after olfactory classical conditioning; memory trace formation by synaptic recruitment. Neuron *42*, 437-449.

Zaslaver, A., Liani, I., Shtangel, O., Ginzburg, S., Yee, L., and Sternberg, P.W. (2015). Hierarchical sparse coding in the sensory system of *Caenorhabditis elegans*. Proceedings of the National Academy of Sciences of the United States of America *112*, 1185-1189.

Zhang, X., and Zhang, Y. (2012). DBL-1, a TGF-beta, is essential for *Caenorhabditis elegans* aversive olfactory learning. Proceedings of the National Academy of Sciences of the United States of America *109*, 17081-17086.

Zhang, Y., Lu, H., and Bargmann, C.I. (2005). Pathogenic bacteria induce aversive olfactory learning in *Caenorhabditis elegans*. Nature *438*, 179-184.

Zheng, Y., Brockie, P.J., Mellem, J.E., Madsen, D.M., and Maricq, A.V. (1999). Neuronal control of locomotion in *C. elegans* is modified by a dominant mutation in the GLR-1 ionotropic glutamate receptor. Neuron *24*, 347-361.